

# **IN SEARCH OF CHAOTIC ELEMENTS IN THE BAY OF FUNDY WATER LEVEL MEASUREMENTS**

**EDWARD BARTLETT**

**February 1999**



**TECHNICAL REPORT  
NO. 197**

## PREFACE

In order to make our extensive series of technical reports more readily available, we have scanned the old master copies and produced electronic versions in Portable Document Format. The quality of the images varies depending on the quality of the originals. The images have not been converted to searchable text.

**IN SEARCH OF CHAOTIC ELEMENTS IN  
THE BAY OF FUNDY WATER LEVEL  
MEASUREMENTS**

Edward Bartlett

Department of Geodesy and Geomatics Engineering  
University of New Brunswick  
P.O. Box 4400  
Fredericton, N.B.  
Canada  
E3B 5A3

February 1999

© Edward Bartlett, 1998

## PREFACE

This technical report is an unedited reproduction of a thesis submitted in partial fulfillment of the requirements for the degree of Master of Science in Engineering in the Department of Geodesy and Geomatics Engineering, January 1998. The research was supervised by Dr. David E. Wells, and it was supported by the University of New Brunswick.

As with any copyrighted material, permission to reprint or quote extensively from this report must be received from the author. The citation to this work should appear as follows:

Bartlett, Edward (1999). *In Search of Chaotic Elements in the Bay of Fundy Water Level Measurements*. M.Sc.E. thesis, Department of Geodesy and Geomatics Engineering Technical Report No. 197, University of New Brunswick, Fredericton, New Brunswick, Canada, 123 pp.

## **Abstract**

The Bay of Fundy has extraordinary water level variations. These variations make accurate prediction using conventional harmonic approaches difficult. A possible approach to improving the predictions is to apply non-linear methods. Since the errors in prediction using harmonic methods appear random, the possibility of this being a system exhibiting chaotic behaviour rather than stochastic behaviour is investigated. Errors in the prediction are dependant upon the chosen method of analysis in the first place, here a least squares spectral analysis is used. The residual time series from the least squares analysis is then subjected to a search for the largest Lyapunov exponent using two algorithms. Existence of a positive Lyapunov exponent is generally accepted as being proof of chaotic behaviour and this existence is investigated. To further enhance the investigation the Correlation Dimension is estimated.

The results are presented and conclusions drawn. With the data sample used no clear indication of chaotic behaviour was identified.

## Table of Contents

<b>Abstract</b>	<b>ii</b>
<b>Table of Contents</b>	<b>iii</b>
<b>List of Figures</b>	<b>vi</b>
<b>Acknowledgements</b>	<b>viii</b>
<b>Approach</b>	<b>1</b>
<b>1.1 Introduction</b>	<b>1</b>
<b>1.2 Aim</b>	<b>2</b>
<b>1.3 Adopted Approach</b>	<b>3</b>
<b>1.4 Analytical Tools Used</b>	<b>4</b>
<b>1.5 Contributions</b>	<b>6</b>
<b>1.6 Outline</b>	<b>7</b>
<b>A Brief Overview of Chaos Theory</b>	<b>8</b>
<b>2.1 Introduction</b>	<b>8</b>
<b>2.2 An Example of a Chaotic System</b>	<b>9</b>
<b>2.3 Fractals</b>	<b>12</b>
<b>2.4 Strange Attractors</b>	<b>13</b>
<b>2.5 Lyapunov or Characteristic Exponents</b>	<b>18</b>
2.5.1 The Multiplicative Ergodic Theorem of Oseledec	20
2.5.2 The Spectrum of Lyapunov Exponents	22
<b>2.6 Correlation Dimension</b>	<b>24</b>
2.6.1 Dimension	24
2.6.2 Fractal (or Mandelbrot) dimension	25
2.6.3 Hausdorff (or Hausdorff-Besicovitch) dimension	25
2.6.4 Correlation dimension	26
<b>2.7 Reconstruction of the Attractor</b>	<b>28</b>

<b>Tides, the Data and Removal of Periodic Components</b>	<b>34</b>
<b>3.1 Introduction</b>	<b>34</b>
<b>3.2 Tides</b>	<b>35</b>
3.2.1 Equilibrium Theory of Tides	36
3.2.2 Dynamic Tide Theory	39
3.2.3 Chaos in the water level measurements	39
<b>3.3 Removal of Periodic Components</b>	<b>42</b>
<b>3.4 Least-Squares Spectral Analysis (LSSA)</b>	<b>44</b>
<b>3.5 Data Requirements</b>	<b>47</b>
3.5.1 Length of the Time Series	48
3.5.2 Sampling Frequency	49
3.5.3 Noise	50
3.5.4 Shortening of the data set	50
<b>3.6 The Delay Portrait</b>	<b>51</b>
<b>Determining Lyapunov Exponents I</b>	<b>54</b>
<b>4.1 Algorithm</b>	<b>54</b>
<b>4.2 Implementation</b>	<b>56</b>
<b>4.3 Interactive Runs</b>	<b>59</b>
<b>4.4 Batch Runs</b>	<b>61</b>
<b>Determining Lyapunov Exponents II</b>	<b>67</b>
<b>5.1 The Algorithm</b>	<b>67</b>
<b>5.2 Implementation</b>	<b>70</b>
<b>Results, Conclusions and Recommendations</b>	<b>77</b>
<b>6.1 Interactive Runs using Wolf's Algorithm</b>	<b>77</b>
<b>6.2 Batch Runs using Wolf's Algorithm</b>	<b>79</b>
<b>6.3 Batch runs Using Rosenstein's Algorithm</b>	<b>87</b>

<b>6.4 Evaluation of a Surrogate Time Series</b>	<b>91</b>
<b>6.5 Conclusions</b>	<b>92</b>
<b>6.6 Recommendations</b>	<b>93</b>
<b>References</b>	<b>95</b>
<b>Bibliography</b>	<b>99</b>
<b>Appendix A</b>	<b>101</b>
<b>A.1 Data Sample</b>	<b>101</b>
<b>Appendix B</b>	<b>103</b>
<b>B.1 LSSA Command File</b>	<b>103</b>
<b>B.2 LSSA Output</b>	<b>103</b>
<b>Appendix C - Source Listings after Wolf et al. (1985).</b>	<b>111</b>
<b>C.1 Source listing for BASGEN</b>	<b>111</b>
<b>C.2 Source listing for FET</b>	<b>114</b>
<b>Appendix D</b>	<b>121</b>
<b>D.1 Autocorrelation computation</b>	<b>121</b>



## List of Figures

2.1 Bifurcation diagram for the logistic map	10
2.2 Time series representing period-2 behaviour	11
2.3 Time series representing chaotic behaviour	12
2.4 Construction of the Cantor set	13
2.5 The Hénon map	15
2.6 The Hénon map enlarged	16
2.7 The Hénon map further enlarged	16
2.8 The stretching and folding of a strange attractor	18
2.9 Reconstructed Hénon attractor	32
2.10 Reconstructed Lorenz attractor	33
3.1 Gravity and the Ocean	35
3.2 Eccentricity of the moon's orbit	38
3.3 First 1000 points of the residual signal	46
3.4 Frequency spectrums for the tide and residual signals	47
3.5 Reconstructed delay portrait	51
3.6 Reconstructed delay portrait using lines	52
4.1 Screen capture from an interactive session	60
4.2 A second example of the interactive graphics	61
4.3 Largest Lyapunov exponent vs embedding dimension	63
4.4 Largest Lyapunov exponent vs evolution time	64
4.5 Largest Lyapunov exponent vs maximum separation	65
4.6 Largest Lyapunov exponent vs tau	66
5.1 Largest Lyapunov exponent estimation	72
5.2 Correlation dimension estimation	73

5.3 MTRCHAOS screen capture	73
5.4 Lyapunov exponent estimation using randomised data	75
5.5 Correlation dimension estimation using randomised data	75
6.1 Screen capture of an interactive session	78
6.2 Screen capture of an interactive session	79
6.3 Lyapunov exponents for increasing dimension	83
6.4 Lyapunov exponents for increasing evolution times	83
6.5 Lyapunov exponents for increasing maximum separation	84
6.6 Lyapunov exponents for increasing minimum separation	85
6.7 Lyapunov exponents for increasing reconstruction delays	86
6.9 Estimated slope for a moving window	89
6.8 Curves for estimating the largest Lyapunov exponent	89
6.10 Curves for estimating the correlation dimension	90
6.11 The first 1000 points of the surrogate data set	91
6.12 Lyapunov curves for the surrogate data	92
6.13 Correlation dimension curves for the surrogate data	92

## **Acknowledgements**

The University of New Brunswick, in particular the Department of Geodesy and Geomatics, enabled the author to study by being extremely flexible with regards to schedules. I wish to thank the university for the freedom of scheduling

Dr Wells provided the guidance in this work by providing advice and supplying material of interest in a number of fields and not by attempting to directly influence my chosen direction. For this academic freedom I wish to thank Dr Wells.

Lastly but not least I wish to thank my wife, Tanya, who checked my English, typing and spelling by proof reading.

# Chapter 1

## Approach

### 1.1 Introduction

Chaotic behaviour is a non-linear phenomenon. One of the characteristics, although not exclusive to chaotic systems, is an extreme sensitivity to initial conditions. For dissipative systems, in a chaotic state, the dynamics are generally constrained to a finite, lower-dimensional region of state space called a 'strange attractor'. Time series from such a system may display apparently stochastic behaviour. The sensitivity to initial conditions in chaotic systems complicates long term predictions, even when the system is known to be purely deterministic. Here a deterministic system is considered to be one which is mathematically defined and under ideal conditions completely known. That is, under conditions of zero noise, perfect knowledge of the system and no computational error, all future states may be predicted. Real systems are never known perfectly and are not noise free. The extreme sensitivity to initial conditions prevents long term predictions in real systems which are chaotic. An improvement in the accuracy with which short term predictions can be made, compared to statistical forecasts, is gained by using the deterministic knowledge.

This apparently stochastic behaviour in chaotic systems has led researchers in many fields to consider the possibility that their data are in fact deterministic chaos rather than noise. Remarkable successes have been achieved in a number of fields. There are also numerous less substantiated claims. Some of the fields where chaos has been claimed are as diverse as medicine (Frank et al., 1990), economics (Brock, 1986), meteorology

(Cuomo et al., 1993), biology (Lloyd and Lloyd, 1995), (Arizmendi et al., 1995), earthquake predictions (Ouchi, 1993) and oceanography (Yan, 1993).

The requirements of researchers to classify the nature of their data more completely has led to the development of a number of algorithms that distinguish deterministic chaos from noise in time series. Two of these were selected and used in this study. It is realised that Wolf's algorithm (Wolf et al., 1985) is not ideal for the analysis of real world data. A principal reason for the lack of suitability to real world data is the use of a fixed time before replacement of the vectors used in the estimation. A consequence of this is that a poor selection of points may contribute significantly to the estimated quantities. It does, however, form an important part of the literature and is referred to extensively, often forming a starting point for further developments. Improved algorithms have subsequently been developed. For this reason the second algorithm used here, developed by Rosenstein (Rosenstein et al. 1993), is also applied to the data. Use of these two approaches by no means exhausts the possibilities, and both suffer from the lack of a 'sanity' check. By a 'sanity' check, a gross test of reasonableness is implied - in a dissipative system the overall system cannot be an expanding one. In Section 6.5 it is shown that this sanity check becomes a moot point.

## **1.2 Aim**

In this work the water level records from the Bay of Fundy, in eastern Canada, are analysed to establish whether deterministic behaviour can be identified. The records used are from the permanent tide gauge at the port of Saint John. Since water level variations are largely periodic in nature, a significant portion of the signal can be predicted using an  $n$  period model. Differences between the predicted and observed water level are referred to here as the residual signal and represent the errors in the prediction. The magnitude of

these errors is significant, up to the order of 1m. In the event that low-dimensional deterministic chaos could be identified in this residual time series, the possibility of increased accuracy in short term predictions would be opened up.

### 1.3 Adopted Approach

The water level record for the period starting from 1/1/1947 and extending for 30 000 samples was used. Section 3.5 deals with the criteria for the selection of this data record. Data were recorded with a sample interval of one hour: 30 000 samples thus represent 30 000 hours, or 1250 days. Since there are a number of well known periodic components in the tidal records, these were removed using a least-squares spectral method. Further spectral analysis was performed to identify remaining periodic components. These too were removed as they were considered predictable. What remains after removal of all the identified periodic components is a residual time series, which may be considered to represent the errors in water level predictions using a particular model. More specifically

$$\mathbf{X}(t) = Z_0(t) + \mathbf{T}(t) + \mathbf{S}(t) \quad 1.1$$

where  $\mathbf{X}(t)$  represents the observed level,  $Z_0(t)$  is the relationship between chart datum and mean sea level,  $\mathbf{T}(t)$  is the harmonic portion of the signal, and  $\mathbf{S}(t)$  is the residual signal. Variations in  $Z_0(t)$  were identified as being negligible and consequently  $Z_0(t)$  was dropped.  $\mathbf{T}(t)$  was removed from the observed time series leading to  $\mathbf{S}(t)$  which becomes the signal of interest.

It is important to note that the time series analysed is a natural system that has been filtered. This manipulation of the data introduces artefacts which almost certainly affect the nature of the data. Since the method of least-squares spectral analysis (LSSA) allows for both the identification of periodic elements and the prediction of future states, it is

argued that the approach remains valid as long as the water level predictions are made using LSSA. If the residual time series could be shown to contain deterministic elements and could be predicted with an accuracy better than that obtainable with stochastic methods, then combining the predicted residual series with the LSSA water level prediction should yield improved results. That is both  $T(t)$  and  $S(t)$  could be predicted instead of only  $T(t)$ . In fact it must be remembered that the time series is already contaminated by elements from the measuring apparatus which, in theory, could be divorced from the 'true' water levels. Merry and Vaníček (1983) use this approach. The difference between this work and that of Merry and Vaníček (1983) is the manner in which the residual time series is analysed.

Modelling of any system occurs in phases which may be broken down into :

- a) Analysis of the data with the aim of identifying their nature.
- b) Interpretation of the data in terms of real world components.
- c) Formulation of the mathematical equations that represent the system which generates these data.
- d) Refinement of the model to an optimal solution (in some sense).
- e) Interpretation of the model results in real world terms.

Only phase a) of this process is undertaken here, and this is undertaken with the specific intention of identifying whether deterministic chaos is present or not.

## **1.4 Analytical Tools Used**

There is a wealth of computer software freely available, it was decided that the most efficient approach was to adopt and use existing software as far as possible. In this regard a number of utilities have been used to manipulate the data, either in their original form or after modification by the author. A brief summary of the software and tools used is given below :

- 1) LSSA - the source code for this algorithm, developed at the University of New Brunswick, is freely available and fully described in Wells et al. (1985). It was used with only minor modifications.
- 2) FET - or the fixed evolution time algorithm by Wolf et al. (1985) which allows for identification of deterministic chaos. The source code for this was used with only slight modifications. In order to improve computational efficiency a second utility BASGEN was used in conjunction with the FET code. This allows for the data to be pre-classified spatially and greatly reduces search times during later analysis.
- 3) MTRLYAP and MTRCHAOS are two utilities written by Rosenstein et al. (1993). The first of these is an analysis tool to assist in the identification of deterministic chaos. The second allows the results to be visualised as well as the original time series to be further manipulated to establish stability in the solution. Both were available only as executable programs and were used unmodified.
- 4) GNUPLOT (Williams and Kelley, 1993) was used for all plotting and visualisation of data. This is a freely available plotting package capable of generating presentation quality output. It is distributed on the Internet and at the time of writing could be found at [http://www.cs.dartmouth.edu/gnuplot\\_info.html](http://www.cs.dartmouth.edu/gnuplot_info.html)
- 5) Mathcad<sup>1</sup> (MathSoft Inc., 1993) is a commercial mathematics package that was used to perform Fourier analyses on the time series. It was also used fairly extensively when initially gaining an understanding of iterated maps and was then used to generate examples of certain maps for presentation.

---

<sup>1</sup>Trademark of MathSoft, Inc.



6) SEARCH (Spratt, 1996) was used to create the example of stretching and folding of a strange attractor in Chapter 2. The procedure is somewhat tedious but useful when gaining an understanding of the nature of strange attractors. The process involves running three programs SEARCH or SIMPANIM, DISPLAY and a utility to create animations. SEARCH and SIMPANIM search for and find suitable candidates from either an iterated map or a set of simple ordinary differential equations. These are saved as a bitmap file which can be converted into individual files using DISPLAY, still in bitmap format. In the event that an animated display is desired the successive frames can be used to generate an animated GIF file. In Chapter 2 the single bitmap file containing the 'panes' is presented, i.e., it is simply the results of SEARCH.

## **1.5 Contributions**

At the time that this work was started the author could find no literature connecting non-linear systems in a chaotic state to water level predictions. Due to the physical nature of water level variations and the many non-linear processes involved water level prediction was believed to be a good candidate. This work is intended to introduce this possibility and to take the first steps to identifying whether such elements are present in a single data set. From the outset there was no intention of progressing to the point of devising models using non-linear processes. It is also hoped that it will initiate a course of interest to others in related disciplines.

During the later stages of this work it came to the author's attention that an as yet unpublished paper claiming to improve on tidal predictions, using chaos theory, has been written (Frison, 1997a).

## 1.6 Outline

In order to introduce the reader to the terminology and a layman's understanding of chaos theory a brief overview is given in Chapter 2. This concentrates on the topics relevant to this work, as developed by others, and makes no attempt to expand on chaos theory.

Tides are a well understood physical phenomenon. Chapter 3 briefly discusses water level variation theory. The likelihood of there being chaotic elements in the water level signal is discussed. Certain types of systems which are not accounted for in later analysis are mentioned. Prior to analysis the measured water level signal is manipulated. How this is done and the reasons why are presented. In addition the data requirements are discussed.

The following two chapters, Chapters 4 and 5, deal with algorithms developed by Wolf et al. (1985) and Rosenstein et al. (1993) respectively. These algorithms are used to analyse the data with the explicit aim of identifying whether it is chaotic or stochastic.

Chapter 6 presents the results obtained from applying the algorithms of Chapters 4 and 5 to the water level data. These results are discussed and conclusions drawn. Finally proposals with regards to how to proceed further with this work are presented.

## **Chapter 2**

### **A Brief Overview of Chaos Theory**

#### **2.1 Introduction**

Before proceeding to the specific algorithms used to evaluate the data a brief overview of chaos theory is given. Aspects that are covered are mainly those used in the subsequent algorithms, however, a more general approach is presented. For a fuller understanding of the concepts the reader is referred to the literature referenced in this section.

As stated in Chapter 1 chaotic behaviour is a non-linear phenomenon, characterised by an extreme sensitivity to initial conditions. For dissipative systems, in a chaotic state, the dynamics are usually constrained to a finite, lower-dimensional, region of state space called a strange attractor. Dissipative systems are ones which 'lose' or dissipate information, thus the sum of all the Lyapunov exponents is negative. Strange attractors and Lyapunov exponents are discussed in Sections 2.4 and 2.5 respectively. Energy and/or matter constantly flow through the system from its environment. This enables the system to remain in a far-from-equilibrium state (Marshall and Zohar, 1997). A chaotic state is considered to be one in which the behaviour is not regular. Time series from such a system may display apparently stochastic behaviour. This chapter expands on these statements and covers the basics of the theory used in later chapters.

After removal of periodic components from observed ocean water levels a signal remains. This signal may be considered as an observation of a single variable in a system. Since no further periodic components can reasonably be identified, the remaining signal can be considered as noise and treated stochastically. Traditionally this

has been the case. An alternative approach is to consider the signal as a deterministic system exhibiting chaotic behaviour. The truth is probably a combination of the two. Analysis of such a signal with the express purpose of identifying deterministic chaos forms the basis of this work and was undertaken using two measures to quantify the system :

- a) Lyapunov exponents
- b) Correlation dimension

## 2.2 An Example of a Chaotic System

Chaotic systems are introduced by means of an example. One of the simplest systems known to exhibit chaotic behaviour is the so-called logistic map. Before proceeding it is worthwhile noting that 'map' here is used to describe a discrete time system. Continuous time systems are referred to as 'flows'.

Casti (1992, p. 255) discusses the growth over time of an insect population in terms of the logistics map. He further notes that the logistic map, in a chaotic region, was often employed as a random number generator in the early days of computing. Kugiumtzis et al. (1994) note that the logistic map has been used to model supply and demand in economics in addition to populations in biology.

The logistic map is an iterated map, it is completely deterministic and defined as follows

$$x_{k+1} = ax_k(1 - x_k) \quad 2.1$$

where  $x$  is the state variable and  $a$  is an independent parameter.

For  $1 \leq a \leq 4$  and an initial condition in the interval  $[0,1]$  the state variable is restricted to the interval  $[0,1]$ . For  $a > 4$  the system was observed to be divergent when

examined numerically. The behaviour of the system is dependant on the value selected for  $a$  and varies, with the asymptotic state (for a particular selection of  $a$ ) changing from a fixed point through stable periodic orbits to chaotic behaviour at  $a \geq 3.57$  as  $a$  is varied (Kugiumtzis et al, 1994). For the case  $x_0 = 0$  the solution is trivial with  $x_k = 0 \quad \forall k$ .

This behaviour is most clearly demonstrated using a bifurcation diagram, Figure 2.1 was generated using Mathcad and iterating the logistic map 30 000 times. In general, the phase portrait changes gradually as the parameters vary. There are usually parameter values for which the phase portrait changes drastically. These abrupt changes in the phase portrait due to changes in the parameters are called *bifurcations* (Hubbard and West, 1990). The phase portrait is a representation of the phase space discussed in Section 2.6. By plotting the state variable,  $x_k$ , against the parameter,  $a$ , these changes in behaviour are apparent. To generate the plot  $a$  was incremented while the system was

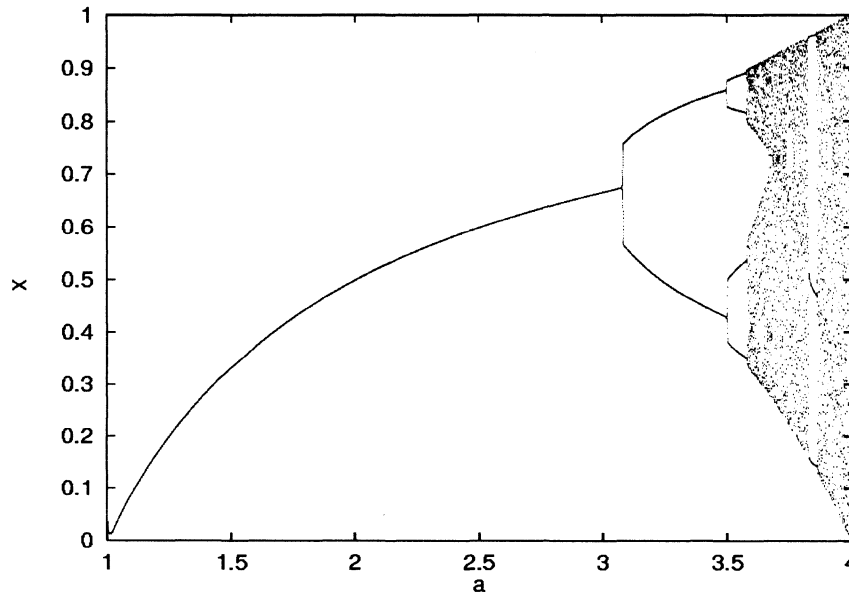


Figure 2.1 - Bifurcation diagram for the logistic map. Evolution of the attractor as the parameter  $a$  increases from 1 to 4 is demonstrated. For the  $a$ -interval 1 to  $\approx 3.08$  the stable solution is a fixed point, from  $\approx 3.08$  to  $\approx 3.5$  a stable period-2 solution exists, from  $\approx 3.5$  to  $\approx 3.57$  a stable period-4 solution exists. As  $a$  is further increased there is an infinite sequence of period-doubling bifurcations before the onset of chaos. A brief period-3 solution occurs around 3.85.

iterated.

The period doubling route to chaos shown in Figure 2.1 is interesting because it may be characterised by certain universal numbers. The spacing between consecutive bifurcations approaches a universal constant, called the Feignbaum number after its discoverer (Baker and Gollub, 1990).

Figures 2.2 and 2.3 are time series plots for two of the different stages of evolution. Values of  $a$  are 3.2 and 3.9 which demonstrate period-2 and chaotic behaviours respectively. Period- $n$  implies that the state variable takes on  $n$  discrete values when the system is iterated. Such time series may represent the observer's knowledge of a system.

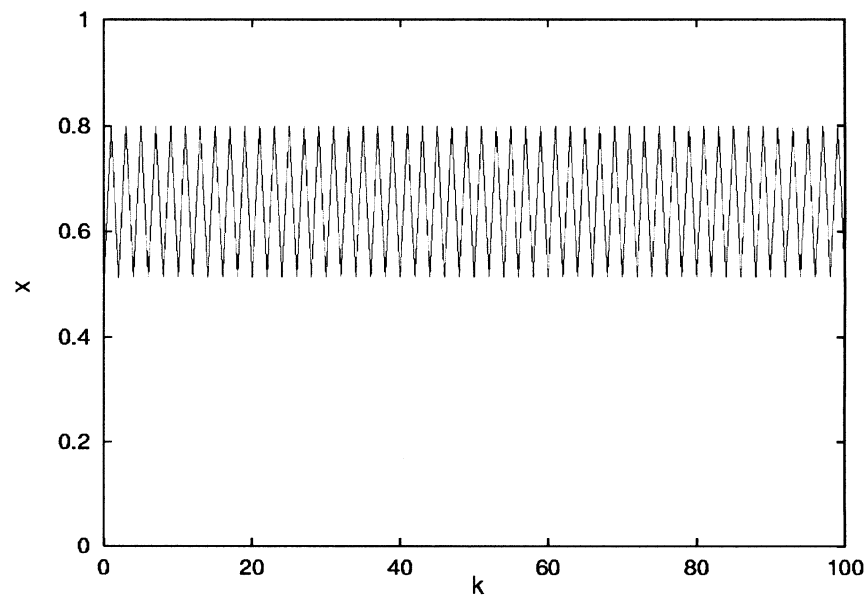


Figure 2.2 - Time series representing period-2 behaviour for the logistic map,  $a = 3.2$ .

Chaotic behaviour in the logistic map is characterised by an autocorrelation function which is essentially zero for all lags except zero and could easily lead to the conclusion that the system is white noise (Kugiumtzis et al., 1994). The autocorrelation may be estimated from a sample by

$$\hat{R}_{xx}(r\Delta t) = \frac{1}{N-r} \sum_{n=1}^{N-r} x_n x_{n+r} \quad r = 0, 1, 2, \dots, m \quad 2.2$$

where  $r$  is the lag,  $m$  is the maximum lag number and,  $N$  is the number of observations (Bendat and Piersol, 1986). It is required that the data be equally spaced, stationary and have a zero mean. The autocorrelation for the logistic map is estimated in Appendix D.

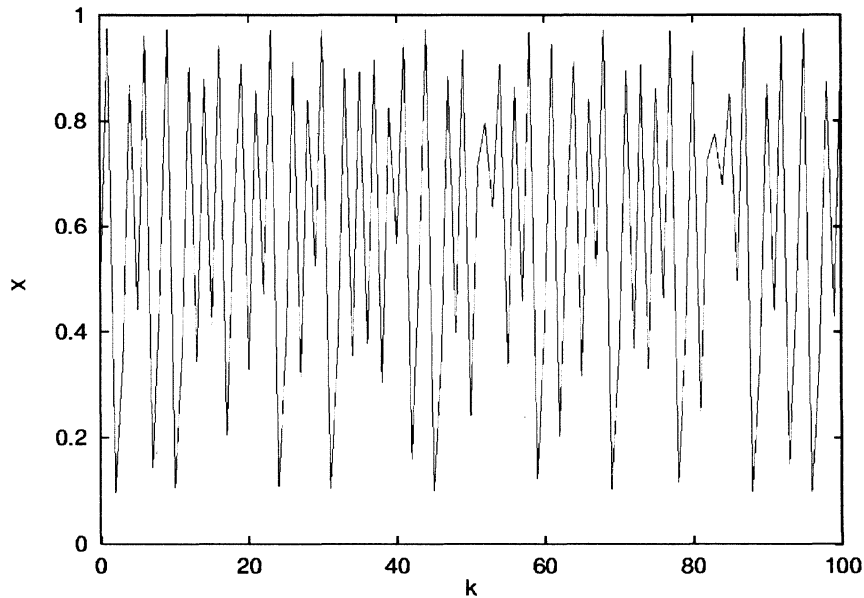


Figure 2.3 - Time series representing chaotic behaviour of the logistic map,  $a = 3.9$ .

### 2.3 Fractals

Broadly speaking a fractal set may be considered as a set which is self-similar under magnification, that is, its appearance remains the same at any magnification. More specifically, a fractal is a set  $F$  which has the property that  $F$  is the union of sets  $\{F_i\}$  for which each  $F_i$  is similar to  $F$  and  $F_i \cap F_j (i \neq j)$  is empty (or negligible in some sense). Each  $F_i$  can also be decomposed in this way and this can be continued indefinitely (Mathematics Dictionary, 1992).

Probably the simplest example of this is the Cantor set. This is created by starting with a line of fixed length, dividing it into three equal portions and deleting the middle third. This yields two lines and a 'gap' of equal length. Each of the remaining lines can be divided in the same manner yielding four lines of equal length and three 'gaps'. This is illustrated by Figure 2.4. Continuing this process indefinitely leads to a set which contains a total line length of zero, given by  $\lim_{n \rightarrow \infty} (2/3)^n$ . There are a number of simple extensions to higher dimensions of this concept such as the Koch Snowflake (Gleick, 1988) and the Sierpinski Gasket (Casti, 1992).

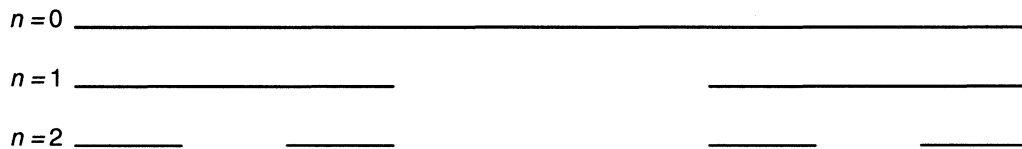


Figure 2.4 - Construction of the Cantor set for the steps up to  $n = 2$ .

## 2.4 Strange Attractors

*Phase space* is the set of states of a system. For instance the *state* of a Newtonian system is specified when both a position and a velocity is known for each component of the system (Hubbard and West, 1990). A trajectory is the path traced by the solution of the equations as a function of time. In conservative or chaotic systems where the attractor is bounded the trajectory will form orbits as it revisits nearby regions of phase space.

Grebogi et al. (1984) define an *attractor* and a *basin of attraction* as :

An attractor is a compact set with a neighborhood such that, for almost every initial condition in this neighborhood, the limit set of the orbit as time tends to  $+\infty$  is the attractor.

The basin of attraction of an attractor is the closure of the set of initial conditions which approach the attractor as time tends to  $+\infty$ .



As a chaotic system evolves the trajectory in phase space is normally constrained to a geometrical structure characterised by *stretching* and *folding*. This geometrical structure is the so-called strange attractor. In a system with  $F$  degrees of freedom an attractor is a lower-dimensional subset of  $F$ -dimensional phase space. Almost all sufficiently close trajectories (all points within the basin of attraction) are attracted asymptotically towards the attractor.

In a dissipative system volume is contracted and the volume of the attractor is always zero, however, with strange attractors the contraction does not occur in all directions. The stretching is caused by the divergence of nearby trajectories, while the folding constrains the dynamics to a finite region. Despite having a zero volume the attractor may exhibit extremely complex structures. The divergence of nearby trajectories is exponential and directly related to the sensitive dependence on initial conditions. This is treated more fully under the section on Lyapunov exponents. Eckmann and Ruelle (1985) define a strange attractor to be an attractor with *sensitive dependence on initial conditions*.

A characteristic of the strange attractor is that its dimension is non-integer, unlike ordinary attractors which have integer dimensions. The subset, to which the strange attractor is confined, has a non-integer dimension  $< m$ , where  $m$  is an integer and is called the *embedding dimension*. There are a number of definitions for non-integer dimensions, some of which are discussed in Section 2.6.

As a result of the repeated stretching and folding the structure becomes multi-sheeted or Cantor-set like in some directions; accordingly it can be considered a fractal. It is a common characteristic of strange attractors that they are fractal in nature. The fractal nature of a strange attractor is demonstrated using the Hénon map. Equation 2.3 defines the map and Figures 2.5, 2.6 and 2.7 show the map and two successive magnifications.

The fractal nature is apparent when the figures are compared, as the geometrical structure repeats itself with the increased magnification.

$$\begin{aligned}x_1(k+1) &= 1 + x_2(k) - ax_1^2(k) \\x_2(k+1) &= bx_1(k).\end{aligned}\tag{2.3}$$

This system is chaotic when  $a = 1.4$  and  $b = 0.3$  (Rosenstein et al., 1993). Figure 2.5 was generated by iterating the system 30 000 times in Mathcad and then plotting each value as a point.

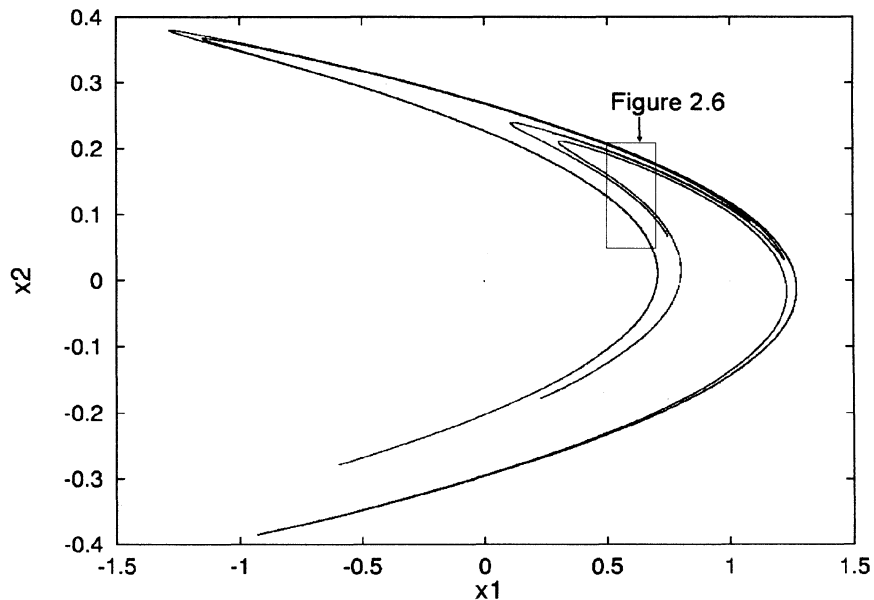


Figure 2.5 - The Hénon map.

Computing successive iterations of the Hénon map shows that using 14 digits' accuracy the error in prediction grows to order 1 by the sixtieth iteration (Eckmann and Ruelle, 1985). This means that the solution may lie anywhere on the attractor and predictions can no longer be made with any greater accuracy than the bounds of the attractor. Computations performed in Mathcad were made using 15 digits of precision. In view of this it is important to note that strictly speaking it is not possible to simulate chaotic systems on a computer because of the finite set of numbers available, however,

for purposes of illustration it suffices. It was supposedly the use of a different calculator, with a different precision, that led Lorenz (1963) to note the sensitivity of his weather prediction system (Marshall and Zohar, 1997). Ruelle (1989, p. 28), puts this into context.

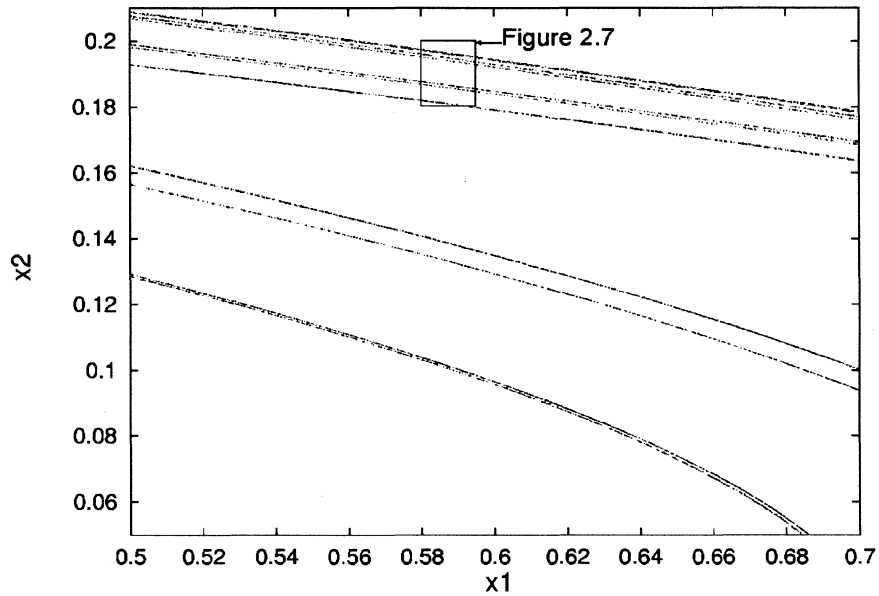


Figure 2.6 - The Hénon map enlarged.

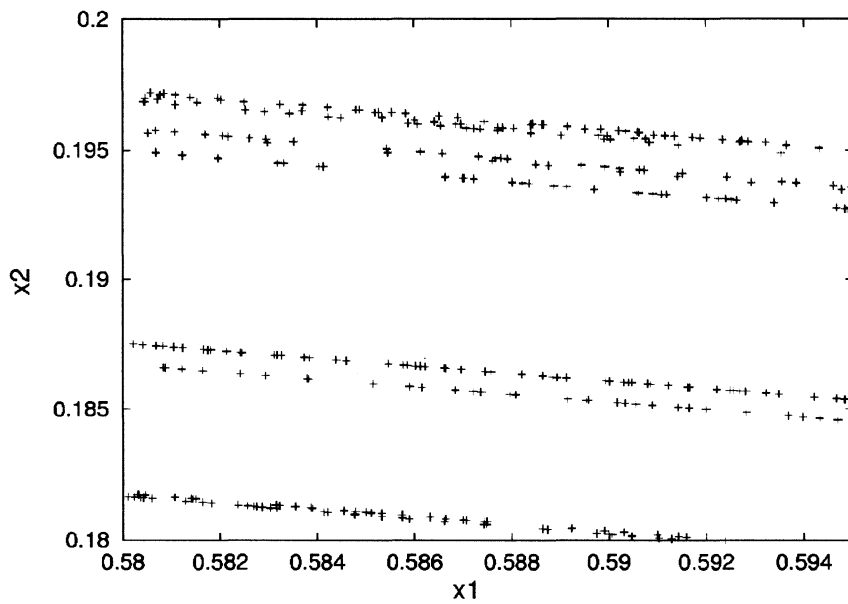


Figure 2.7 - The Hénon map further enlarged.

Hence, we can ask why should we compute 10 000 points if after 60 the results are already meaningless. *The point is that we have to reformulate what is considered as meaningful.* In fact, it is clear that if one does not make more precise computations, the exact position of the 60th point of the orbit is *completely indeterminate*: it could be anywhere on the attractor; however, as far as the *statistical* properties of the orbit are concerned, this must not trouble us because they do not depend on the details of the calculations and therefore the existence of the attractor is not in question.

Although many chaotic systems exhibit fractal structures in phase space there is no direct connection between strange attractors and fractals. For example, the attractor for the logistic map is observed to consist of a finite number of disjoint intervals in  $0 \leq x \leq 1$  (Grebogi et al., 1984). This attractor is not strange and does not exhibit a fractal nature. Grebogi et al. (1984) also provide examples of non-chaotic strange attractors, in particular they examine a non-linear oscillator forced at two incommensurate frequencies,

$$\begin{aligned} x_{n+1} &= f(x_n, \theta_n) \\ \theta_{n+1} &= [\theta_n + 2\pi\omega] \pmod{2\pi}, \end{aligned} \tag{2.4}$$

where  $f(x, \theta) = f(x, \theta + 2\pi)$ .

The definitions adopted by Grebogi et al. (1984) help to clarify the relationship between chaos and strange attractors. These are :

*Chaotic* refers to the dynamics on the attractor.  
*Strange* refers to the geometrical structure of the attractor.

For a rigorous treatment of strange attractors the reader is referred to Ruelle (1989).

A clear demonstration of many of the characteristics discussed in this section is achieved by viewing an attractor at successive times. In particular the stretching and folding of the attractor are apparent. Using software written by Sprott (1996) Figure 2.8 was generated. Here a quadratic map given by

$$\begin{aligned}
 x_{k+1} &= -0.1 + 0.2x_k + 0.1x_k^2 + 0.8y_k + 0.7z_k + -0.5\sin\left(\frac{\pi t}{8}\right) \\
 y_{k+1} &= x_k \\
 z_{k+1} &= y_k
 \end{aligned}
 \tag{2.5}$$

is iterated with the attractor being displayed for successive times given by  $t \bmod 16$ .

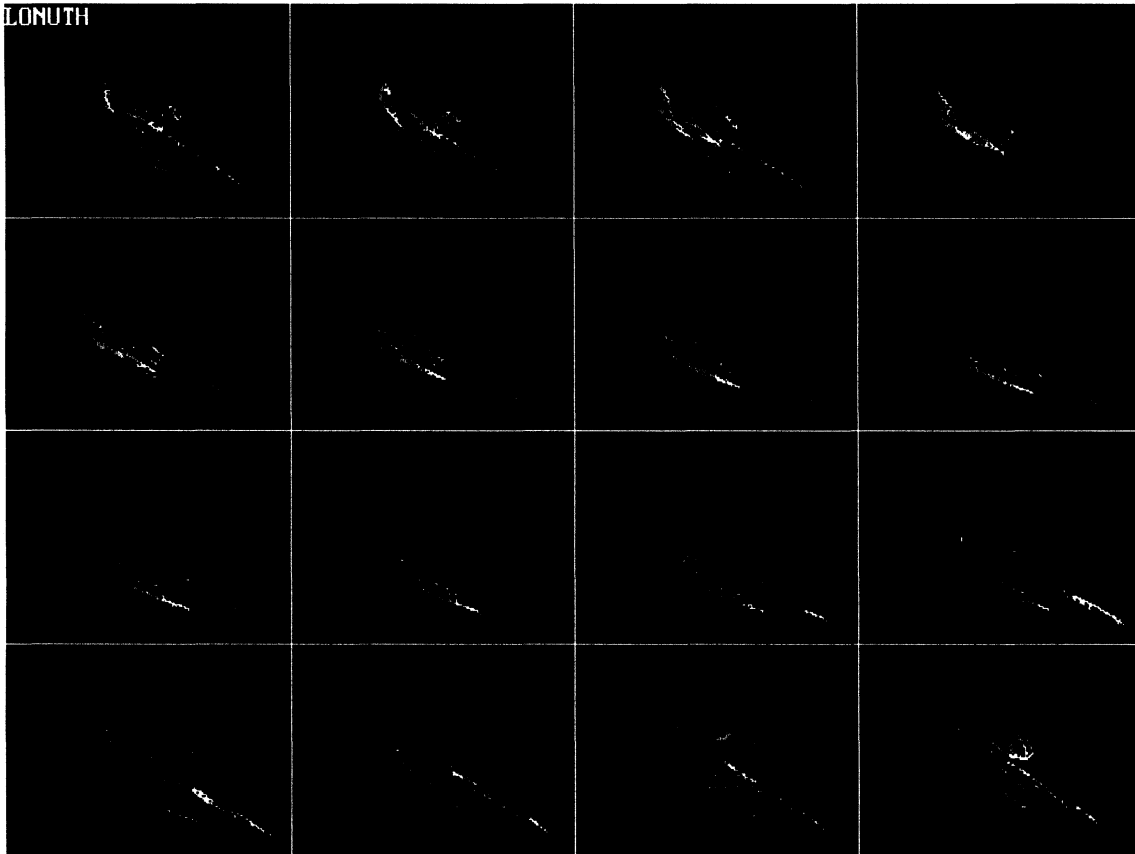


Figure 2.8 - The stretching and folding of a strange attractor.

## 2.5 Lyapunov or Characteristic Exponents

Chaotic systems are characterised by the exponential divergence of 'close' trajectories. Lyapunov exponents (or characteristic exponents) may be considered a measure of this divergence. Lyapunov exponents quantify the rate at which a small perturbation to the system will vary, either increase or decrease, that is the average

exponential rates of divergence or convergence of nearby orbits in phase space. The following description, after Kugiumtzis et al. (1994), defines Lyapunov exponents in a non-rigorous manner and allows one to visualise their computation using local Jacobians (local linearization) :

Lyapunov exponents are defined as the logarithms of the absolute value of the eigenvalues of the linearized dynamics averaged over the attractor.

This concept is formalised in Section 2.5.1.

In order to estimate the Lyapunov exponents we resort to statistics and assume the existence of an ergodic probability measure on the attractor. Ruelle (1989, p. 38), gives the following definition :

*Ergodicity.* An invariant probability measure  $\rho$  is *ergodic* or *indecomposable* if it does not have a nontrivial convex decomposition :

$$\rho = \alpha\rho_1 + (1 - \alpha)\rho_2 \text{ with } \alpha \in ]0,1[ \tag{2.6}$$

where  $\rho_1$  and  $\rho_2$  are again invariant probability measures and  $\rho_1 \neq \rho_2$ .

It does not make sense to say that  $f^t$  is ergodic if it is not stated with regards to what measure  $\rho$ . If  $f^t$  is a dissipative system, one has to specify which ergodic measure  $\rho$  one considers (Ruelle, 1989). Ruelle (1989, p. 44), clarifies this for Lyapunov exponents:

In general, it is exceptional that an attractor carries only one ergodic invariant measure  $\rho$ . In typical cases there are uncountably many distinct ergodic measures. Nevertheless, as we have already mentioned in part I, in physical experiment and in computer simulations it seems that one invariant probability measure  $\rho$  is produced more or less automatically by the time that the system spends in various part of the space  $M$ . Thus, there is a selection process of the so-called *physical measure*  $\rho$ .

The advantage of the ergodic approach lies in the fact that there are important theorems which apply to *all* ergodic measures, and we do not have to worry immediately about which ergodic measure is physical. (Furthermore, as noted earlier, there are always *some* ergodic measures on a compact invariant set.)

.....

However, many important results of ergodic theory hold for an arbitrary invariant measure  $\rho$ . This is the case, for example, of the existence of characteristic exponents.

It is important to note that in the statistical analysis of time series we deal directly with time averages. Statistical analysis of chaos does not have very much to do with the ergodic problem. It focuses its attention on invariant measures carried by attractors, which are *assumed* to be ergodic (Ruelle, 1989).

Consider a discrete time evolution equation

$$x(n+1) = f(x(n)), \quad x(i) \in R, \quad 2.7$$

and the rate at which nearby orbits are separated. The average rate of growth may be defined as the number

$$\lambda = \lim_{n \rightarrow \infty} \frac{1}{n} \log |D_{x(0)} f^n \delta x(0)|, \quad 2.8$$

where  $Df^n$  is the derivative of  $f$  composed with itself  $n$  times (Ruelle, 1989). In the special case of a one-dimensional map there is a single Lyapunov exponent given by Equation 2.8. Existence of the limit in Equation 2.8 is guaranteed by the ergodic theorem. The existence of this limit can be extended to higher dimensions than 1. This is guaranteed by a generalisation of the ergodic theorem to products of matrices; the multiplicative ergodic theorem of Oseledec (Ruelle, 1989). This theorem is stated as it leads to the formal definition of Lyapunov exponents.

### 2.5.1 The Multiplicative Ergodic Theorem of Oseledec

This section follows Eckmann and Ruelle, (1985) :

*Theorem* Let  $\rho$  be a probability measure on a space  $M$ , and  $f: M \rightarrow M$  a measure preserving map such that  $\rho$  is ergodic. Let also  $T: M \rightarrow m \times m$  matrices be a measurable map such that

$$\int \rho(dx) \log^+ \|T(x)\| < \infty, \quad 2.9$$

where  $\log^+ u = \max(0, \log u)$ .

Define the matrix  $T_x^n = T(f^{n-1}x) \cdots T(fx)T(x)$ . Then, for  $\rho$ -almost all  $x$  the following limit exists:

$$\lim_{n \rightarrow \infty} \sqrt[n]{T_x^{n*} T_x^n} = \Lambda_x \quad 2.10$$

where  $T_x^{n*}$  represents the adjoint of  $T_x^n$ .

The logarithms of the eigenvalues of  $\Lambda_x$  are called *characteristic exponents* (*Lyapunov exponents*). They are denoted by  $\lambda_1 \geq \lambda_2 \geq \dots$ . They are almost everywhere constant if  $\rho$  is ergodic. Let  $\lambda^{(1)} > \lambda^{(2)} > \dots$  be the characteristic exponents no longer repeated by multiplicity; we call  $m^{(i)}$  the multiplicity of  $\lambda^{(i)}$ . Let  $E_x^{(i)}$  be the subspace of  $\mathbf{R}^m$  corresponding to the eigenvalues  $\leq \exp \lambda^{(i)}$  of  $\Lambda_x$ . Then  $\mathbf{R}^m = E_x^{(1)} \supset E_x^{(2)} \supset \dots$  and the following holds

*Theorem.* For  $\rho$ -almost all  $x$ ,

$$\lim_{n \rightarrow \infty} \frac{1}{n} \log \|T_x^n u\| = \lambda^{(i)} \quad 2.11$$

if  $u \in E_x^{(i)} \setminus E_x^{(i+1)}$ . In particular, for all vectors  $u$  that are not in the subspace  $E_x^{(2)}$  (viz., almost all  $u$ ), the limit is the largest characteristic exponent  $\lambda^{(1)}$ .

Under certain circumstances it is necessary to extend the above theorems, this is noted by Ruelle (1989, p. 47) :

In some physical applications, like those concerning hydrodynamical systems, we shall need a version of these theorems where  $\mathbf{R}^m$  is replaced by an infinite-dimensional space, like a Banach space or a Hilbert space  $E$  and the  $T(x)$  are bounded operators.

Ruelle (1989) proceeds to show that the theory extends without difficult for certain classes of systems.



## 2.5.2 The Spectrum of Lyapunov Exponents

The spectrum of the Lyapunov exponents is useful as an indicator of the type of system being described. Using a notation developed by Crutchfield (noted by Ruelle, (1989)) we can describe the following systems in three-dimensional space :

Attracting fixed point       $(-, -, -)$

Attracting limit cycle       $(0, -, -)$

Quasiperiodic attractor       $(0, 0, -)$

Strange attractor       $(+, 0, -)$

In three-dimensional space there are three Lyapunov exponents; these may each be described as +, 0, or -. The above notation represents the three Lyapunov exponents in decreasing order of magnitude. The existence of at least one positive Lyapunov exponent is often taken to indicate chaos in systems which are bounded. Gao and Zheng (1994) show that the existence of a positive exponent alone is not sufficient to justify an underlying strange attractor. In fact they provide an argument that leads to the conclusion that white noise will produce a positive exponent, the size of which can be varied arbitrarily given a sufficiently large data set.

Ruelle (1987, p. 56), makes the following notes :

For a discrete time system with  $t \geq 0$ , chaos may occur in *one* (or more) dimension(s).

.....

In the case of a diffeomorphism, i.e. for a discrete time dynamical system where  $t$  may be negative as well as positive, chaos occurs only in *two* (or more) dimensions.

.....

For a continuous time dynamical system (i.e. a flow) chaos occurs only in *three* (or more) dimensions.

For a flow there must be at least one local Lyapunov exponent that is zero when the system is chaotic (Abarbanel, 1996). Local Lyapunov exponents are a measure of the divergence (or contraction) at a point in phase space.

In a continuous four-dimensional dissipative system there are three possible types of strange attractors, (+, +, 0, -), (+, 0, 0, -) and (+, 0, -, -). Changes in the system's parameters will generally change the Lyapunov spectrum and may also change the type of attractor (Wolf et al., 1985).

Returning to the sensitive dependence, we note that the magnitudes of the Lyapunov exponents quantify the dynamics of an attractor in information theory terms. They provide a measure for the rate at which the system processes information, that is, the rate at which information is created or destroyed. This leads to the exponents being expressed in (bits of information)/s or bits/orbit for continuous systems and bits/iteration for discrete systems. The exponents are not always expressed in this form in the literature. In order to illustrate this concept as well as that of sensitive dependence consider the Lorenz (1963) attractor. Three equations define the system

$$\begin{aligned}\dot{X} &= \sigma(Y - X) \\ \dot{Y} &= X(R - Z) - Y \\ \dot{Z} &= XY - bZ\end{aligned}\tag{2.12}$$

Selecting the parameters to be  $\sigma = 16.0$ ,  $R = 45.92$  and  $b = 4.0$  results in a positive Lyapunov exponent of  $2.16 \text{ bits/s}$ . Specifying an initial point to a given accuracy determines the time for which predictions can be made. Using the Lorenz system with parameters as above and specifying an initial point with an accuracy of 20 bits (1 part per million), we cannot predict further than  $20 \text{ bits} / (2.16 \text{ bits/s})$ , or about 9s. Any

uncertainty in the initial point will essentially cover the entire attractor after this time, reflecting 20 bits of new information that can be gained from an additional measurement of the system (Wolf et al., 1985).

For a detailed treatment of this subject see Eckmann and Ruelle (1985) and Ruelle (1989).

## 2.6 Correlation Dimension

A second property which is often used to quantify chaos is the correlation dimension. Correlation dimension is a characteristic measure of strange attractors (Grassberger and Procaccia, 1983). Before proceeding with a discussion of the correlation dimension a more general approach to the concept of dimension is taken. Let us introduce the definitions of several 'dimensions'. The definitions in Sections 2.6.1, 2.6.2 and 2.6.3 are taken from the *Mathematics Dictionary* (1992, p.123).

### 2.6.1 Dimension

Refers to those properties called length, area, and volume. A configuration having length only is said to be of one dimension; area and not volume, two dimensions; volume, three dimensions. A geometric configuration is of dimension  $n$  if  $n$  is the least number of real valued parameters which can be used to (continuously) determine the points of the configuration; *i.e.*, if there are  $n$  degrees of freedom, or the configuration is (locally) topologically equivalent to a subspace of  $n$ -dimensional Euclidean space.

For more general sets of points it is necessary to use a different definition of dimension. Two of these are the fractal (or Mandelbrot) dimension and the Hausdorff (or Hausdorff-Besicovitch) dimension.

### 2.6.2 Fractal (or Mandelbrot) dimension

Let  $X$  be a metric space. For each positive number  $\varepsilon$ , let  $N(X, \varepsilon)$  be the least positive integer  $M$  for which there are  $M$  balls of radius less than  $\varepsilon$  whose union contains  $X$ . Then the fractal dimension of  $X$  is

$$D_f = \lim_{\varepsilon \rightarrow 0} \frac{\log N(X, \varepsilon)}{\log 1/\varepsilon}, \quad 2.13$$

which is also the greatest lower bound of positive numbers  $d$  such that

$$\limsup_{\varepsilon \rightarrow 0} \varepsilon^d N(X, \varepsilon) = 0.$$

If  $X$  is a fractal that can be divided into  $N$  congruent subsets each of which can be made congruent to  $X$  by magnifying it by a factor of  $r$ , then the fractal dimension of  $X$  is equal to

$$D_f = \frac{\log N}{\log r}. \quad 2.14$$

An example is the Cantor set which has a fractal dimension of  $(\log 2)/(\log 3)$ .

### 2.6.3 Hausdorff (or Hausdorff-Besicovitch) dimension

Let  $X$  be a metric space. For positive numbers  $\varepsilon$  and  $p$ , define  $m_p^\varepsilon(X)$  to be the greatest lower bound of

$$\sum_{k=1}^{\infty} [\text{diameter of } A_k]^p \quad 2.15$$

where  $\cup_{k=1}^{\infty} A_k = X$  and the diameter of each  $A_k$  is less than  $\varepsilon$ . If  $X$  is compact, one need use only finitely many such  $A_k$ . Now define

$$m_p(X) = \lim_{\varepsilon \rightarrow 0} m_p^\varepsilon(X). \quad 2.16$$

The Hausdorff dimension of  $X$  is the greatest lower bound of all  $p$  for which  $m_p(X) = 0$ , or equivalently, the least upper bound of all  $p$  for which  $m_p(X) = \infty$ , that is

$$D_h = \liminf_{\varepsilon \rightarrow 0} \{m_p^\varepsilon(X) = 0\} = \limsup_{\varepsilon \rightarrow 0} \{m_p^\varepsilon(X) = +\infty\} \quad 2.17$$

An example is the Cantor set which has Hausdorff dimension of  $(\log 2)/(\log 3)$ . For any metric space the Hausdorff dimension is less than or equal to the fractal dimension. The quantity  $m^\varepsilon(X) = \lim_{\rho \rightarrow \infty} m_\rho^\varepsilon(X)$  is known as the Hausdorff measure in dimension  $\varepsilon$ .

Some confusion exists in the literature regarding the names used for the above dimensions. The fractal dimension is also the *capacity* in Kolmogorov terminology. Further, Mandelbrot introduced the phrase *fractal dimension* to denote the Hausdorff dimension (Ruelle, 1989). Here fractal dimension is taken to mean the capacity in Kolmogorov terminology and the Hausdorff dimension is referred to as such. Further, different authors start with differing concepts regarding the geometrical shape used to cover the attractor. Here 'balls' are used, following the *Mathematics Dictionary* (1992), however, some authors in the literature, Grassberger and Procaccia (1983), Kugiumtzis et al. (1994) use hypercubes of a given dimension and side length.

#### 2.6.4 Correlation dimension

The fractal dimension takes only the geometrical structure of the attractor into account. No consideration is given to the *distribution* of points on the attractor. This has the disadvantage that all balls count the same irrespective of the frequencies with which they are visited, possibly even developing singularities (Grassberger and Procaccia, 1983). The *information dimension* is one measure which accounts for this. It can be described as the minimum information necessary to specify a point in a set to a given accuracy. Let us introduce a probability measure  $\rho$  carried by the attractor. The information dimension may then be defined as the minimum Hausdorff dimension of the sets  $X$  for which  $\rho(X)=1$  (Ruelle, 1989). Following Kugiumtzis et al. (1994) the information may be measured by

$$S(\varepsilon) = \sum_{i=1}^M \rho_i \log \rho_i \tag{2.18}$$

where  $\rho_i$  is the probability of a point being in the  $i$ th set defined as  $\rho_i = \mu_i/N$ ,  $N \rightarrow \infty$  and  $\mu_i$  is the number of points in the  $i$ th set, and  $\varepsilon$  is the required accuracy.  $M$  is, as defined above, the least integer number of balls required to cover the attractor. The information dimension is then given by

$$\sigma = \lim_{\varepsilon \rightarrow 0} \frac{-S(\varepsilon)}{\log \varepsilon}. \quad 2.19$$

Finally we arrive at the *correlation dimension*, which may be thought of as a simplification of the information dimension. The correlation dimension was first defined by Grassberger and Procaccia (1983). Their arguments are followed here with some changes to terminology to remain consistent with the preceding material. This measure is obtained from the correlations between random points on the attractor. Consider the set  $\{X_i, i = 1 \dots N\}$  of points on an attractor obtained from a time series. Then

$$X_i \equiv X(t + i\tau) \quad 2.20$$

where  $\tau$  is a fixed time increment between successive measurements. Since trajectories diverge exponentially most pairs of points on the attractor,  $(X_i, X_j), i \neq j$  will be *dynamically* (temporally) uncorrelated pairs of essentially random points. Since trajectories are constrained to the finite region of the attractor they will be spatially correlated. This spatial correlation is defined as

$$C(l) = \lim_{N \rightarrow \infty} \frac{1}{N^2} \times \left\{ \text{number of pairs } (i, j) \text{ whose distance } |X_i - X_j| < l \right\}. \quad 2.21$$

Grassberger and Procaccia (1983) proceed in their paper to establish that for small  $l$ 's,  $C(l)$  grows like a power  $C(l) \sim l^\nu$  where  $\nu$  is the correlation dimension. The correlation dimension may be computed from

$$v = \lim_{l \rightarrow 0} \frac{\log \langle \mu_l \rangle_x}{\log l} \quad 2.22$$

where  $\mu_l$  is the number of points in the  $l$ th set for a ball with centre  $x$  and  $\langle \bullet \rangle_x$  denotes the average over all points  $x$ . It can also be argued that the correlation dimension provides an estimate of other dimensions as the following relationship holds in general

$$v \leq \sigma \leq D_f . \quad 2.23$$

The advantage of the correlation dimension over others is its simplicity of computation while still providing a useful indicator.

## 2.7 Reconstruction of the Attractor

Section 2.5.2 discusses the minimum dimensions under which chaos may occur. Often only a single variable is observed. It is therefore necessary to reconstruct a higher dimensional space in order to investigate the behaviour of the system.

Several algorithms have been developed to differentiate between stochastic and deterministic systems which display chaotic behaviour, using different quantities to characterise chaos. In particular, these algorithms concentrate on the ability to differentiate when only a single variable from the system has been observed over a time period, i.e., when a single variable time series is available. These algorithms almost universally use reconstruction of the attractor, also referred to as phase space reconstruction, as the first step. By reconstruction we imply that the attractor can be characterised; at least its ‘nature’ can be if not its exact form. In particular we wish to preserve the evolution in time of the unknown dynamics (Abarbanel, 1996). Reconstruction using time derivatives is often difficult or impossible and an alternate approach using time delays is used. The reconstructed attractor is often referred to in the

literature as a delay portrait. Casti (1992, p. 311) states that, “...we will obtain a manifold having the same geometrical properties as the original phase portrait.”

More specifically let us denote a time series which represents a discrete scalar observation of a chaotic time series by  $x(t)$ . Note that the system function  $f$ , the attractor dimension  $d$  and the measurement function  $h$  are unknown. We now seek an *embedding* space in which we can reconstruct the attractor in such a manner that the invariant measures are preserved. The simplest method of achieving this reconstruction is by the method of *delay co-ordinates* or *time delays* proposed by Ruelle and noted by Packard et al. (1980). Let  $k = 1, \dots, m$  from which we generate scalar signals  $x_k(t)$  such that

$$x_k(t) = x(t + (k - 1)\tau) \quad 2.24$$

where  $\tau$ , called the *time delay*, is an integer multiple of the sample interval for continuous systems or the time interval for discrete systems. This leads directly to an  $m$  dimensional signal represented by

$$\mathbf{x}(t) = \begin{pmatrix} x(t) \\ x(t + \tau) \\ \vdots \\ x(t + (m - 1)\tau) \end{pmatrix}. \quad 2.25$$

Takens's theorem guarantees that for an infinite noise free data series one can almost always find an embedding dimension  $m$  preserving the invariant measures. He further proves that it is sufficient that  $m \geq 2d + 1$  (Takens, 1981). This latter condition is sufficient but not necessary and in practice an attractor may be successfully restored with an embedding dimension as low as  $d$  (Kugiumtzis et al., 1994).

In theory the actual values for the time delay and the sample interval are irrelevant; in practice, however, this is not the case (Kugiumtzis et al., 1994). The sample interval is



often restricted or defined by practical considerations. Ideally the sample interval should be sufficiently dense to reveal the structure but not overly dense so as to impose too high a computational load. It has been suggested by Wolf et al. (1985) that around 12 points per mean orbital period is ideal, and that the number of orbits sampled should never be sacrificed for an increase in the number of samples per orbit. Selection of the time delay can be achieved by several methods, however, it is important that the researcher establish the stability of the recovered solutions by varying the time delay. If such stability cannot be demonstrated then the solution must be brought into question. What one wishes to achieve by the choice of time delays is summarised by Abarbanel (1996) as :

- i) It must be some multiple of the sampling time.
- ii) If the time delay is too short the coordinates  $x(t)$  and  $x(t + \tau)$  will not be sufficiently independent.
- iii) Due to the sensitivity of chaotic systems to initial conditions  $x(t)$  and  $x(t + \tau)$  are numerically tantamount to being random with respect to each other if the time delay is too long.

This is not a precise requirement. It is therefore necessary to use a prescription. Two such prescriptions that have been used are (Abarbanel, 1996):

- i) The first zero of the linear autocorrelation function, Equation 2.2.
- ii) The first minimum of the average mutual information.

Only the autocorrelation function was used by the author. The interested reader is referred to Abarbanel (1996) for a description of the average mutual information.

Selection of the embedding dimension is often required with no *a priori* information about the dimension of the original system. What we are seeking is an embedding dimension which unfolds observed orbits from self overlaps due to projecting the attractor onto a too low dimensional space. If we measure two quantities  $x_a(t)$  and  $x_b(t)$

from the same system, there is no guarantee that the embedding dimension will be the same for each quantity (Abarbanel, 1996). Since the only systems that are of interest are low-dimensional systems it is feasible to use increasing embedding dimensions. These may then be tested using global false nearest neighbours to ascertain when the attractor has been unfolded. Global false nearest neighbours were not used in this work and the reader is referred to Abarbanel (1996) for an understanding of this technique.

It is also feasible to test the estimated measures (largest Lyapunov exponent and correlation dimension) for stationarity, in fact it is advisable to do so (Wolf et al., 1984). Too high an embedding dimension will not affect the reconstruction adversely for noise free data, however, it is desirable to identify the lowest meaningful embedding dimension. If the embedding dimension used is too high for noisy data, the effect is an unnecessary contamination of the data (Wolf et al., 1984). Too low an embedding dimension will result in a reconstruction which fails to unfold the attractor. This means that the estimates will stabilise above a certain embedding dimension. The lowest of these may then be adopted (Rosenstein et al., 1992). It should be noted that the amount of data required to successfully reconstruct an attractor increases exponentially with the dimension, however, this is largely dependant on the quality of the data (Eckmann and Ruelle, 1992).

In order to demonstrate the technique we return to the Hénon attractor (Equation 2.3). A single time series, in this case  $x_1(k)$ , is extracted and the attractor reconstructed. The reconstructed attractor is shown in Figure 2.9. As the system is well known and the data are virtually free from noise, the stability of the solution is not tested. The geometrical nature of the attractor is clearly visible in the reconstructed attractor. A time delay of one sample interval is used.

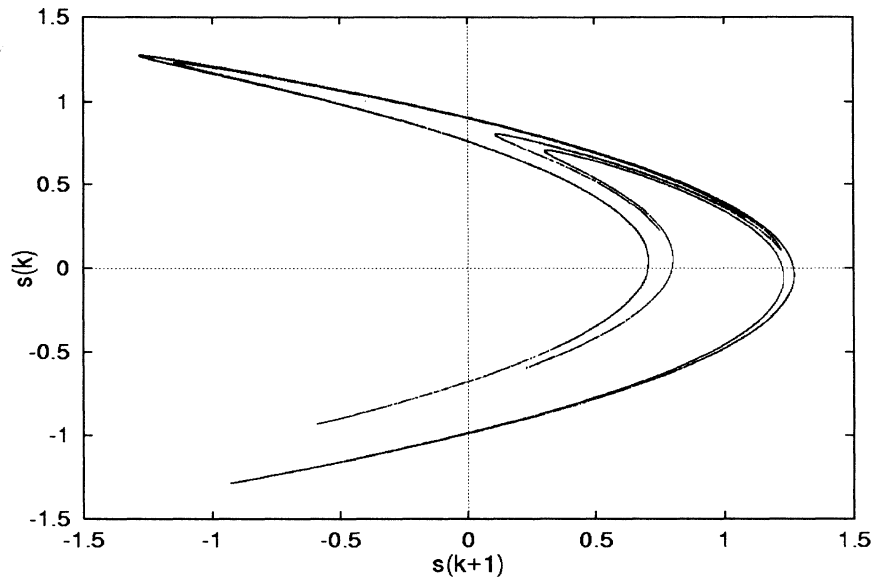


Figure 2.9 - Reconstructed Hénon attractor.

Since the above example is an iterated map and a discrete time system the question of whether an attractor generated by a flow can be recovered is raised. In order to offer the reader some confidence, but not a rigorous proof, let us consider the Lorenz attractor, as given in Equation 2.12. Using a single variable  $X(t)$ , a time delay of one sample, and an embedding dimension of 3, Figure 2.10 was generated. An interval of 0.01 was used to generate the time series and represents the sample interval. It is evident that the reconstructed attractor has some geometrical structure and does not comprise random data. The fractal dimension of the Lorenz system is  $\approx 2.06$ . This would lead us to anticipate an embedding dimension of 5 to unfold the attractor. Using  $X(t)$  we find that an embedding dimension of 3 is sufficient (Abarbanel, 1996).

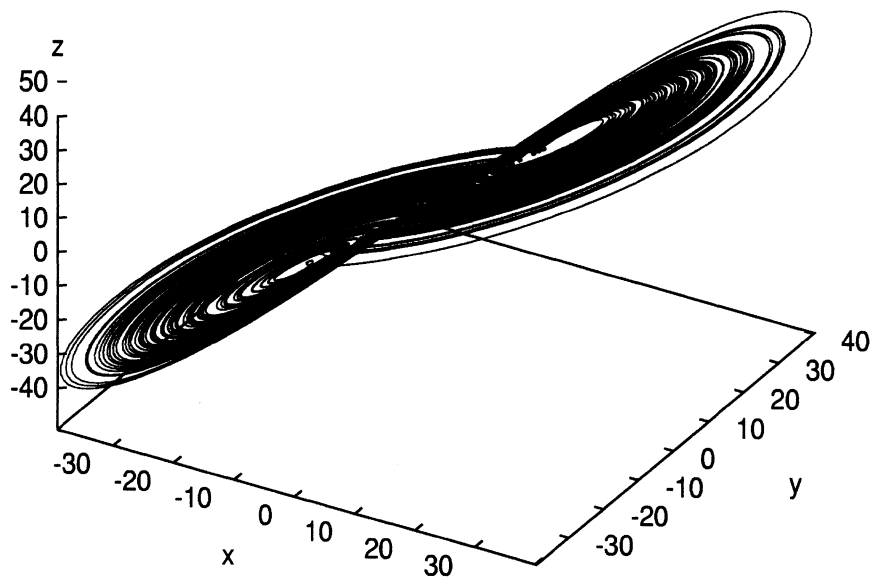


Figure 2.10 - Reconstructed Lorenz attractor.

## Chapter 3

### Tides, the Data and Removal of Periodic Components

#### 3.1. Introduction

Section 3.2 introduces tidal theory and water level variations. A postulate is made as to why water level variations are a likely candidate to contain a chaotic component. The remaining sections discuss the actual data used, removal of periodic components and data requirements. Reasons for wishing to remove the periodic component are discussed in Section 3.3.

To extract information from a time series in order to reconstruct an attractor and to estimate ergodic measures of probability, there have been a number of estimates regarding the length of the required time series. Irrespective of which algorithm is being used, the longer the data series the higher the probability that the correct solution, or at least a repeatable one, is extracted. Since chaos theory is still relatively young, algorithms concentrate on extracting the correct information using ideal data sets rather than the treatment of irregularly sampled data or data sets with gaps.

It was with the constraints of

- a) no gaps, and
- b) as long a continuous data set as possible,

that the start and end points were selected. These requirements are discussed in more detail in Section 3.5.

The water level data supplied extended from 1/1/1947 to 31/12/1992 but contained a number of gaps. The data were sampled every hour. Gunaratne (1994) identified the gaps

in the data. Using his work the longest, continuous data set was identified. This was initially used but later shortened to data starting from 1/1/1947 and extending for 30 000 samples. Reasons for this are discussed in Section 3.5.4. The relevant data were extracted, the headers removed and a pseudo time stamp, incrementing by 1 for each observation, was added. This was reformatted to a sequential ASCII file (an extract is given in Appendix A) and the mean subtracted to yield a zero mean time series.

### 3.2. Tides

Tides should be considered a combined or integrated response to a variety of natural phenomena (Thompson, 1981). Figure 3.1 illustrates some of the major interactions. The tidal phenomenon is purely periodic (Vaníček and Krakiwsky, 1986). Water levels represent a combination of the tidal phenomenon and non-astronomic elements which may or may not be periodic.

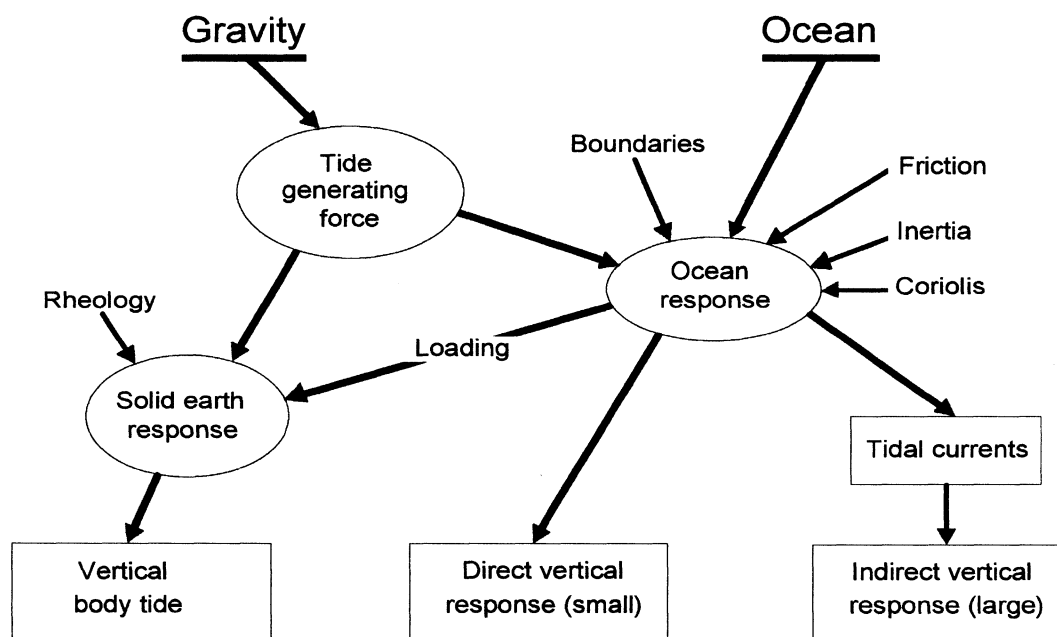


Figure 3.1 - Gravity and the ocean. Some of the influences and relationships which complicate the tidal phenomenon (after Wells, 1993).

The predictability of contributing elements is considered and reasons why certain elements are considered likely candidates for a chaotic system postulated.

### **3.2.1. Equilibrium Theory of Tides**

In 1687 Sir Isaac Newton published his *Equilibrium Theory of Tides*. This is the simplest of the tidal models and assumes an equilibrium state. The assumption requires that the earth be covered with water of uniform density to a uniform depth, has a uniform atmosphere, no inertia and is not rotating (Wells, 1993).

The single most important factor in producing tides is the combined gravitational attraction of the moon and sun on the earth. Detailed accounts of how the gravitational attractions of the three bodies combine to produce the tide generating force are given in Pugh (1996), Thompson (1981) and Wells (1993). This represents the equilibrium theory, also known as the astronomic or gravitation tide theory. In this work it is of interest to understand which features are explained by the theory and what limitations exist.

The notion of an equilibrium tide is a useful concept to account for the fundamental nature of tidal fluctuations (Thompson, 1981). Some of the characteristics and complexities that can be explained are:

- a) Daily and diurnal tides due to the earth's rotation.
- b) Declinational-type tides which cause the diurnal inequality as well as constituting one reason for the biweekly tidal cycle.
- c) Synodic-type tides which result in the quasi-biweekly tidal cycle of spring and neap tides. This is related to the phases of the moon which has a period of approximately 15 days, hence quasi-biweekly. It should be noted that there is a

variability in the periods associated with synodic-type tides. These variations result from the orientation of the moon's elliptical orbit to the earth and sun. Figure 3.2 illustrates this variation. Due to the eccentricity of the orbit, the moon travels slowest at apogee (point A) and fastest at perigee (point P). In travelling from apogee to perigee and back the speed of the moon will vary, however, the time taken to travel from A to P will equal the time taken to travel from P to A. The time taken is 14 days, 18 h, 22 min and represents half a synodic month (29.5 days). In the upper part of Figure 3.2 this represents the time taken to transition from full moon to new moon and back due to the sun lying along the direction AP. Consider now the situation where the sun lies along the direction DC. The time to transition from full moon (point D) to new moon (point C) is 13 days, 22 h, 32 min while the transition from new moon (point C) back to full moon (point D) requires 15 days, 14 h, 12 min (Thompson, 1981).

- d) Anomalistic-type tides resulting from the eccentricity of the moon's orbit. The eccentricity results in the moon being closer to the earth at perigee and consequently influencing the tide more at perigee. These variations have a period of 27.5 days.
- e) Bi-annual changes due to the varying declination of the sun.
- f) Annual variation due to the eccentricity of the earth's orbit around the sun.
- g) An 18.6 year period results from the precession of the intersection of the orbital planes of the moon and earth. Moon's precession of node.
- h) The moon's precession of perigee results in an 8.85 year period.



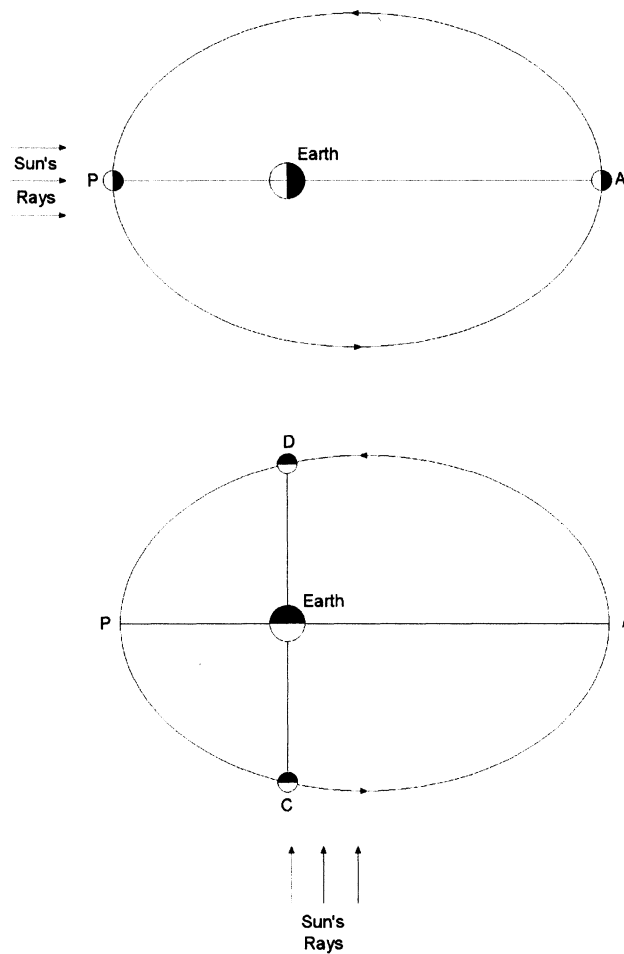


Figure 3.2 - The eccentricity (exaggerated) of the moon's orbit and the relative position of the sun to the orbit (after Thompson, 1981).

Factors which are not accounted for by the equilibrium theory include, but are not limited to.

- a) Friction between the water and the ocean bottom.
- b) Inertia of the water mass.
- c) Coriolis force.
- d) Continents interrupt the passage of the tidal wave (or tidal bulge) as it travels around the globe every 24 hours. In addition the effects of irregular coasts and continental shelves need to be accounted for.

- e) The configuration of ocean basins. These introduce resonance and amplification effects.
- f) To support long wavelength propagation it is necessary for the water depth to be greater than half the wavelength. The average depth of the oceans is only a few kilometres while the semidiurnal equilibrium tide has a wavelength of half the earth's circumference, or greater than the earth's radius. For a shallow water wave the requirement is a uniform depth of 20 km (Wells, 1993).

### **3.2.2. Dynamic Tide Theory**

Any theory which wishes to approximate reality must include non astronomic factors such as those listed in a) to f) in Section 3.2.1. The first step towards such a dynamic tide theory was taken by Laplace in 1775, about one hundred years after Newton formed the equilibrium theory. There is still not a complete dynamic theory. Detailed development of aspects of the dynamic theory may be found in Wells (1993) and Pugh (1996).

The dynamic theory results in a set of differential equations. Solution of these equations is difficult and simplifications are required. Laplace was the first to undertake this. He made considerable simplifications. A result of his work was a set of three equations which are known as the Laplace Tidal Equations (LTE). These have formed the starting point for the development of tidal theories for the past two hundred years.

### **3.2.3. Chaos in the water level measurements**

Clearly there is a significant portion of the water level signal which is periodic. Periodic components are largely the result of astronomic elements but may also result from natural frequencies within basins. The equilibrium theory gives us a global characterisation while the dynamic theory takes into account more specific effects.

Schwiderski (1981) is arguably the most successful at applying the dynamic theory. This is achieved by quantifying the Laplace tidal equations as fully as possible.

Since the most significant portion of the water level variation is periodic and predictable, good approximations can be obtained in general. These models then allow for long term prediction with considerable accuracy. In an area such as the Bay of Fundy the tides are amplified and predictions, using periodic models, do not produce the same quality of results. Carrera (1995) analysed water level differences derived from the observed and predicted values for a number of stations including St John, New Brunswick. Carrera (1995, p. 4) makes the following observation.

The same vertical and horizontal scales were used in all plots to facilitate their comparison. However, in at least one instance, St John, NB, difference values fall outside the plotted area. The difference values are so large in this case that the vertical scale needed to display them would have made it impossible to portray meaningfully the output from all other ports.

It is postulated that these large discrepancies are the result of non-periodic effects in the water level being amplified due to the unique nature of the basin. The non-periodic effects are known to be caused, at least partially, by the influence of natural systems. Some of the non-periodic elements are :

- a) Air pressure results in an inverse barometer effect. This has a seasonal variation as the mean air pressure varies between summer and winter as well as short term variations.
- b) Seasonal changes in water temperature result in variations in the water density. These are known as steric effects.
- c) Piling up or draining of water due to prevailing winds. During storms, surges of this nature are often significant.
- d) Non-linearities in the measuring apparatus.

Identification of chaos in a number of systems that have an effect on water level have been claimed, for example in meteorology (Cuomo et al., 1993), in earthquake predictions (Ouchi, 1993) and in oceanography (Yan, 1993). The author believes that the possibility exists for such chaotic signals to propagate into the water level signal.

Further the dynamic tidal theory uses a system of differential equations to represent tides. For certain parameters such systems may exhibit chaotic behaviour. The possibility that the boundary conditions in the Bay of Fundy provide such a set of parameters cannot be discarded.

Fang and Cao (1995) discuss the difference between structure invariant systems, ones in which all the parameters are fixed, and structure variable systems, where not all parameters are fixed. It is arguable that many natural systems fall into the latter class. Ricard and Bascompt (1993) discuss the problem of transients in natural systems, that is the possibility of systems evolving from one attractor to another. Further, the possibility of chaotic motion shown by spatially extended systems is discussed. The implication of this is that the data sets are not sufficiently long to identify a particular attractor using Lyapunov exponents or correlation dimensions. Alternatively, computations are blurred across attractors. The analysis performed in this study does not take these possibilities into account.

During the course of this investigation it came to the author's attention that identification of chaos in tides is being claimed by (Frison, 1997a) and (Frison, 1997b). Baltimore and other stations in the Chesapeake Bay have been examined by Frison (1997a). Frison (1997c) claims that a predictor based on non-linear dynamics that they have developed is better than the US government approved predictor (a harmonic model).

### **3.3. Removal of Periodic Components**

The most commonly used tidal predictions are based on a harmonic analysis of the data, using frequencies related to astronomical constituents. It is widely acknowledged that this accounts for the majority of the regular or periodic components in the data. Which constituents are used to describe a particular tide is partly based on the amount of data and the quality of the data available. A general rule that has been applied in many cases is the Rayleigh criteria (Pugh, 1996). This requires that the constituents be separated from their neighbouring constituents by at least one full period over the length of the data. Using this criteria, a series of length 30 000 hours and a 12 hour period it is possible to separate neighbours further than approximately 0.005 hours away. No attempt was made to identify periods this finely.

In addition to astronomic constituents, it is usual to include shallow water terms when making shallow water predictions. Shallow water components represented as periodic constituents provide a useful approximation of the effects but do not fully model such phenomena.

Further, it is possible that periodic components due to other phenomena, such as resonance, may exist.

In order to improve the probability of the Lyapunov exponent algorithm's success it is desirable to have an attractor which is as densely covered by the trajectories as possible. When the attractor contains periodic components it may result in trajectories from a chaotic signal being spatially separated. Using the algorithms presented in Chapters 4 and 5 it is readily seen that this will adversely affect the chances of success. By removing the periodic components the volume of the attractor is reduced and the

density of the trajectories increased. It is for these reasons that the periodic components are removed from the water level signal prior to analysis.

Removal of the periodic component of the water level series results in a 'residual' series, often referred to as the meteorological surge component (Pugh, 1996). More formally, this may be expressed as

$$\mathbf{X}(t) = Z_0(t) + \mathbf{T}(t) + \mathbf{S}(t) \quad 3.1$$

where  $\mathbf{X}(t)$  represents the observed level,  $Z_0(t)$  is the relationship between chart datum and mean sea level,  $\mathbf{T}(t)$  is the periodic portion of the signal, and  $\mathbf{S}(t)$  is the meteorological surge component. In this work  $\mathbf{T}(t)$  is not restricted to only astronomical components.

Several methods were considered for the removal of the periodic components including :

- a) Application of the existing tidal analysis or 'Blue Book' data.
- b) Digital filtering techniques using an application package such as Matlab.
- c) A spectral analysis with associated removal of components based on the UNB least-squares approach.

It rapidly became apparent that the last approach was the most suitable one of the above and this was then adopted and used. Since the data had been analysed previously using this tool by Gunaratne (1994) his results were used as a starting point. It should be noted that he analysed the whole data series. This meant that he was using a 'gappy' data series as well as one which spanned alterations made to the recording gauge. Alterations made to the tide gauge include extension of the inlet to the stilling well. Such changes

will affect the nature of the signal by altering the damping. It is believed that the tide gauge was not altered during the period used for this study. Consequently the results obtained by Gunaratne (1994) were found to be less than ideal and further analysis was performed.

### **3.4. Least-Squares Spectral Analysis (LSSA)**

This method along with the associated software is well described by Wells et al. (1985). The interested reader is invited to pursue the subject in the above reference. An application of the method is described here.

Since the source code is freely available at the University of New Brunswick it was modified and compiled to run on an IBM compatible PC. Due to the length of the data series it was necessary to increase the size of many of the arrays. The result was source code which would not compile and run under DOS. In order to work around this as well as allowing for multiple runs to be executed simultaneously a PC running OS/2 was used. The software was compiled to run as a native OS/2 application. It is suggested that the approach used was not an elegant one and probably not the most efficient, however, it was implemented expediently, with minimal changes to the code. Once compiled the software was tested using the supplied test data. Since modifications to the software were superficial no code listing is included.

After adopting frequencies which showed significant power in the analysis performed by Gunaratne (1994), successive runs were made to identify further periodic components. These were then introduced into the LSSA as forcing periods. Following each run a spectrum of the remaining signal was plotted and examined. In total approximately 50 runs were performed using different forcing periods. Appendix B contains the results from the run that was finally adopted. A total of 78 periods are

included. These are identified purely through the spectral analysis and have not been selected to specifically represent astronomical or other identified periodic components. As discussed in Section 3.3 the reason for removing periodic components was to reduce the volume of the attractor. Once a point was reached where no further ‘significant’ reduction to the magnitude of the residual time series was reached, the process was terminated. As there is no means of quantifying ‘significant’ in this sense the selection was somewhat arbitrary. It can be seen from Appendix B that there are significant correlations between some constituents. Further the threshold of 25% of estimated magnitude for the standard deviation of constituents is often exceeded, however, all constituents exceeding 50% were rejected.

In Equation 3.1 allowance for a trend component is made, that is temporal variation in the relationship between chart datum and mean sea level, represented by  $Z_0(t)$ . In the Bay of Fundy a trend of approximately 3mm/year has been identified (Godin, 1994). In this case, through the LSSA the trend was identified as being indistinguishable from zero and was therefore ignored. For a data series that spans 30 000 hours the trend would amount to approximately 1cm. The observations are made at the cm level making the trend indistinguishable. This results in Equation 3.1 being simplified to

$$\mathbf{X}(t) = \mathbf{T}(t) + \mathbf{S}(t) \quad 3.2$$

In principal then the 'best fit' signal based on selected forcing periods is computed as  $\mathbf{T}(t)$ , through LSSA, and removed from the observed time series. This yields the residual time series  $\mathbf{S}(t)$  which becomes the signal for further analysis.

No datum biases were included in the analysis. Justification for this was twofold:

- a) There are no obvious changes throughout the time series.



- b) The stability of the tide gauge was confirmed by telephone with the Canadian authorities for the period used in this analysis.

The residual time signal has a larger magnitude than normally expected in tidal analysis. Comparison with the residual signal obtained by Carrera (1995) shows that the LSSA returns a smaller residual time series. However, the LSSA and Carrera (1995) results are of a similar order of magnitude.

Figure 3.3 shows the first 1000 points of the residual time series.

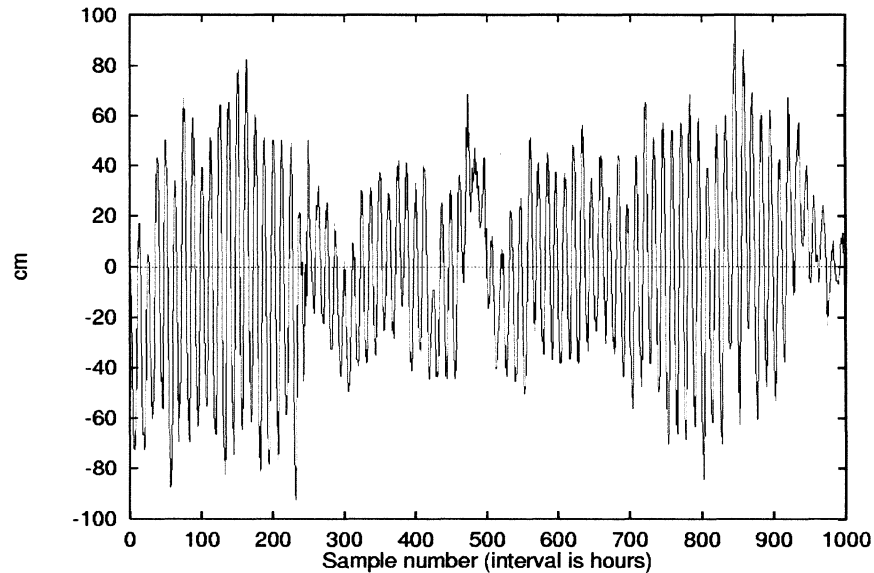


Figure 3.3 - Running LSSA on the data produces a residual time series. The first 1000 points of this residual time series are shown.

The spectrum of a chaotic system may well display characteristic frequencies and not a strictly uniform spectrum as in white noise (or band limited white noise). In fact it is generally important that a mean orbital period be established. In retrospect it may have been more useful to remove fewer components. This is discussed in the conclusions Section 6.6. Figure 3.4 shows the spectrums for the data series before and after removal of the periodic components. When the LSSA software was initially compiled and run the

results of the spectra produced were checked using Fourier analysis. The spectra shown in Figure 3.4 are from a Fourier analysis of the data and not the results of the LSSA, however, both exhibit exactly the same characteristics.

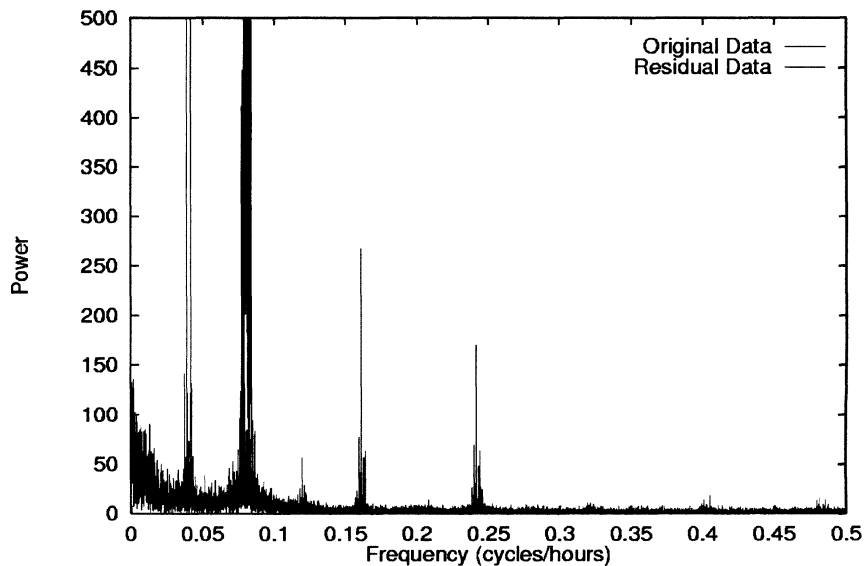


Figure 3.4 - Frequency spectra for the time series before and after removal of the periodic components. The spectra were generated by running an FFT on the first  $2^{14}$  points.

### 3.5. Data Requirements

In order to reliably recover the structure of an attractor and estimates of the defining characteristics from a time series the data needs to be considered in terms of :

- a) length of the time series, that is, number of samples;
- b) sampling frequency;
- c) quality of the data or signal to noise ratio.

Chapters 4 and 5 present the two algorithms used for the estimation of Lyapunov exponents in this study. Both of these algorithms require that the data be regularly sampled and that there are no gaps. A further constraint of these algorithms is that they assume that the system being analysed is invariant in terms of the defining parameters, or

at least that the parameters vary sufficiently slowly. It is for this reason that a period of uninterrupted sampling was selected, in addition to one during which it is believed that the characteristics of the equipment used to sample the data were not changed significantly.

### 3.5.1. Length of the Time Series

The question of how many samples are required to recover estimates for Lyapunov exponents and correlation dimensions is still subject to study. A widely recognised paper in this regard is one by Eckmann and Ruelle (1992). Their conclusion is presented.

When measuring the rate of divergence of trajectories with nearby initial conditions, a number of neighbours are required for a given reference point. If the reconstructed attractor has a diameter  $d$  then these neighbours should lie in a ball ( $n$  sphere) of radius  $r$ , where  $r$  is small with respect to  $d$ .

$$\frac{r}{d} \equiv \rho \ll 1 \quad 3.3$$

Eckmann and Ruelle (1992) suggest  $\rho \leq 0.1$ .

They then proceed to the conclusion that the requirement for the length of a data set is given by

$$\log N > D \log \left( \frac{1}{\rho} \right), \quad 3.4$$

where  $N$  is the number of data points and  $D$  is the dimension of the attractor. For  $\rho = 0.1$ , Equation 3.4 directs us to choose  $N$  such that  $N > 10^D$ .

There are numerous examples where it is claimed that chaos has been identified using time series that are far shorter than this criteria, as well as a number of examples

where it is claimed that this is too pessimistic (Kugiumtzis et. al. 1993). If Eckmann and Ruelle (1992)'s criteria is to be strictly adhered to it should be noted that the time series used in this study, which comprises 30 000 points is only sufficient to estimate dimensions and Lyapunov exponents of up to dimension 4. This, however, is not a well defined requirement. The algorithms presented in Chapters 4 and 5 were in fact used to far higher dimensions.

### **3.5.2. Sampling Frequency**

In order to obtain estimates of the ergodic characteristics of an attractor it is important that the divergence be monitored for sufficient periods. Since the trajectories are followed, what is required is that they are followed for a sufficient distance to ensure that the divergence has been correctly estimated. Thus the sampling frequency is as important as the number of data points. If the sampling frequency is too high then excessive computation time is used and if the sampling frequency is too low then the nature of the divergence cannot be tracked. In the presence of noise too high a sampling frequency may introduce difficulties in selecting points from different trajectories.

Wolf et al. (1985) suggest that a sample frequency of about 12 samples per mean orbit is close to ideal. It is accepted that given a trade-off between samples per mean orbit and the number of orbits it is preferable to increase the number of orbits, provided that a minimum of 4 to 6 samples per orbit is maintained.

After removal of the periodic components the dominant period is 12 hours. This results in a mean orbital period of 12 hours. As the data are sampled every hour this provides 12 samples per mean orbit.

### 3.5.3. Noise

Recovery of chaotic systems is simplified as the noise level of the data is reduced. When working with known systems to demonstrate an algorithm, it is possible to quantify the noise level and to demonstrate robustness in the presence of noise. In real life data this is far more difficult as often the aim of the exercise is to differentiate between noise and a deterministic signal, that is, to identify whether the signal is stochastic or deterministic in nature. When both components are present the task of identifying determinism becomes increasingly difficult as the noise level increases. There is no *a priori* way of assessing the level of noise in the data. Normally in tidal analysis the residual signal is considered as noise and discarded. In this study the periodic portion is discarded and the residual signal retained.

### 3.5.4. Shortening of the data set

Initially a data set comprising around 100 000 observations was used. This represented the longest continuous sequence of observations. After running the algorithms described in Chapters 4 and 5 for a number of parameters it was noted that the solution obtained a steady state fairly rapidly. Solutions were then sought using an embedding dimension of 10. These solutions also achieved a steady state long before the full data set had been used, typically by 20 000 observations. Since the computation time using 30 000 is approximately an order of magnitude less it was decided to use only the first 30 000 observations when batch processing solutions.

An alternative approach was to ‘thin’ the data by using only every third observation. Section 3.5.2 would indicate this to be a better alternative. One of the uncertainties in the data is at what points changes were made to the tide gauge. In order to minimise the probability of this being the case a data set using a shorter time span was selected.

### 3.6. The Delay Portrait

As mentioned in Section 2.7, a first step in the algorithms employed is the reconstruction of the attractor in state space. This provides a useful means of visualising the data, however, it is important that a sufficiently high dimension be used to 'unfold' the attractor in the event of a strange attractor existing. Consequently delay portraits were generated for increasing embedding dimensions with differing time delays. No significant change in the nature of the portraits was noted. An example, using an embedding dimension of 5 and a time delay of 3 hours (samples) is given in Figure 3.5. As discussed in Section 2.7 the evolution in time (the trajectories) of the unknown dynamics can be preserved. The delay portrait is a projection onto a plane of the trajectories in reconstructed phase space.

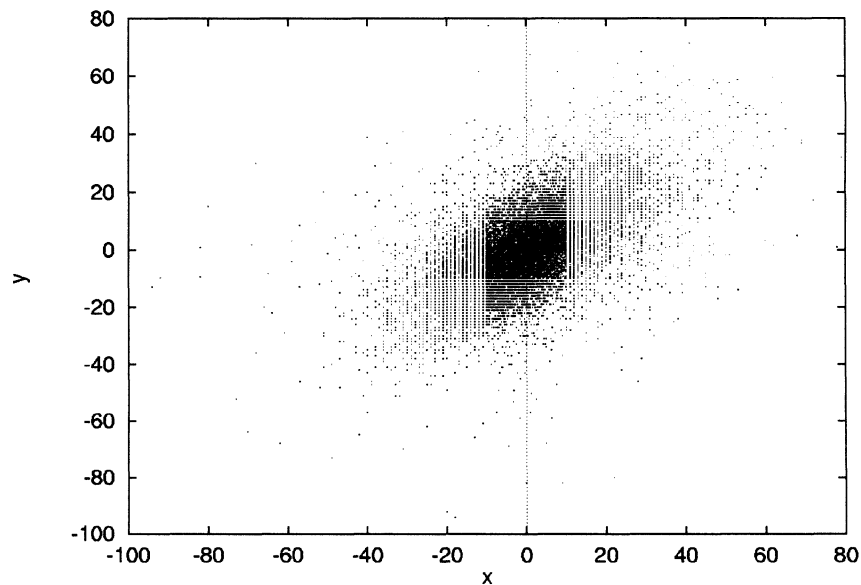


Figure 3.5 - Delay portrait of the reconstructed attractor projected onto the XY plane.

Reconstruction of the attractor is achieved using the method described in Section 2.7. As the time series is sampled and not continuous,  $\tau$  in Equation 2.25, is constrained to an integer multiple of the sample interval. In the water level data the sample interval is 1

hour. Using an embedding dimension of 5 and a time delay of 3 hours this leads to the system being described by

$$\mathbf{S}(t) = \begin{pmatrix} s(t) \\ s(t+3) \\ s(t+6) \\ s(t+9) \\ s(t+12) \end{pmatrix} \quad 3.5$$

where  $s(t)$  represents the residual time series.

The XY plane is formed using the first two vectors of Equation 3.5, with the X vector being formed by  $s(t)$  and the Y vector being formed by  $s(t+3)$ .

The use of dots does not allow a feeling for phase 'continuity', however, lines clutter the plot badly. In order to generate the feeling for phase 'continuity' a second plot using only the first 200 points is given in Figure 3.6.

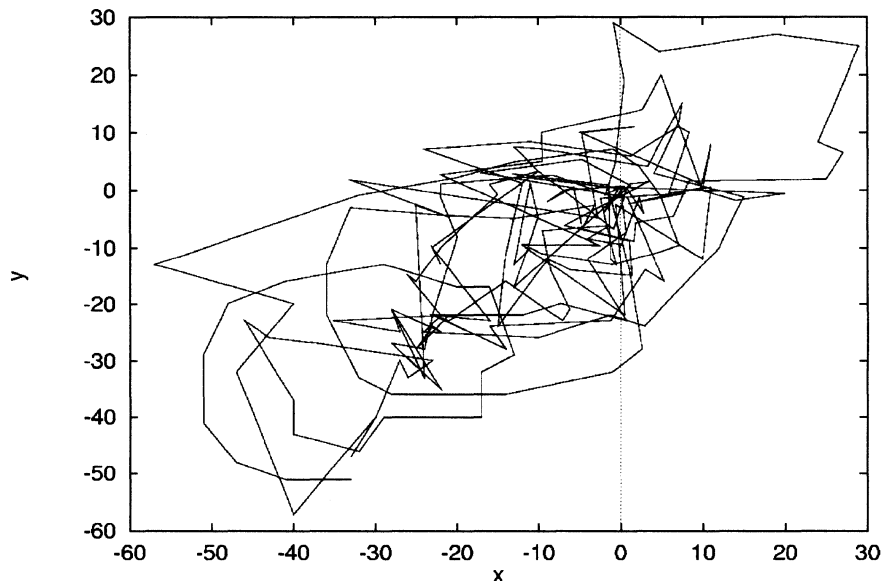


Figure 3.6 - Delay portrait of the reconstructed attractor projected onto the XY plane using only the first 200 points.

Prior to removal of the periodic components the delay portrait represented a torus. This is not surprising and the author believes that a  $n$ -period signal may reconstruct to an  $n$ -torus. Consider a single period signal. Such a signal can be represented by a circle. Next consider a signal composed of two periods. If the two signals are orthogonal the second period can be represented as a circle which is perpendicular to the first at any given point. Evolving such a signal over time forms a 2-torus. Expanding this notion to an  $n$ -period signal would result in an  $n$ -torus representation.



## Chapter 4

### Determining Lyapunov Exponents I

The first of two algorithms used to determine Lyapunov exponents is presented in this chapter. Wolf et al. (1985) is the source to which the reader is referred.

#### 4.1. Algorithm

Wolf et al. (1985) provide a definition of Lyapunov exponents which is relevant to spectral calculations. As this is the manner in which the calculations are performed, the exponents are once again defined. In an  $n$ -dimensional space with a continuous dynamical system, an infinitesimal  $n$ -sphere will deform due to the expanding or contracting nature of the flow. This locally deforming nature will cause the  $n$ -sphere to become an  $n$ -ellipsoid and the  $i$ th Lyapunov exponent is then defined in terms of the length of the principal ellipsoidal axis  $p_i(t)$  as

$$\lambda_i = \lim_{t \rightarrow \infty} \frac{1}{t} \log_2 \frac{p_i(t)}{p_i(0)}. \quad 4.1$$

In Section 4.4 the estimated exponent is given in *bits/s*. In order to return the information in this form  $\log_2$  replaces  $\log$  as used in Equations 2.8 and 2.11, and a time average is used. The orientation of the ellipsoid varies continuously, therefore there is no well-defined direction associated with a given exponent. Wolf et al (1985, p. 286) state :

Notice that the linear extent of the ellipsoid grows as  $2^{\lambda_i t}$ , the area defined by the first two principal axes grows as  $2^{(\lambda_1 + \lambda_2)t}$ , the volume defined by the first three principal axes grows as  $2^{(\lambda_1 + \lambda_2 + \lambda_3)t}$ , and so on. This property yields another definition of the spectrum of exponents: the sum of the first  $j$  exponents is defined by the long term exponential growth rate of a  $j$ -volume element. This alternate definition will provide the basis of our spectral technique for experimental data.

Before considering experimental data Wolf et al. (1985) discuss the computation of Lyapunov exponents when the equations of motion are known. Monitoring of the *long term* growth of the axes of an infinitesimal sphere could be implemented by defining principal axes with initial conditions which are small, and evolving these with the nonlinear equations of motion. It is important to recall that there is a limitation to how small the initial separation, between trajectories, can be selected due to computer limitations. In order for the spectrum of exponents to converge it may be necessary to monitor the system for many orbital periods. There is then a likelihood of the principal axes finding the global 'fold' on a chaotic attractor. What is actually required is to probe the local 'stretch'.

In order to probe only the local stretch Wolf et al. (1985) introduce the concept of using a phase space plus tangent space. A “fiducial” trajectory is defined as that generated by the actions of the nonlinear equations on the centre of the sphere. Wolf et al. (1985, p. 290) state that :

Trajectories of points on the surface of the sphere are defined by the action of the linearized equations of motion on points infinitesimally separated from the fiducial trajectory. In particular, the principal axes are defined by the evolution via the linearized equations of an initially orthonormal vector frame anchored to the fiducial trajectory. By definition, *principal axes defined by the linear system are always infinitesimal relative to the attractor.*

They proceed by simultaneously integrating the nonlinear equations of motion and  $n$  different initial conditions to create the fiducial trajectory and an arbitrarily oriented frame of  $n$  orthonormal vectors respectively. When applied to systems with known equations, the limitations of computer arithmetic manifest themselves by causing the axes to collapse to a single direction. In order to avoid this Wolf et al. (1985) use repeated Gram-Schmidt reorthonormalisation of the vector frame.

For experimental data, typically discrete measurement of a single observable, a similar approach is adopted. In order to proceed, the phase space is reconstructed using the method of delay co-ordinates as discussed in Section 2.7. Since all points then lie on the same trajectory, it is necessary to select initial points which are nearby but separated temporally by at least one orbital period. The first point can be considered to define the fiducial trajectory and the second the principal axis which is sufficiently small that the linear approximation holds. The rate of growth of the principal axis, or separation of the two points is then monitored. When the separation becomes too large the non-fiducial point is replaced with a close point. In order to maintain the orientation, normalisation of the vector is required. A replacement point is therefore chosen which preserves the orientation within limits and minimises the separation. Each vector is subsequently evolved, the exponential growth of these vectors yielding an estimate of  $\lambda_1$ .

## 4.2. Implementation

The source code, executable files and documentation for this algorithm have been released to the public domain Wolf (1995). The source code was modified to use the graphics libraries available to the author and to accommodate large data sets, although the data set was later shortened to a length that would fit into the original code. The reason for shortening the time series was not because of a computational limitation but to avoid the pitfalls discussed in Section 3.5. All routines were compiled to run as native OS/2 software to enable multiple runs during batch processing. Wolf et al. (1985) have published a number of routines. The routine used was 'FET' or the fixed evolution time routine for the estimation of the largest Lyapunov exponent. In order to improve computational efficiency, a routine was run on the data before FET. This routine, 'BASGEN', optimises the search functions in FET by limiting the data to be searched for each replacement.

A much simplified description of the process followed by FET is extracted from the documentation which accompanies the software, Wolf (1995, p. 6) :

- 1) FET creates a multi-dimensional phase space orbit from a one-dimensional time series by delay reconstruction.
- 2) Using the database created by BASGEN ....., FET locates a pair of points that are very close to each other in the reconstructed phase space orbit.
- 3) FET follows each of the points as they travel a short distance along the phase space orbit. We can compare the initial separation (ordinary Euclidean distance) of these points to their separation at the end of the interval. The logarithm (base 2) of the ratio of final to initial separation of these points is a local estimate of orbital divergence.
- 4) If the two points are still fairly close together at the end of this interval, we keep both of them, evolve them a bit further along the orbit, and compute the next local value of orbital divergence. If the points have grown much further apart, we keep one of the points, and use the database to find an appropriate replacement for the other point.
- 5) By averaging the local rates of orbital divergence and dividing by the total travel time along the orbit we obtain the long time average rate of divergence of nearby orbits. The word nearby is important -- our contributions come from orbital segments that are reasonably close together at all times.

The above does not replace a careful reading of Wolf et al. (1985).

Prior to running FET it is necessary to run BASGEN. BASGEN will perform the time delay reconstruction and generate a database which is optimised for the search functions used in FET. User input required for BASGEN is :

- 1) The number of data points. The data may be in an ASCII format or BASGEN format.
- 2) The time delay (tau or  $\tau$ ).

3) Embedding dimension.

4) Grid resolution. BASGEN 'bins' data into a grid, FET searches appropriate bins thus reducing the number of points to be searched. Within reasonable bounds selection of this parameter will affect the efficiency of the computations but not the accuracy of the estimates. BASGEN will report the number of non-empty 'boxes', a rule of thumb is to aim for an average of 100 points per box.

FET may then be run on the database generated by BASGEN. User input required for FET is :

- 1) Time step. The time between samples in the time series in seconds. FET will multiply the estimate by this value to produce an estimate in *bits/s*. If a value of 1 is entered the estimate is in *bits/sample*.
- 2) Evolution time. The number of samples for which the trajectories must be evolved before searching for a replacement point.
- 3) Minimum separation. When either the initial points or a replacement point is selected a close point is chosen. Errors in the data may result in a large relative error in our knowledge of the initial separation. To reduce this relative error it may be desirable to impose a minimum separation. It is interesting to note that the longer the time series the higher the likelihood of a very close point being found. Thus with very long time series a minimum other than zero might be preferable, even if the data are virtually noise free.
- 4) Maximum separation. After evolving the trajectories for the user specified number of samples, the separation is tested to determine whether it should be evolved

further, or a replacement point sought. The maximum separation parameter defines the largest length scale on which orbital divergence is to be monitored.

- 5) Maximum orientation error. FET attempts to preserve the orientation of the line segment being evolved. The maximum orientation error specifies the allowable change in orientation at replacement.

There were essentially two phases to the analysis of the data using this software; the first part being interactive, the second being batch runs. During the interactive phase the output is a graphical representation of the two trajectories being monitored. The input parameters are varied and divergence characterised by 'observing'.

Batch runs are necessary in order to test the stability of any solution. These runs are used to compute the estimated exponent while varying the input parameters. The computed exponent should show a large degree of independence from these parameters. A number of plots showing these results, along with the parameters used, are presented in Sections 4.3 and 4.4. Data used throughout this chapter was extracted from the Lorenz system, given by Equation 2.12. The parameters used when generating the time series from the Lorenz system were  $\sigma = 16.0$ ,  $R = 45.92$  and  $b = 4.0$ . This has the advantage of allowing the behaviour of the algorithm to be demonstrated against a known result. The time series of the  $X(t)$  state was sampled with an interval of 0.05s.

### **4.3. Interactive Runs**

The graphics implementation is primitive and the rate at which information is displayed to the screen leaves the user somewhat unsure of exactly what has been observed. What is displayed is the divergence of selected points when the trajectories are tracked. As new points are selected, so the trajectories are replaced and the divergence

repeated. Since the software was run on a moderately high performance PC, the rate at which information was processed was too rapid. In order to work around this the software was compiled as a DOS program and executed in a virtual DOS machine under OS/2. By lowering the priority of the session the speed of execution can be greatly reduced. This also allows for the screen to be captured, and two examples are given in Figures 4.1 and 4.2

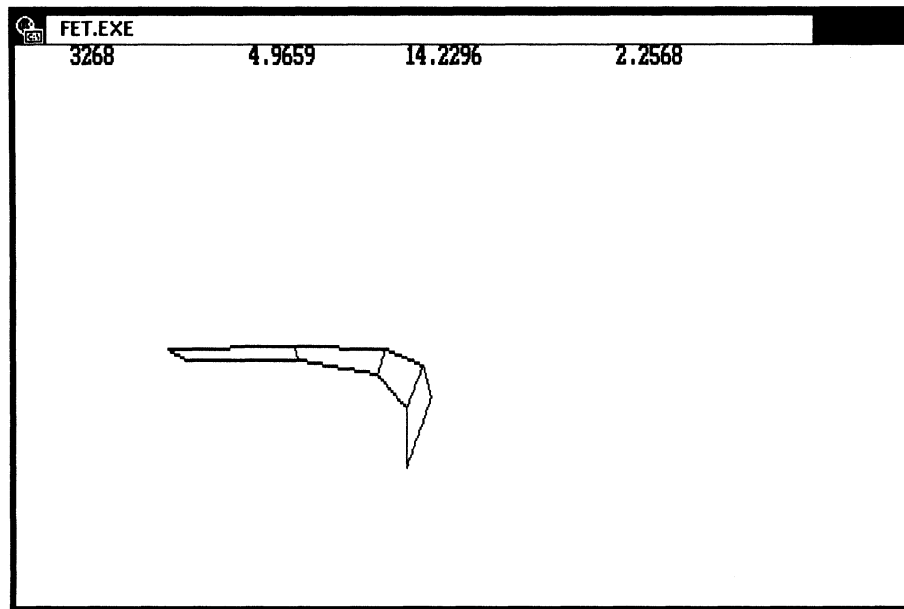


Figure 4.1 - An interactive screen capture using data from the Lorenz attractor.

Where Figure 4.1 showed the divergence quite clearly the angle that the segment in Figure 4.2 is viewed from is not as informative, however, the divergence of the trajectories can still be perceived. It is necessary to view a significant number of evolutions to gain a feeling for the behaviour of the data.

In both Figures 4.1 and 4.2 parameters were used which are known to be correct. The values used were :

Sample interval	0.05s
Minimum separation	0.0001

Maximum separation	8
Maximum orientation error	30
tau	3

The evolution time that the solution was tracked for was 4 samples for Figure 4.1 and 6 samples for Figure 4.2.

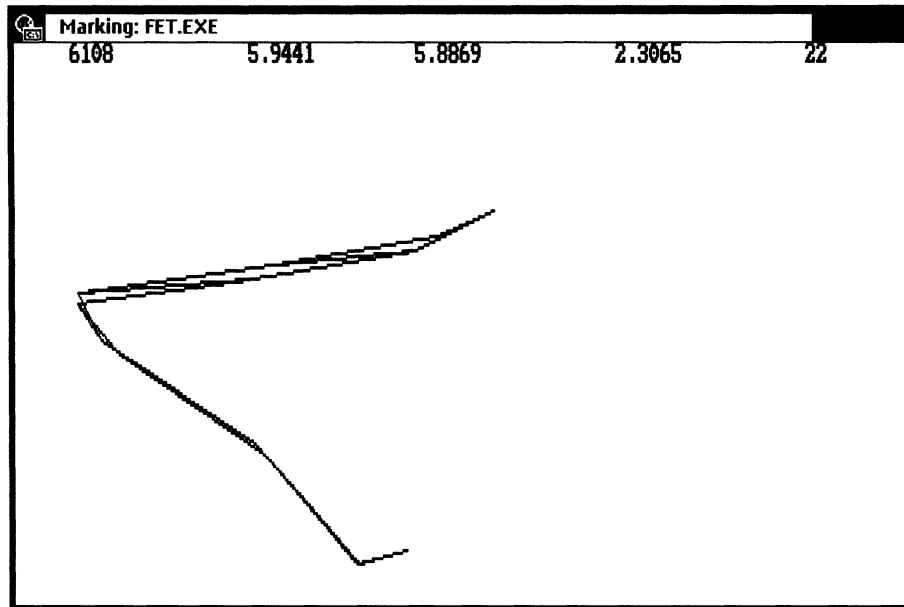


Figure 4.2 - A second example of the interactive graphics

#### 4.4. Batch Runs

The largest Lyapunov exponent was calculated for the data series using a number of different parameters. In each case a single parameter was varied while the rest were held constant and the exponent estimated. What is required from the algorithm is a positive exponent, however, it is equally important that the solution is shown to be stable. Here “stable” is used in the sense that it does not exhibit excessive dependence on the input parameters used in the algorithm. Stability of the solution is demonstrated here for four of the input parameters. The four parameters that were varied are :

- 1) embedding dimension,
- 2) evolution time,



- 3) maximum separation,
- 4) increasing delay ( $\tau$ ) used in the phase space reconstruction.

Choice of the limits that the values can reasonably be varied between is briefly discussed.

- 1) The embedding dimension cannot be smaller than 2 and has a practical upper limitation since we are interested in low-dimensional chaos. Further the data requirements become excessive for higher orders and even the limit of 10 imposed is questionably high. A further practical constraint is the processing time required as the dimension increases.
- 2) Evolution time has a lower limit which is one sample. The upper limit can only reasonably be a few mean orbital periods. This is important to ensure that the local stretching is being probed and not the global folding of the attractor. Once an estimate of the exponent has been obtained, the rate at which information is generated (or lost) is available and uncertainty in future positions may be roughly estimated.
- 3) Maximum separation has upper and lower bounds which correspond to the size of the attractor and the minimum separation respectively.
- 4) Time delay ( $\tau$ ) has a lower bound of one sample. No upper bound is defined, apart from that imposed by the length of the data series and the embedding dimension selected, however, a practical upper bound of several orbits is realistic. In theory selection of this parameter is arbitrary; in practice this proves not to be the case due to errors in the data.

Details of each run are given with the results being plotted in Figures 4.3, 4.4, 4.5 and 4.6.

1) Estimated largest Lyapunov exponent for increasing embedding dimension.

Parameters used :

Time step	0.05
Evolution time	4 (samples)
Min separating	0.0001
Max separating	8
Max orientation error	30
tau	3 (samples)

Estimated largest Lyapunov exponent for dimensions 3 to 10.

Results are plotted in Figure 4.3

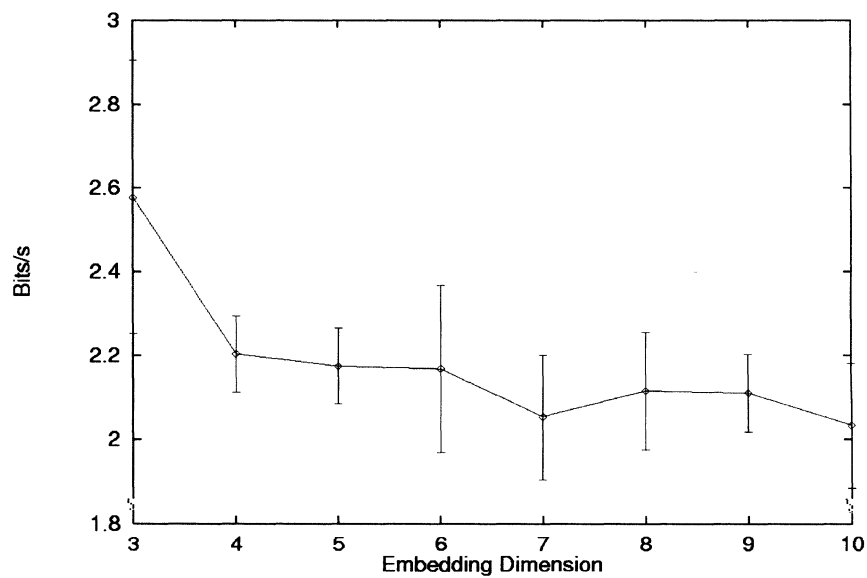


Figure 4.3 - Estimates for the largest Lyapunov exponent computed for increasing embedding dimensions.

The error bars in Figures 4.3, 4.4, 4.5 and 4.6 show the associated confidence for the estimates that the algorithm returns.

2) Estimated largest Lyapunov exponent for increasing evolution times.

Parameters used :

Time step	0.05
Min separating	0.0001
Max separating	8
Max orientation error	30
Embedding dimension	4
tau	3 (samples)

The evolution time is varied from 1 to 10 samples.

Results are plotted in Figure 4.4

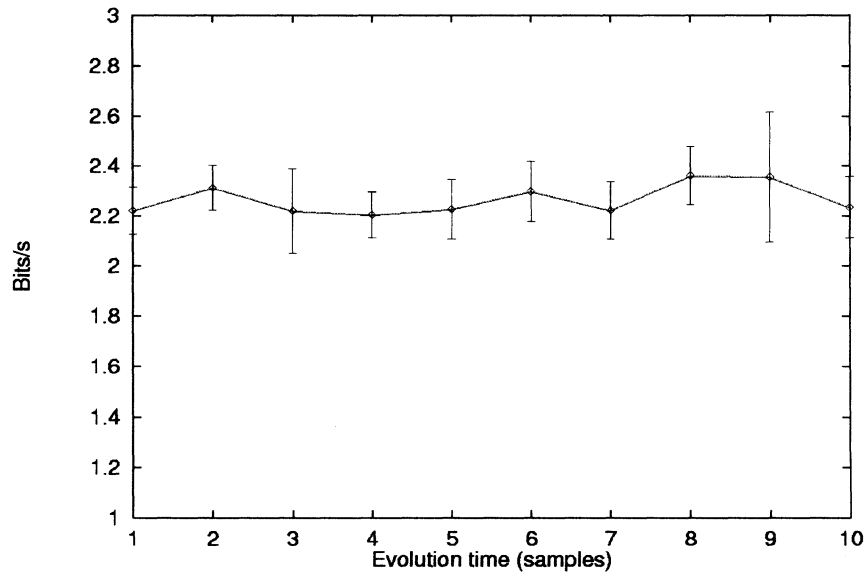


Figure 4.4 - Estimated largest Lyapunov exponent for increasing evolution times.

3) Estimated largest Lyapunov exponent for varying maximum separating values.

Parameters used :

Time step	0.05
Evolution time	4 (samples)
Min separating	0.0001
Max orientation error	30
Embedding dimension	4
tau	3 (samples)

The maximum separation is varied from 1 to 15.

Results are plotted in Figure 4.5.

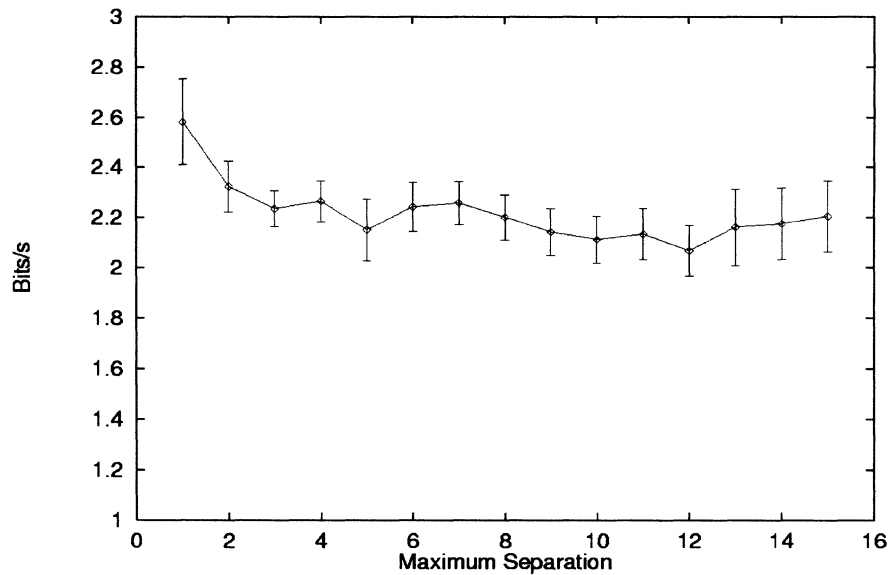


Figure 4.5 - Estimated largest Lyapunov exponent as the maximum separation before replacement of the vector being monitored is increased.

4) Estimated largest Lyapunov exponent for increasing delay ( $\tau$ ) values.

Parameters used :

Time step	0.05
Evolution time	4 (samples)
Min separating	.0001
Max separating	8
Max orientation error	30
Embedding dimension	4

$\tau$  is varied from 1 to 10 samples.

Results are plotted in Figure 4.6

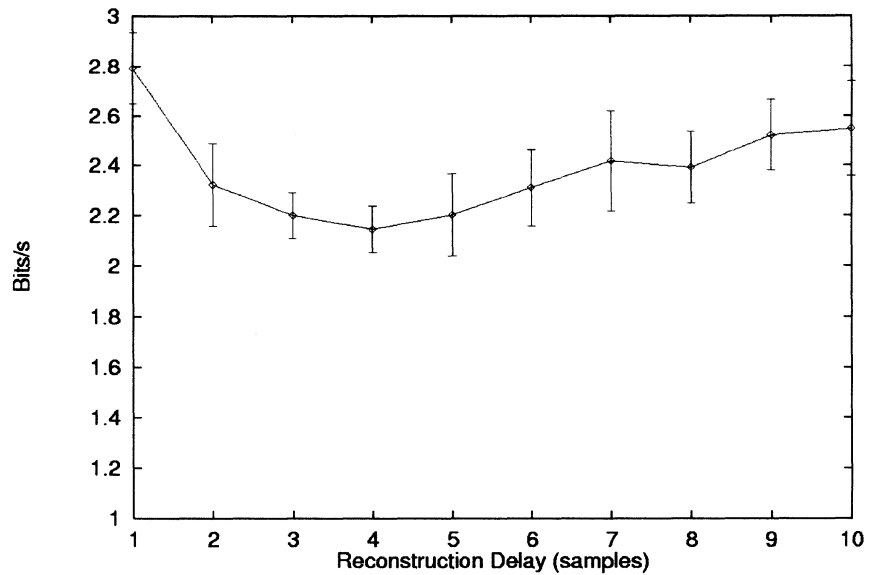


Figure 4.6 - Estimation of the largest Lyapunov exponent for increasing values of tau (delay).

It is readily seen in Figures 4.3 through 4.6 that the estimated exponent does not vary significantly and in all cases returns a value close to the known value of 2.16 *bits/s*.

No attempt is made to establish how robust the algorithm is to noise in the data. In reality the algorithm is probably quite sensitive to noise. Wolf et al (1985) discuss the use of low pass filtering to remove noise and show that sensitivity to filtering is system dependant. In the analysis of water level data, filtering is performed in the sense of removing 'known' components, not to remove noise due to high frequency white noise.

## Chapter 5

### Determining Lyapunov Exponents II

A second approach to determining Lyapunov exponents is introduced and used to analyse the data. In addition to estimating the largest Lyapunov exponent this algorithm estimates the correlation dimension. For a comprehensive description of the methods set out below, the interested reader is referred to the original paper by Rosenstein et al. (1993).

#### 5.1. The Algorithm

It is suggested by Rosenstein et al. (1993) that alternative algorithms all suffer from one or more of the following drawbacks, they are

- 1) unreliable for small data sets,
- 2) computationally intensive,
- 3) difficult to implement.

Rosenstein et al. (1993) propose an algorithm which they claim avoids these drawbacks and is robust to variations in the embedding dimension, number of data points, reconstruction delay, and noise level. A summary of their algorithm, which follows the original work closely, is given below.

Consider again the infinitesimal  $n$ -sphere as it evolves. As discussed in Section 4.1 the growth of the principal axis leads to an estimate of the largest Lyapunov exponent. This may be considered as measuring the separation along the Lyapunov directions, which are dependant on the system flow and are defined using the Jacobian matrix, i.e., the tangent map at each point of interest along the flow (Eckmann and Ruelle, 1985). In order to compute the Lyapunov spectrum it is thus necessary to preserve the proper

phase space orientation by approximation of the tangent map. Rosenstein et al. (1993, p. 119) use the following argument to support their claim that it is unnecessary to preserve orientation when estimating only the largest Lyapunov exponent.

If we assume that there exists an ergodic measure of the system, then the multiplicative ergodic theorem of Oseledec [26] justifies the use of arbitrary phase space directions when calculating the largest Lyapunov exponent with smooth dynamical systems. We can expect (with probability 1) that two randomly chosen initial conditions will diverge exponentially at a rate given by the largest Lyapunov exponent [6,15]. In other words, we can expect that a random vector of initial conditions will converge to the most unstable manifold since exponential growth in this direction quickly dominates growth (or contraction) along the other Lyapunov directions. Thus the largest Lyapunov exponent can be defined using the following equation where  $d(t)$  is the average divergence at time  $t$  and  $C$  is a constant that normalises the initial separation :

$$d(t) = Ce^{\lambda t} . \tag{5.1}$$

In order to proceed the phase space is reconstructed. This is achieved using the method of time delays. Rosenstein et al. (1993, p. 120) use a prescription based on the autocorrelation function to estimate the lag, “...the lag where the autocorrelation function drops to  $1 - \frac{1}{e}$  of its initial value.” The reconstructed trajectory can then be expressed as a matrix where each row is a phase space vector. Let these phase space vectors be represented by  $X_i$  for  $i = 1 \dots n$ . A starting point is selected and the nearest neighbour located. The mean rate of separation of these points is then used as an estimate of the largest Lyapunov exponent. The nearest neighbour,  $X_j$ , is selected by searching for the point that minimises the distance to the particular reference point,  $X_i$ , with the constraint that the temporal separation is greater than one mean orbital period. Distance is defined in terms of the Euclidean norm. Each pair of neighbours can then be treated as nearby initial conditions for different trajectories with the initial separation defined as

$$d_j(0) = \min_{X_j} \|X_j - X_j\| . \quad 5.2$$

More precisely the estimate of the largest Lyapunov exponent is obtained from

$$\lambda_1(i) = \frac{1}{i\Delta t} \frac{1}{(M-i)} \sum_{j=1}^{M-i} \ln \frac{d_j(i)}{d_j(0)} \quad 5.3$$

where  $\Delta t$  is the sample interval,  $d_j(i)$  is the distance between the  $j$ th pair of nearest neighbours after  $i$  discrete time steps ( $i\Delta t$  seconds).  $M$  is the number of reconstructed points given by

$$M = N - (m-1)J \quad 5.4$$

where  $J$  is the reconstruction delay,  $m$  is the embedding dimension and  $N$  is the number of points in the time series. Using the definition of  $\lambda_1$  given in Equation 5.1 it is assumed that the  $j$ th pair of nearest neighbours diverge at a rate given (approximately) by

$$d_j(i) \approx C_j e^{\lambda_1(i\Delta t)} \quad 5.5$$

where  $C_j$  is the initial separation. Taking the logarithm of each side yields

$$\ln d_j(i) \approx \ln C_j + \lambda_1(i\Delta t) \quad 5.6$$

which represents a set of approximately parallel lines, for  $j = 1, 2, \dots, M$ , each with a slope roughly proportional to  $\lambda_1$ . The largest Lyapunov exponent is then calculated using a least-squares fit to the average line defined by

$$y(i) = \frac{1}{i\Delta t} \langle \ln d_j(i) \rangle \quad 5.7$$

where  $\langle \bullet \rangle$  denotes the average over all values of  $j$ .



An important difference to the approach used by Wolf et al. (1985) is now noted. Since Wolf et al. (1985) focus on a single 'fiducial' trajectory the algorithm fails to take advantage of all the data. By using 'all' of the data it is argued that smaller data sets may be used or an improvement under noisy conditions noted.

Since Rosenstein et al. (1993) use natural logs in their calculations the estimated exponent is not in *bits/s*. The relationship to *bits/s* is then simply the relationship of  $\log_2$  to  $\ln$ , given by

$$\log_2 \lambda \approx 1.44 \ln \lambda . \quad 5.8$$

An additional advantage of this approach is that the correlation dimension is simultaneously calculated with the largest Lyapunov exponent. An implementation of the correlation dimension computations was proposed by Grassberger and Procaccia (1983). This algorithm is used by Rosenstein et al. (1993). For a given embedding dimension  $m$  let  $M$  be the number of balls needed to cover the attractor. Then the correlation sum may be estimated by

$$C_m(r) = \frac{2}{M(M-1)} \sum_{i \neq k} \theta(r - \|X_i - X_k\|) \quad 5.9$$

where  $\theta(\ )$  is the Heavside function (Grassberger and Procaccia, 1983).  $C_m(r)$  may be interpreted as the fraction of pairs of points that are separated by a distance less than or equal to  $r$ .

## 5.2. Implementation

Software based on the above algorithms is freely distributed by Rosenstein et al. (1993). It is in the form of two DOS executable files: MTRCHAOS and MTRLYAP. The latter is used to estimate the largest Lyapunov exponent as well as the correlation

dimension. It has the advantage of allowing for computations to be run in batch mode. The former is used to 'examine' the data and the results of the estimates for Lyapunov exponents and correlation dimension. MTRCHAOS allows the user to generate data sets for a few systems, create delay portraits, compute frequency spectra, generate surrogate data sets, estimate delays, and interpret the results from MTRLYAP.

MTRLYAP is run either from the command line or a batch file. A number of parameters are required by the program. These are :

- 1) File name. Data is supplied to the routine in an ASCII format. The data file may contain time series information from more than a single state of the system.
- 2) Time series number. Which of the multiple time series in the file are to be used.
- 3) The number of data points to be used.
- 4) Embedding dimension.
- 5) Reconstruction delay.
- 6) Mean orbital period.
- 7) Duration for which the divergence is to be tracked.

MTRLYAP is used to generate the 'analysis' files, from time series data, by estimating the curves as described in Section 5.1. MTRCHAOS is then used to plot the curves and estimate the slope for a selected portion of the curve. In order to illustrate the performance, MTRLYAP is run on a time series derived from the Lorenz system, given by Equation 2.12. By using data from a system which is known to be chaotic the software is easier to understand than when used on unknown data. Further it provides the reader with a reference when examining the results in Chapter 6. The parameters used when generating the time series from the Lorenz system were  $\sigma = 16.0$ ,  $R = 45.92$  and  $b = 4.0$ . The time series of the  $X(t)$  state was sampled with an interval of 0.01s. MTRLYAP was run in batch mode to generate curves for embedding dimensions from 3 to 10. All other parameters were held constant for these computations. Values used were:

Number of data points	4000
Reconstruction delay	7 samples
Mean orbital period	114 samples
Monitoring period	300 samples

These have been graphed using GNUPLOT and are given in Figure 5.1.

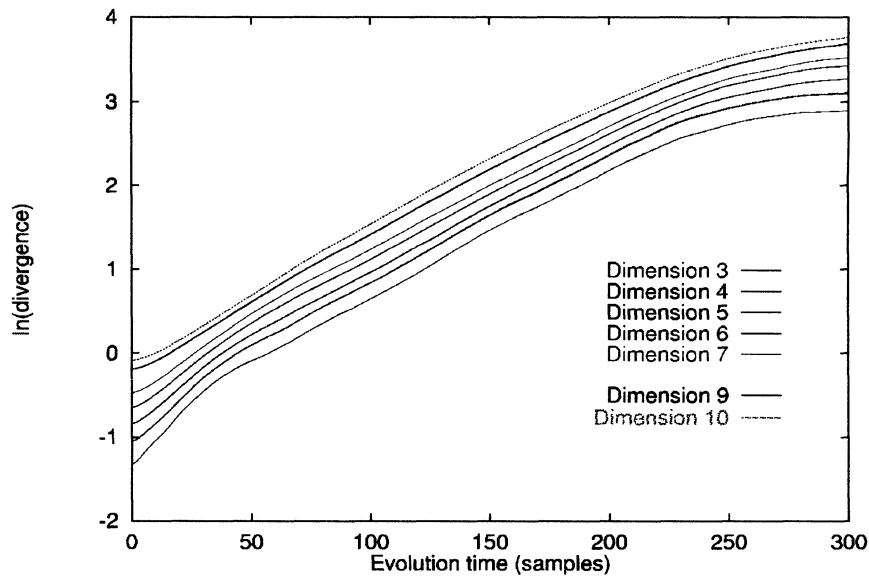


Figure 5.1 - Curves used for estimating the largest Lyapunov exponent.

The correlation dimension which was simultaneously computed is plotted. These curves are given in Figure 5.2

In both cases a 'straight' portion of the line is required which can be used to obtain a good estimate of the slope. For both sets of curves the loss of linearity as time and radius increase respectively is expected as the limits of the attractor are reached. MTRCHAOS is used to compute the slope of the selected portion of the curve. The slope may be interpreted as the largest Lyapunov exponent. Equation 5.7 is used to obtain a least-squares estimate of the slope. In order to illustrate this a screen capture of MTRCHAOS is given as Figure 5.3. The estimated value of 1.519 for the largest Lyapunov exponent

compares well with the expected value of 1.5 (Rosenstein et al., 1993). Using the relationship given in Equation 5.8 this can be converted to *bits/s*. A value of 2.16 *bits/s* is obtained, this is in good agreement with Wolf et al. (1985).

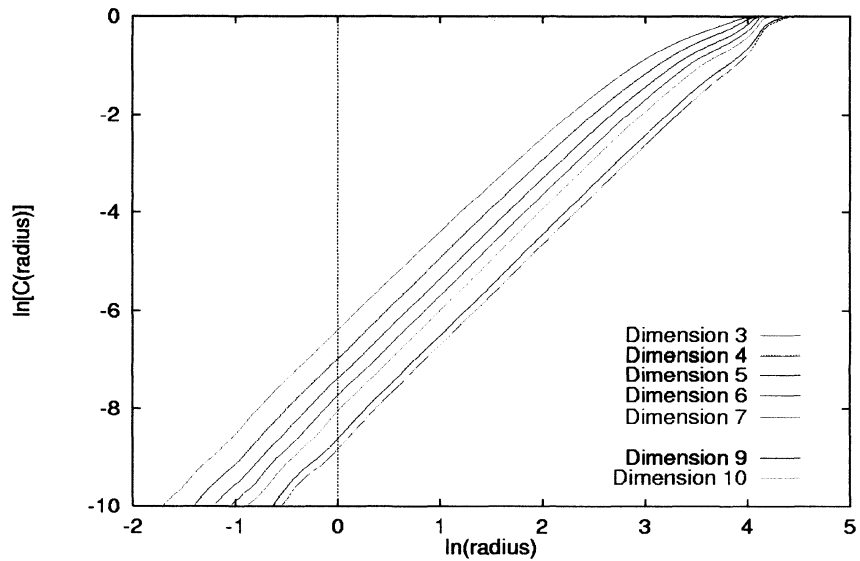


Figure 5.2 - Curves used to estimate the correlation dimension.

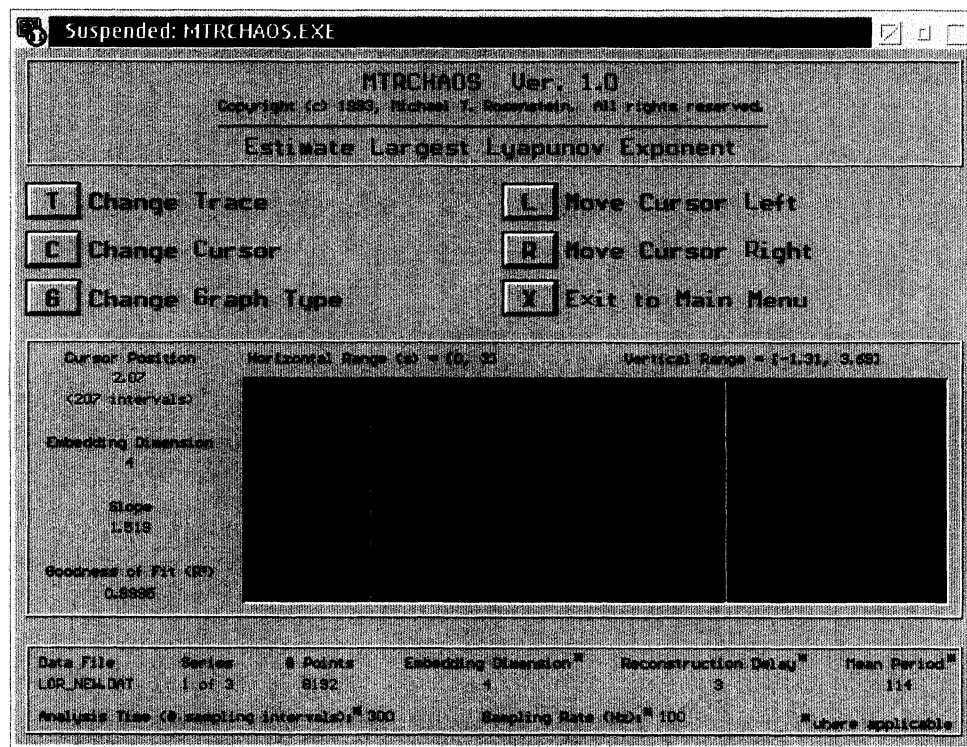


Figure 5.3 - A screen capture of MTRCHAOS for the Lorenz data.

MTRCHAOS allows for the time series in use to be randomised in four different ways :

- a) sequence randomised,
- b) phase randomised, no windowing,
- c) phase randomised, windowed,
- d) Gaussian scaled.

Randomising the time series and running the analysis a second time allows the user to compare the results of the original data to what is known to be a stochastic time series. If the characteristics of the first series are not clear and not significantly different from the randomised sequence, the inference is that the original data are from a random sequence. It is also worth noting that non-chaotic systems will not return curves of the expected form. These aspects are dealt with in Rosenstein et al. (1993).

As an illustration of the effect of randomising the data, the same series that was used in the above plots was randomised using phase randomisation (no windowing) and the curves regenerated. The results of the exponent estimates are given in Figure 5.4 and the correlation dimension in Figure 5.5. What is noticed immediately is that the exponent curves fail to exhibit a linear portion which is parallel among the curves and that the correlation curves fail to exhibit the parallel nature seen in Figure 5.2.

An advantage of this software over that used in Chapter 4 is the ability to view a delay portrait of the reconstructed attractor. This offers the user a graphical visualisation of the reconstructed attractor and leads to a first impression as to whether there is any deterministic structure to the data. Unfortunately the implementation is not very sophisticated and somewhat limiting in how the reconstructed attractor can be viewed. It is only possible to view the projection on a single plane; it is not possible to rotate the reconstructed attractor or to view a projection on an alternate plane.

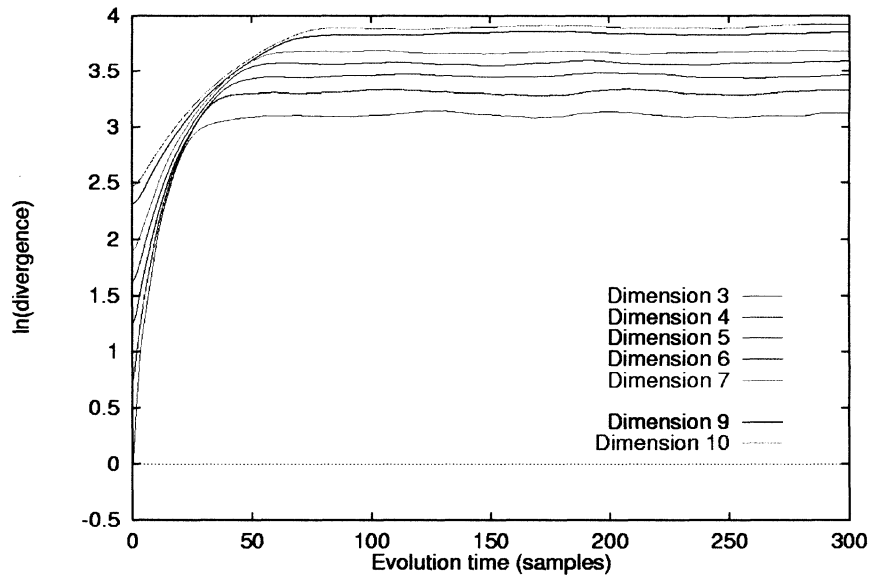


Figure 5.4 - Curves for estimating the largest Lyapunov exponent of the Lorenz data after randomising it.

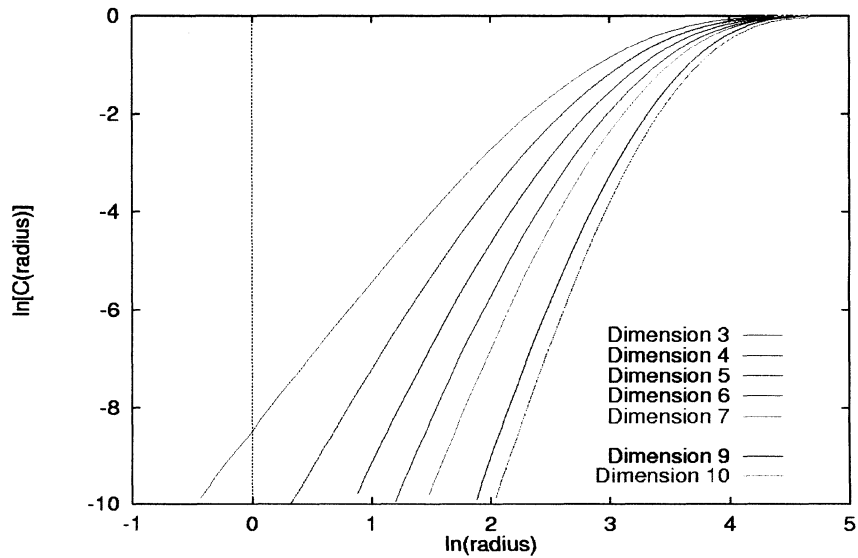


Figure 5.5 - Curves for the estimation of the correlation dimension after randomising data from the Lorenz system.

Although the software was compiled to run on DOS, it partially overcomes the problem of not being able to multitask by allowing for batch runs when computing estimates of the largest Lyapunov exponent and correlation dimension. Since the present

investigation involved a lengthy time series and the author wished to derive estimates for a number of parameters the computational time was significant. At the same time the estimates were being derived simultaneously with those from the algorithm by Wolf et al. (1985). Since the software from Wolf et al. (1985) had been recompiled to run on OS/2 it was decided to use a virtual DOS machine under OS/2 for these computations. This proved to work well and left the computer available for alternative work while computations were performed in the background. It also allowed multiple copies of the software to be run simultaneously.

## Chapter 6

### Results, Conclusions and Recommendations

As discussed in Section 2.5.2 the existence of at least one positive Lyapunov exponent is often taken to indicate chaos in a bounded system. If no positive Lyapunov exponents can be identified then the existence of deterministic chaos becomes highly unlikely, at least within the parameters examined.

#### 6.1. Interactive Runs using Wolf's Algorithm

The implementation, execution and expected results of these interactive runs using the algorithm of Wolf et al. (1985) are presented in Chapter 4. A considerable amount of time was spent observing behaviours exhibited using a variety of parameters. The graphics implementation in Wolf et. al.'s (1985) algorithm is primitive. Section 4.3. discusses the displayed information. Each session involves observing the divergence of trajectories as they evolve with time. The manner in which the divergence is presented is by projecting the two trajectories being tracked onto a plane. This results in considerable loss of information as the projection distorts the separation. The separation of nearby trajectories is precisely what the observer wishes to monitor. By observing sufficient data the user develops up an understanding of how the system behaves. Running the algorithm on a long data set results in thousands of graphic presentations for each set of parameters. Presenting many thousands of images in this document is not practical. As a compromise two screen captures are included. The author's observations are presented.

This interactive approach does not allow the user to quantify the data, rather it aids in the development of an understanding of the behaviour. The author believes that the behaviour was erratic and probably more closely aligned to that expected of a stochastic,



or very noisy system, rather than a largely deterministic one. Replacements of trajectories occur more frequently than desired and the divergence tends to be very erratic.

Figure 6.1 was generated using the following parameters:

Time step	1 hour (sample)
Evolution time	3 hours (samples)
Min separation	1 cm
Max separation	30 cm
Max orientation error	30°
Tau	3 hours (samples)
Embedding dimension	5

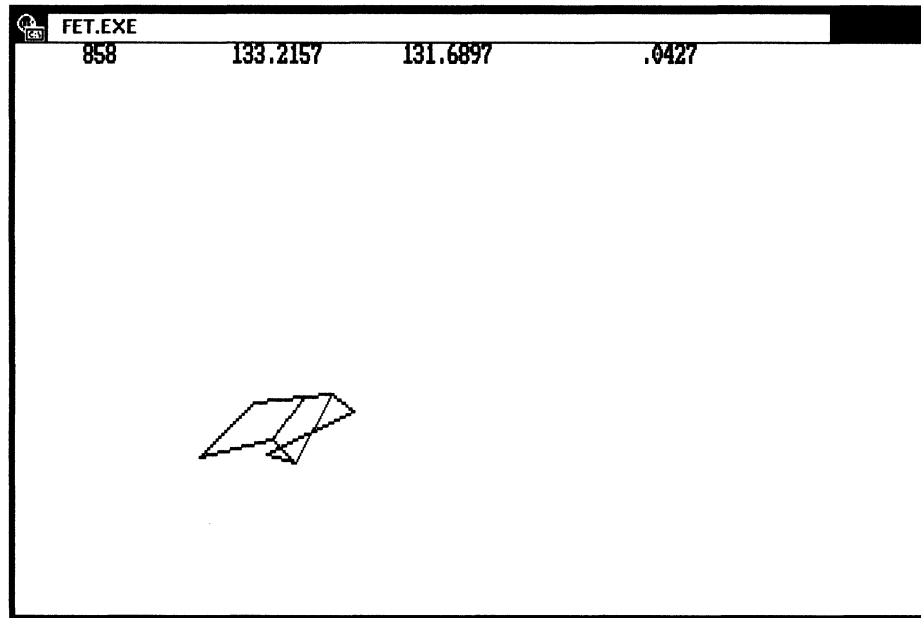


Figure 6.1 - Screen capture from an interactive session.

Any divergence is small, possibly negative. Figure 6.1 does not represent clear divergence of the trajectories as expected for a chaotic system. It is possible that the lack of divergence is the result of the projection distorting the image as the trajectories are tracked. That is the trajectories are moving further from the plane they are projected onto as they evolve. It is only by observing sufficient data that the user understands whether

this is the dominant behaviour. Comparison with Figures 4.1 and 4.2 clearly illustrate the difference in behaviour when compared to a system which is known to be chaotic.

A second example is given in Figure 6.2. The same parameters, as used for Figure 6.1, were used to generate this example. Here divergence is clearly visible. Figure 6.2 represents a promising result. After observing sufficient data and varying the parameters the user develops an understanding for the nature of the divergence.

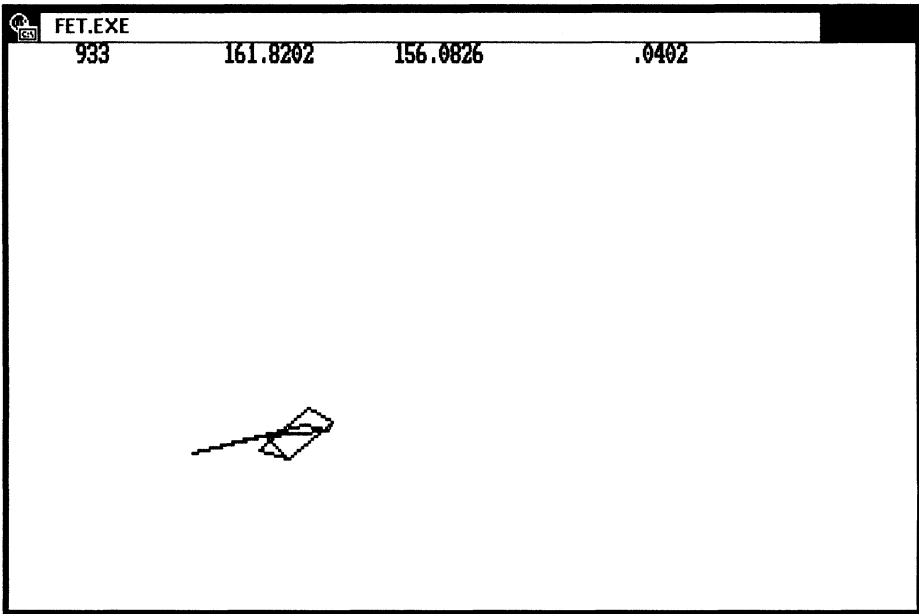


Figure 6.2 - A second example of the interactive graphics.

The authors understanding, from observing the data with many parameters in this manner was that Figure 6.1 exhibits the dominant characteristic.

### 6.2. Batch Runs using Wolf's Algorithm

The largest Lyapunov exponent was calculated for the data series using a number of different parameters. In total many runs were performed, however, they may be grouped into five 'batches'. What is required from the algorithm is a positive exponent. It is

equally important that the solution is shown to be stable in the sense that it is not too sensitive to the input parameters. This concept was demonstrated in Section 4.4 where the algorithm was used on a known system. The five parameters that were varied are:

- 1) Embedding dimension
- 2) Evolution time - the duration over which the evolution is 'tracked' in the algorithm
- 3) Maximum separation before replacement
- 4) Minimum separation, if this is too small the signal and noise are not differentiated
- 5) Increasing delay ( $\tau$ ) used in the phase space reconstruction

Section 4.1 discusses estimation of the largest Lyapunov exponent using the algorithm of Wolf et al. (1985). Section 4.2 presents the actual implementation of this algorithm. It is seen that the result is presented in the form of *bits/s* or *bits/sample*, depending on the parameters used. In this work all computations are performed using a time step of 1 hour. This results in the Lyapunov exponent estimates having units of *bits/sample*, since the sample interval is one hour this translates into *bits/hour*. Section 2.5.5 discusses how Lyapunov exponents quantify an attractor in terms of information theory. In the event that a stable estimate for positive Lyapunov exponent is obtained it could then be interpreted as the number of *bits* of information that the system generates per *hour*. The system represented is that formed by the residual time series after removing the periodic components from the water level measurements. It would therefore include contributions from the water level variations and artefacts introduced by the instrument. This would further lead to an estimate of how predictable the system is.

Choice of the limits that the values were varied between are based on the criteria given below. A summary of these limits and the reasons for their selection follows.

- 1) Embedding dimension cannot be smaller than 2 and has a practical upper limitation since we are interested in low dimensional chaos. This led to 2 being used as the lower limit. An upper limit of 10 was used. Practical considerations regarding the computation time involved largely dictated this selection. Data requirements versus dimension are discussed in Section 3.5.1. Precise requirements remain an open question. This uncertainty is what led to the somewhat arbitrary choice of the upper limit.
- 2) Evolution time has a lower limit which is one sample. The upper limit can only reasonably be a few mean orbital periods. As the mean orbital period is considered to be close to 12 hours (samples) for the data this lead to the upper limit of 36 hours (samples). The lower limit was set to 1 hour (sample).
- 3) Maximum separation has upper and lower bounds which correspond to the size of the attractor and the minimum separation respectively. Since a minimum separation of 1 cm was used the maximum separation used started at 2 cm. The largest value used was 40 cm, this represents approximately 25% of the maximum range of the time series. The author believes that larger values would fail to probe the local behaviour. As initial points are selected which are 'close' a growth beyond 25% of the size of the attractor, over a period of several samples, would most likely represent an error in selection, of the initial points, rather than meaningful orbital divergence. By selecting points which diverge to 25% of the size of the attractor within a few hours (samples) it is likely that they have been selected over a fold in the attractor.
- 4) Minimum separation has upper and lower bounds which correspond to the maximum separation and the resolution of the data respectively. The maximum separation used was 30 cm. This places an upper bound of 29 cm on the minimum

separation. A value of 0 cm was used as the lower bound even though it is unlikely to distinguish between noise and signal at this level. Since the noise level is not apparent the lower bound is not immediately evident.

- 5) Time delay ( $\tau$ ) has a lower bound of 1 hour (sample). This is used as the starting value. A maximum value of 20 hours (samples) is used for the reconstruction delay, this corresponds to nearly two orbits. In theory the selection of this parameter is arbitrary, the results show that it does in fact impact the results.

Details of each run are given with the results being plotted.

- 1) Estimated largest Lyapunov exponent for increasing embedding dimension.

All runs for calculation of the Lyapunov exponents used the following parameters:

Time step	1 hour (sample)
Evolution time	3 hours (samples)
Min separation	1 cm
Max separation	30 cm
Max orientation error	30°
Tau	3 hours (samples)

The embedding dimension was varied from 2 to 10.

Since the time step used is 1 and the samples are hourly, the computed exponents represent *bits/sample* or *bits/hour*. The results are plotted in Figure 6.3. Error bars on the plot show the associated confidence the algorithm returns for each estimate.

- 2) Estimated largest Lyapunov exponent for increasing evolution times.

All runs for calculation of the Lyapunov exponents used the following parameters:

Time step	1 hour (sample)
Min separation	1 cm
Max separation	30 cm
Max orientation error	30°

Tau 3 hours (samples)  
 Embedding dimension 5

Evolution time was varied from 1 hour (sample) to 36 hours (samples).

Since the time step used is 1 and the samples are hourly, the computed exponents represent *bits/sample* or *bits/hour*. The results are plotted in Figure 6.4

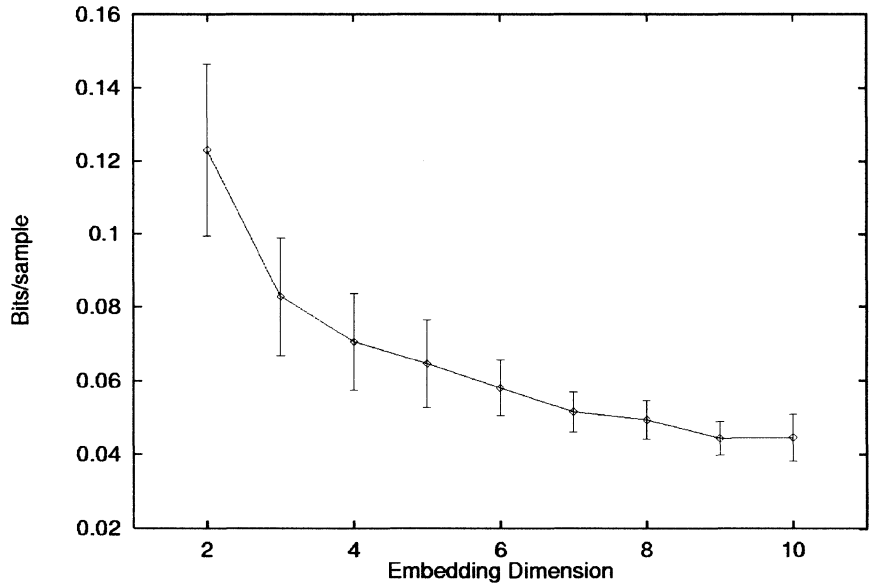


Figure 6.3 - Estimates of the largest Lyapunov exponent, computed for increasing embedding dimensions.

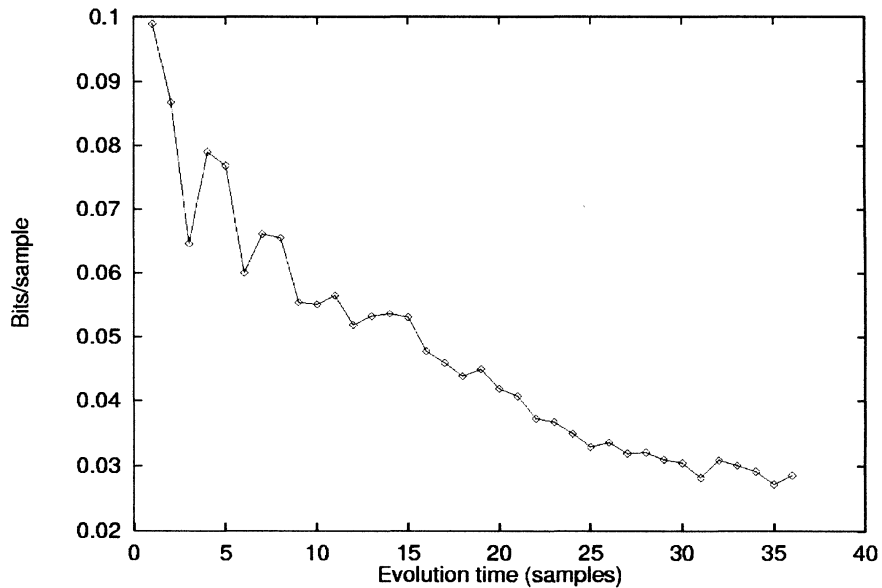


Figure 6.4 - Estimates of the largest Lyapunov exponent computed for increasing evolution times.

3) Estimated largest Lyapunov exponent for varying maximum separation values.

All runs for calculation of the Lyapunov exponents used the following parameters:

Time step	1 hour (sample)
Evolution time	3 hours (samples)
Min separation	1 cm
Max orientation error	30°
Tau is	3 hours (samples)
Embedding dimension	5

The maximum separation was varied from 2 cm to 40 cm.

Since the time step used is 1 and the samples are hourly, the computed exponents represent *bits/sample* or *bits/hour*. The results are plotted in Figure 6.5.

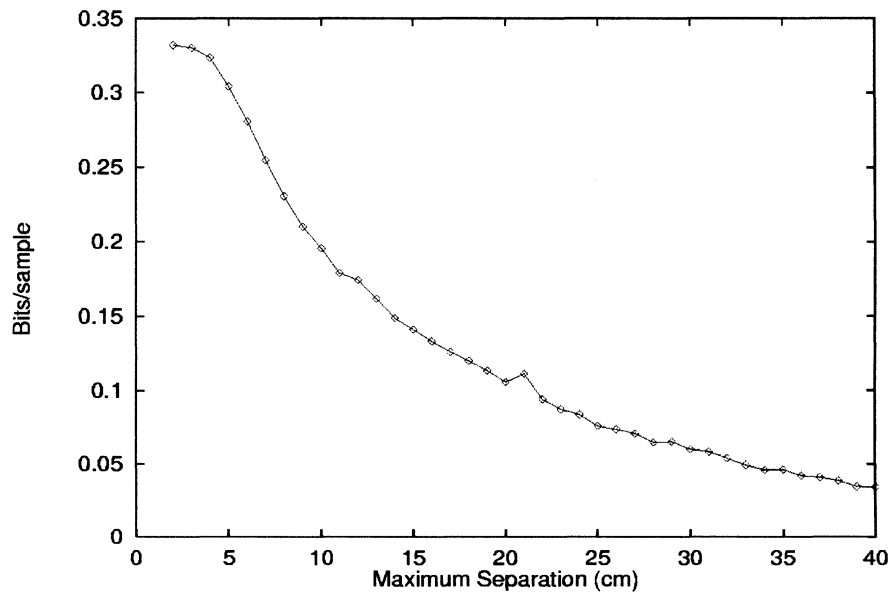


Figure 6.5 - Estimates of the largest Lyapunov exponent computed for increasing maximum separation.

4) Estimated largest Lyapunov exponent for increasing minimum separation values.

All runs for calculation of the Lyapunov exponents used the following parameters:

Time step	1 hour (sample)
Evolution time	3 hours (samples)

Max separation	30 cm
Max orientation error	30°
Tau	3 hours (samples)
Embedding dimension	5

The minimum separation was varied from 0 cm to 29 cm.

Since the time step used is 1 and the samples are hourly, the computed exponents represent *bits/sample* or *bits/hour*. The results are plotted in Figure 6.6.

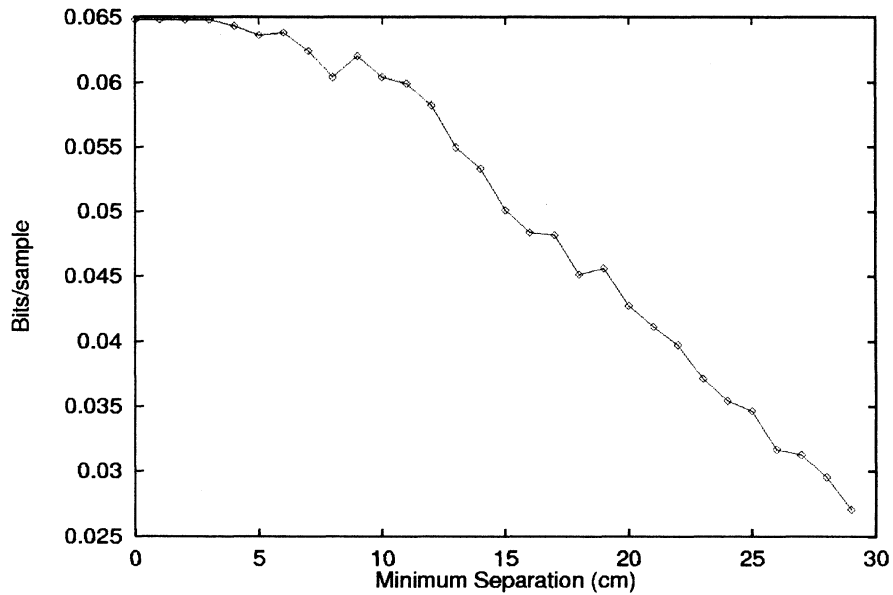


Figure 6.6 - Estimates of the largest Lyapunov exponent computed for increasing minimum separations.

5) Estimated largest Lyapunov exponent for increasing delay ( $\tau$ ) values.

All runs for calculation of the Lyapunov exponents used the following parameters:

Time step	1 hour (sample)
Evolution time	3 hours (samples)
Min separation	1 cm
Max separation	30 cm
Max orientation error	30°
Embedding dimension	5

$\tau$  was varied between 1 hour (sample) and 20 hours (samples).



Since the time step used is 1 and the samples are hourly, the computed exponents represent *bits/sample* or *bits/hour*. The results are plotted in Figure 6.7.

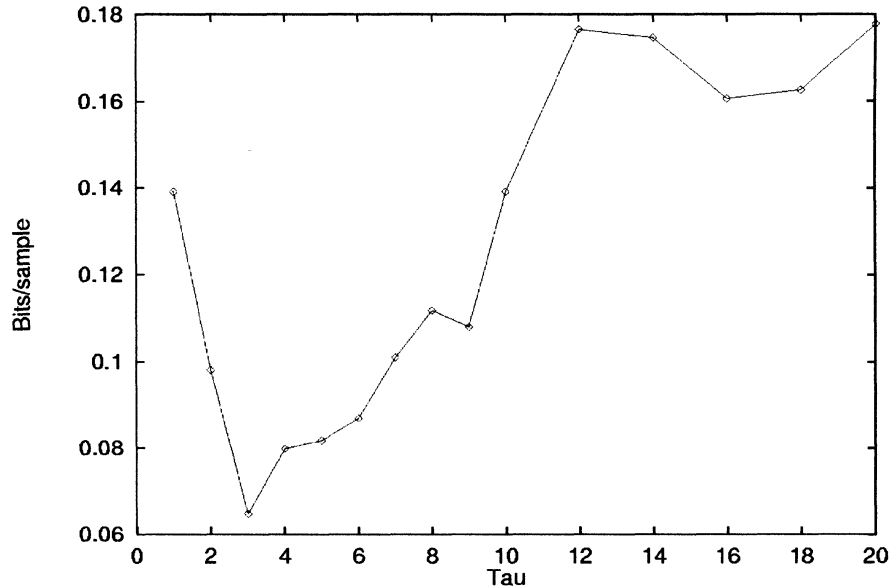


Figure 6.7 - Estimates of the largest Lyapunov exponent computed for increasing reconstruction delays.

Although all of the computations return a positive Lyapunov exponent and some of the interactive displays show the behaviour expected, the results cannot be considered conclusive. In the interactive sessions the occurrences of clearly divergent traces were too erratic to provide confidence in the existence of an invariant measure representing divergence i.e. the existence of a positive Lyapunov exponent. In the batch runs the solutions show a clear lack of stability and marked dependence on the selected values for all parameters. This inevitably leads to the conclusion that the exponent cannot be accurately estimated and in fact its existence must be brought into question. Once the existence of a positive Lyapunov exponent is doubted, the determinism of the system is also brought into question. The doubt exists for the information available, from the system, and the parameters under which the behaviour was examined. It does not rule out the possible existence of determinism completely.

### 6.3. Batch runs Using Rosenstein's Algorithm

Based on the work done using Wolf et al.'s (1985) algorithm a reconstruction delay of 4 hours (samples) was selected. Rosenstein et al. (1993) suggest that a suitable reconstruction delay may be selected using the autocorrelation function. This is implemented in their (Rosenstein et al., 1993) software using a fast Fourier transform for efficiency and returned a delay of 3 hours (samples).

In order to compute the largest Lyapunov exponent the divergence is tracked for a selected period, the  $\ln(\textit{divergence})$  is then plotted against time. Since the divergence in chaotic systems is exponential this should yield a straight line. Recall from Section 5.8 that the relationship between the slope of the straight portion of the line and *bits/sample* is given by :

$$\log_2 \lambda \approx 1.44 \ln \lambda \quad 6.1$$

By computing the average slope of the straight portion of the line and multiplying by a factor of 1.44 the rate at which information is generated (or dissipated) may be computed in terms of *bits/sample*. For the data examined in this work the slope would represent the information generated (or dissipated) by the system in units of *bits/hour*. If the divergence is tracked for too long the separation cannot continue to increase due to the bounds of the attractor, resulting in a flattening of the curve. By tracking the divergence over long periods the algorithm attempts to probe the divergence over folds in the attractor. Since the system is bounded this would result in a value that would asymptotically approach zero. Such a result reveals nothing useful about the data in terms of chaotic behaviour. It would also reveal nothing useful about the natural system being studied. By working with data interactively a suitable evolution period or 'total divergence' can be selected. All runs were performed by monitoring the evolution for

300 hours (samples). However, this was too long as the curve flattened indicating that the attractors bounds had been reached. The data is therefore presented for an evolution time of 100 hours (samples). Section 5.1 describes the algorithm in greater detail.

Reconstruction delays of 3 hours (samples) and 4 hours (samples) were used with no apparent differences in the results, those obtained using a reconstruction delay of 4 hours (samples) are presented. The mean orbital period was taken to be 12 hours (samples) throughout.

In order to estimate the largest Lyapunov exponent it is necessary to estimate the slope of the curve  $\ln(\textit{divergence})$  versus time. Sections 5.1 and 5.2 discuss this. It is required that a linear portion of the curve be identified. Figure 5.1 shows curves for various dimension of a known, chaotic system. The linear portions of the curves are evident. Figure 5.3 illustrates the computation of the slope for such portions of the curves. To relate this to values computed using Wolf et al.'s (1985) algorithm it is necessary to use the relationship given by Equation 5.8. For the water level data analysed this would then quantify the attractor in terms of information theory as discussed in Section 6.2.

Computation of the curves is performed for embedding dimensions from 3 to 10. Figure 6.8 represents the resulting curves when a reconstruction delay of 4 is used and the evolution tracked for 300 samples. Computation of the slope is then performed. In order to present the slope for the whole curve it is computed piece-wise. A 25 point 'rolling' interval is used and a least squares estimate for the slope obtained for each interval. The initial interval comprised samples 1 to 25, the second 2 to 26 through to 275 to 300. In the event of there being a linear portion to the curves this would result in a clear 'plateau' in the curve, representing a near constant slope. These slope computations are presented in Figure 6.9.

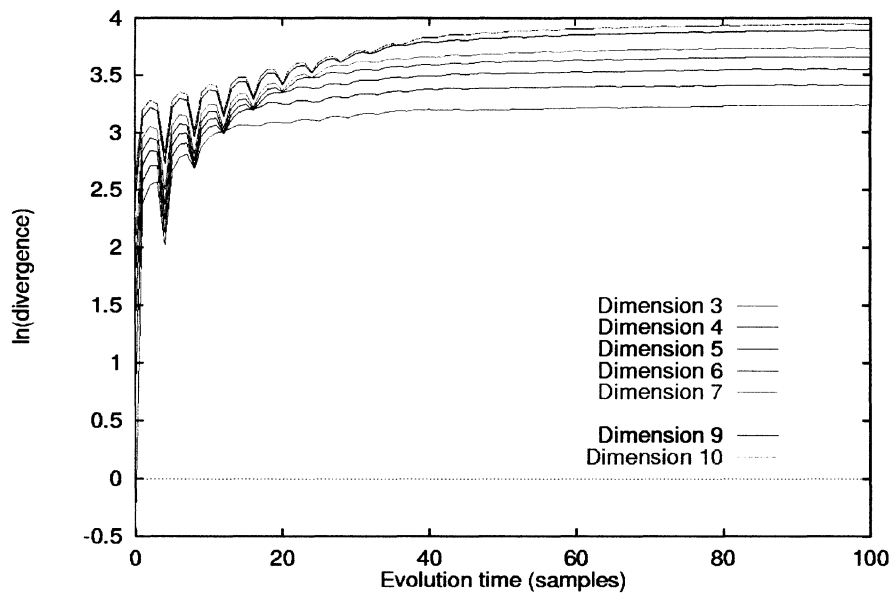


Figure 6.8 - Curves for estimating the largest Lyapunov exponent for embedding dimensions 3 to 10.

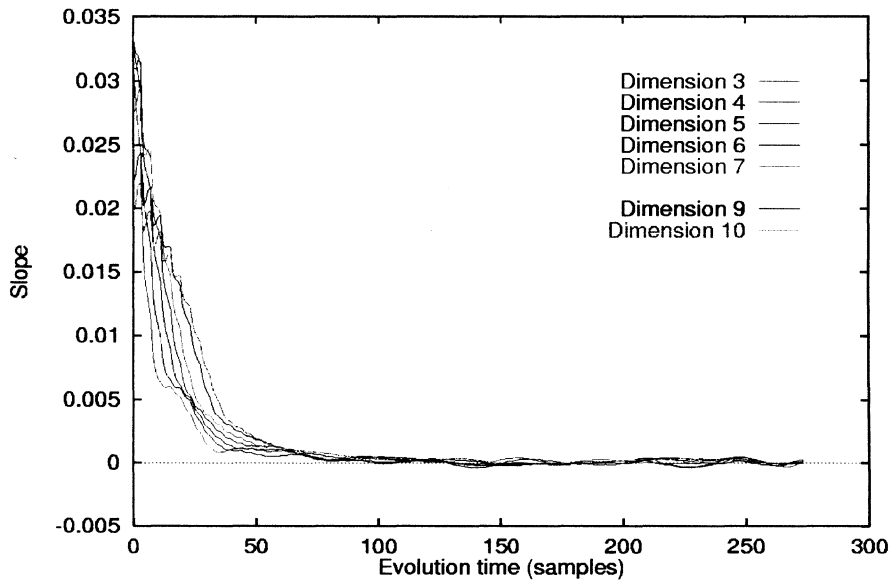


Figure 6.9 - Least squares estimates for the slope using a moving window of 25 points.

It is readily apparent from Figures 6.8 and 6.9 that the algorithm fails to return a single value for the largest exponent. Figure 6.8 would show linear portions for all

curves with a sufficiently high embedding dimension. This in turn would translate into a clear plateau in Figure 6.9 as opposed to a near constant value of 0.

Correlation dimension is simultaneously estimated as described in Section 5.1. The correlation dimension curves should exhibit a parallel, linear nature. Clearly this is absent even for the higher dimensions as seen in Figure 6.10. This introduces doubt about the existence of a positive Lyapunov exponent. The doubt exists for the information available, from the system, and the parameters under which the behaviour was examined. It does not rule out the possible existence of determinism completely.

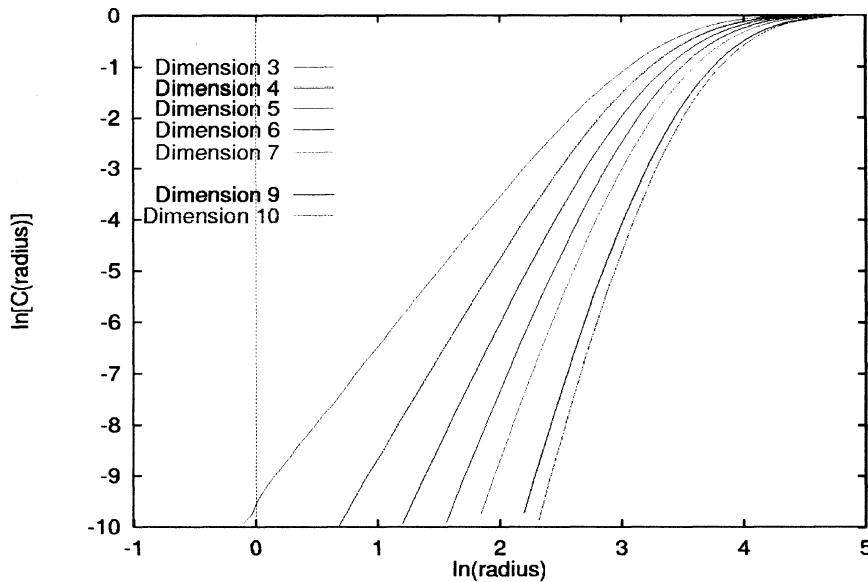


Figure 6.10 - Curves for estimation of the correlation dimension.

Despite the clear indications that the algorithm had failed to identify determinism in the solution it was decided to continue the analysis with a surrogate data set. Section 5.2 discusses the use of surrogate data sets. In all probability the time series being analysed contains both deterministic and stochastic elements. It was felt that randomising the time series and repeating the analysis would illustrate a change in behaviour which could be attributed partially to the fact that both elements exist.

## 6.4. Evaluation of a Surrogate Time Series

In order to remove any determinism from the data series and allow a comparison to the analysis using the original data set the time series was phase randomised. The choice to use phase randomisation was arbitrary. Figure 6.11 is a plot of the first 1000 points of this randomised data. Figure 3.3 shows the first 1000 points of the residual water level signal before randomisation. A comparison of Figures 6.11 and 3.3 shows the effect of randomisation and the removal of a mean period.

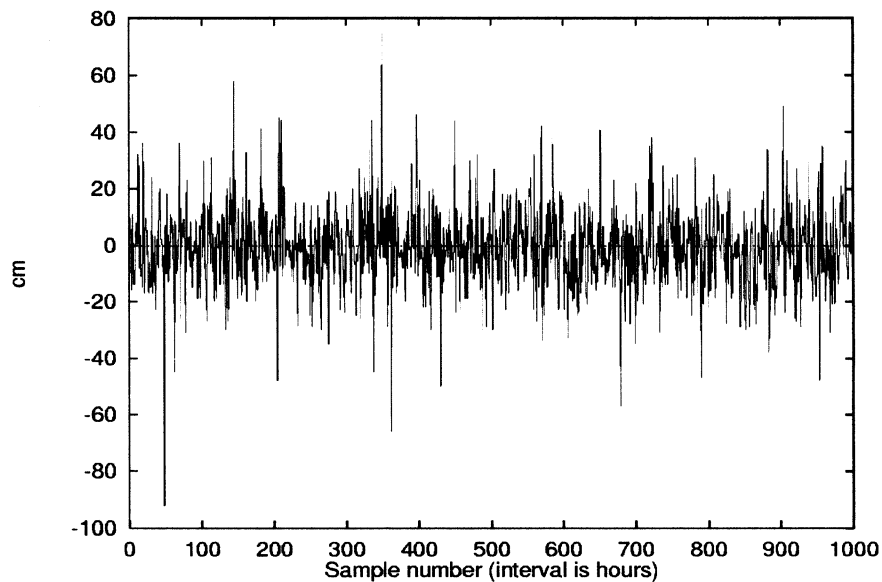


Figure 6.11 - First 1000 points of the data after phase randomising it.

Exactly the same analysis as was performed on the original data was then performed on the surrogate data set. Figures 6.12 and 6.13 show the plots used to estimate the largest exponent and the correlation dimension respectively. A comparison of these plots with those in Figures 6.8 and 6.10 show relatively little difference leading to the conclusion that the data used to generate Figures 6.8 to 6.10 (the data before randomisation) was largely stochastic in nature.

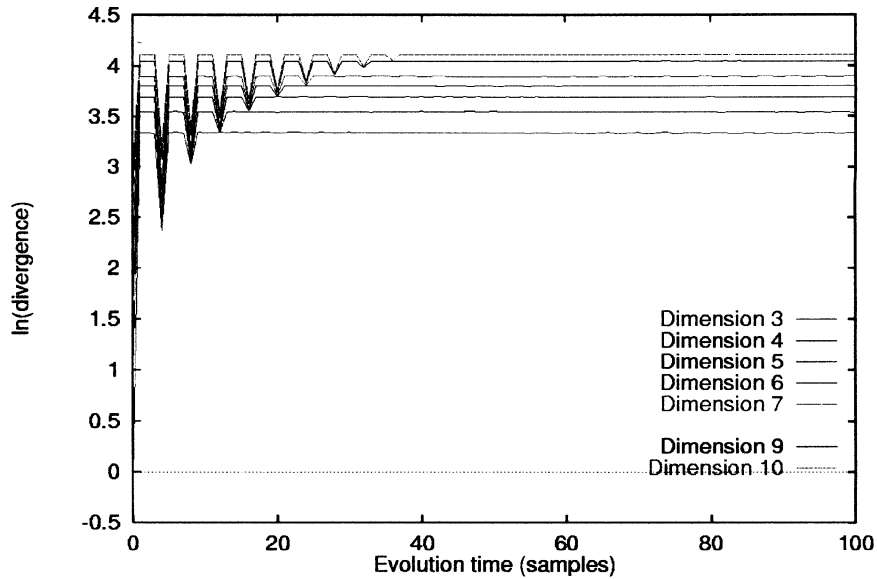


Figure 6.12 - Curves for estimating the largest Lyapunov exponent for embedding dimensions 3 to 10 and the surrogate data set.

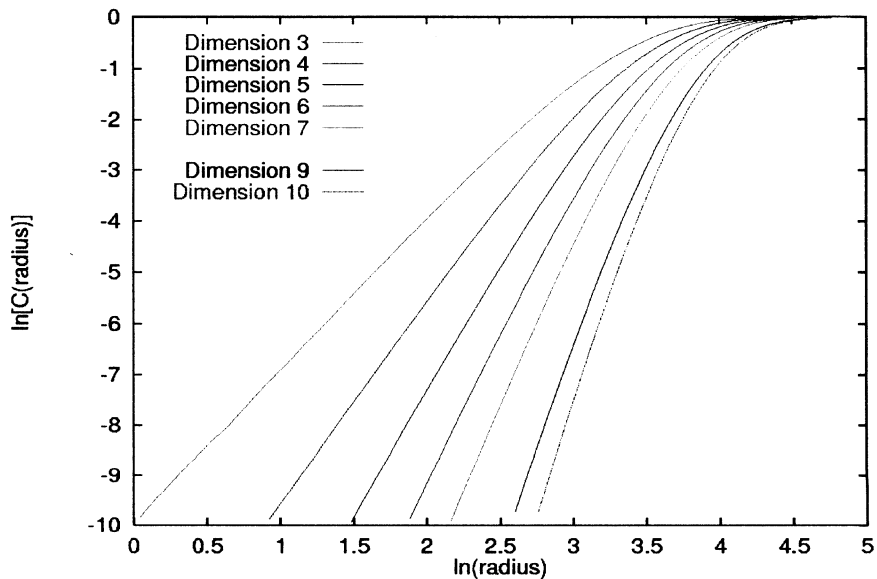


Figure 6.13 - Curves for estimation of the correlation dimension using the surrogate data set.

## 6.5. Conclusions

Although both algorithms return a positive largest exponent neither show any stability. It must therefore be concluded that neither of these methods indicate deterministic chaos in the time series analysed.

This, however, does not rule out the possibility of deterministic elements existing.

Possible reasons for their existence being masked may be :

- 1) The mean orbit has been incorrectly identified due to the data sampling interval being too infrequent.
- 2) The data are too noisy.
- 3) The determinism exists but at too high a dimension to be useful.
- 4) Performance of the algorithms is poor when used on real data.
- 5) Identification and removal of 'known' constituents is invalid.
- 6) The system's parameters vary with time.

## **6.6. Recommendations**

To progress further the author believes the following directions should be pursued.

- 1) Obtain a data set which is more frequently sampled. Frison (1997b) suggests that a sample interval as short as 7 minutes may be required.
- 2) There have been advances in the algorithms used. Significant improvements in the performance of algorithms when applying them to real world data have been achieved. Obtain and make use of more sophisticated software. Possibly from Abarbanel (1996) as he discusses the availability in the preface to his book.
- 3) In Section 3.2.3 the possibility of a structure variable system is mentioned. The possibility that the Bay of Fundy tides comprise such a system is worth pursuing. Fang and Cao (1995) may provide a starting point for such an investigation.



4) The existence of transients, as mentioned in Section 3.2.3, could be investigated. Approaches have been proposed to cope with these types of data and may include the investigation of windowed exponents and local Lyapunov exponents. Ricard and Bascompt (1993) may provide a starting point for such an investigation.

## References

- Abarbanel, H.D.I. (1996). *Analysis of Observed Chaotic Data*. Springer, New York.
- Arizmendi, C. M., J. R. Sanchez and M. A. Foti (1995). "Randomness in Airborne Pollen: Chaos or Noise?" *Fractals*, Vol. 3, No. 1, pp. 155-160.
- Baker G. L. and J. P. Gollub (1996). *Chaotic dynamics an introduction*. 2nd ed. Press Syndicate of the University of Cambridge, New York.
- Bendat, J.S. and A.G. Piersol (1986). *Random Data Analysis and Measurement Procedures*. 2nd ed. John Wiley & Sons, New York.
- Bergamasco, L., M. Serio and A. R. Osborne (1995). "Finite Correlation dimension and Positive Lyapunov Exponents for Surface Wace Data in the Adriatic Sea near Venice." *Fractals*, Vol. 3, No. 1, pp. 55-78
- Brock, W.A. (1986). "Distinguishing random and deterministic Systems: Abridged Version." *Journal of Economic Theory*, Vol. 40, pp. 168-195.
- Carrera, G. (1995). "A Statistical Survey of Tidal Water Levels Predicted by the Canadian Tide and Current tables for the East Coast of Canada." Contract report prepared by Geometrix - Geodetic & Hydrographic Reaserach Inc, for the Canadian Hydrographic Service. pp.63.
- Casti, J.L. (1989). *Alternate Realities Mathematical Models of Nature and Man*. John Wiley & Sons, New York.
- Casti, J.L. (1992). *Reality Rules: 1 Picturing the World in Mathematics -The Fundamentals-*. John Wiley & Sons, New York.
- Cuomo, V., Serio C., Crisciani F. and Ferraro A (1994). "Discriminating randomness from chaos with application to a weather time series." *Tellus Series A-Dynamic Meteorology and Oceanography*, Vol. 46, No. 3, pp. 299-313.
- Crutchfield, J., D. Farmer, N. Packard, R. Shaw, G. Jones and R.J. Donnelly (1980). "Power Spectral Analysis of a Dynamical System." *Physical Letters*, Vol. 76A, No. 1, pp. 1-4
- Eckmann, J. P. and D. Ruelle (1985). "Ergodic theory of chaos and strange attractors." *Reviews of Modern Physics*, Vol. 57, No. 3, Part 1, pp. 617-656.

- Eckmann, J. P. and D. Ruelle (1992). "Fundamental limitations for estimating dimensions and Lyapunov exponents in dynamical systems." *Physica D*, Vol. 56 pp. 185-187.
- Eckmann, J. P., S. O. Kamphorst, D. Rulle and S. Ciliberto (1986). "Liapunov [sic] exponents from time series." *Physical Review A*, Vol. 34, No. 6, pp. 4971-4979.
- Fowler, A. D. and D. E. Roach (1993). "Dimensionality Analysis of Time-Series Data: Nonlinear Methods." *Computers and Geosciences*, Vol. 19, No. 1, pp. 41-52.
- Frank, G. W., T. Lookman, M. A. H. Nerenberg, C. Essex, J. Lemieux and W. Blume (1990). "Chaotic time series analysis of epileptic seizures." *Physica D*, Vol. 46 pp. 427
- Frison, T. (1997a). "Fun with Fundy." Personal e-mail, ted@chaotic.com, Randle, Inc., Great Falls, VA 22066, 13 March.
- Frison, T. (1997b). "It's all in the exponents." Personal e-mail, ted@chaotic.com, Randle, Inc., Great Falls, VA 22066, 14 March.
- Frison, T. (1997c). "Tide paper." Personal e-mail, ted@chaotic.com, Randle, Inc., Great Falls, VA 22066, 7 September.
- Gleick, J. (1988). *Chaos Making a New Science*. Penguin Books, New York.
- Godin G. (1994). "Confirmation of the Trends Suspected to be Present in the Tide of the Bay of Fundy." *International Hydrographic Review*, September 1994, Vol. 71, pp. 103-117.
- Grassberger, P. and I. Procaccia (1983). "Characterization of strange attractors." *Physical Review Letters*, Vol. 50, No. 5, pp. 346-349.
- Grebogi, C., E. Ott, S. Pelikan and J. A. Yorke (1984). "Strange Attractors that are not Chaotic." *Physica D*, Vol. 13 pp. 261-268.
- Gunaratne, G. D. (1994) *Spectral Analysis of Long Gappy Tidal Records: A Comparison of Two Algorithms*. M.Eng. thesis, Department of Surveying Engineering, University of New Brunswick, Fredericton, N.B., Canada, 115 pp.
- Kugiumtzis D., B. Lillekjendlie, and N. Christophersen (1994). "Chaotic time series Part 1 : Estimation of some invariant properties in state space." *Modeling, Identification and Control*, Vol. 15, No. 4, pp. 205-224.
- Lloyd, A. L. and D. Lloyd (1995). "Chaos: Its Significance and detection in Biology." *Biological Rhythm Research*, Vol. 26, No. 2, pp. 233-252.

Lorenz, E. N. (1963). "Deterministic Nonperiodic Flow." *Journal of Atmospheric Sciences*, Vol. 20, pp. 130-141.

*Mathematics Dictionary* (1992). "James and James." 5th ed., Chapman and Hall, New York.

MathSoft Inc. (1993). *Mathcad 4.0*, Cambridge, Massachusetts, USA.

Merry, C. L. and P. Vaníček (1993). "Investigation of Local Variations of Sea-surface Topography." *Marine Geodesy*, Vol. 7, No. 1-4, pp. 101-126.

Ouchi, T. (1993). "Population Dynamics of earthquakes and Mathematical Modeling." *Pure and Applied Geophysics*, Vol. 140, No. 1, pp 15-28.

Packard, N., J. Crutchfield, J. D. Farmer, and R. Shaw (1980). "Geometry from a time series." *Physical Review Letters*, Vol. 45 pp. 712-716.

Pugh, D.T. (1996). *Tides, Surges and Mean Sea-Level*. John Wiley & Sons Ltd. New York

Rosenstein, M. T., J. J. Collins and C. J. De Luca (1993). "A practical method for calculating largest Lyapunov exponents from small data sets." *Physica D*, Vol. 65, pp. 117-134.

Ruelle, D. (1989). *Chaotic Evolution and Strange Attractors*. University Press, Cambridge, UK.

Sprott, J. C. (1996). *Sprott's Fractal Gallery*. University of Wisconsin. <http://sprott.physics.wisc.edu/fractals.htm>.

Takens, F. (1981). *Dynamical Systems and Turbulence, Warwick 1980*. Eds. D. Rand and L. S. Young, Springer, Berlin.

Thompson, R. E. (1981). *Oceanography of the British Columbia Coast*. Canadian Special Publication of Fisheries and Aquatic Sciences 56, Department of Fisheries and Oceans.

US Department of Commerce (n.d.). *Our restless tides*. Available from the Superintendent of Documents.

Vaníček, P. and E. J. Krakiwsky (1986). *Geodesy: The Concepts*. 2nd rev. ed., North-Holland, Amsterdam

Wells, D. E., P. Vaníček and S. Pagiatakis (1985). *Least Squares Analysis Revisited*. Technical Report No. 84, Department of Surveying Engineering, University of New Brunswick, Fredericton, N.B., Canada.

Weltner, K., J. Grosjean, P. Schuster, and W.J. Weber (1991). *Mathematics for Engineers and Scientists*. Stanley Thornes (Publishers) Ltd, Leckhampton, England.

Williams, T. and Kelley, C. (1993). *GNUPLOT, an interactive plotting program*. University of Dartmouth, <http://www.cs.dartmouth.edu/gnuplot/gnuplot.html>.

Wolf, A., J. B. Swift, H. L. Swinney, and J. A. Vastano (1985). "Determining Lyapunov exponents from a time series." *Physica D*, Vol. 16, pp. 285-317.

Wolf, A. (1995). *Alan Wolf's Home Page*. The Department of Physics, The Cooper Union, <http://www.users.interport.net/~wolf>.

Yan, J. (1993). "Ray chaos in underwater acoustics in view of local instability." *Journal of the Acoustical Society of America*, Vol. 94 (5), pp. 2739-2745.

## Bibliography

Box, G.E.P and G.M. Jenkins (1976). *Time Series Analysis Forecasting and Control*. Holden-Day Inc., San Francisco.

Brown, R., N. F. Rulkov and E. R. Tracy (1994). "Modeling and synchronizing chaotic systems from time-series data." *Physical Review E*, Vol. 49, No. 5, pp. 3784-49.

Cao, L., Y. Hong, H. Fang and G. He (1995). "Predicting chaotic time series with wavelet networks." *Physica D*, Vol. 85, No. 1-2, pp. 225-238.

Carrera, G. (1995). "A Statistical Survey of Tidal Water Levels Predicted by the Canadian Tide and Current Tables for the East Coast of Canada." *Contract Report for the Canadian Hydrographic Service, Atlantic Region, May 1995*. pp63.

Chui, K. C. (1992). *An Introduction to Wavelets*. Academic Press, Inc, New York.

Cortini, M. and Barton C. C. (1993). "Nonlinear Forecasting analysis of inflation-deflation patterns of an active caldera (Campi Flegrei, Italy)." *Geology*, Vol. 21, pp. 239-242.

Egolf, D. A. and H. S. Greenside (1994). "Relation between fractal dimension and spatial correlation length for extensive chaos." *Nature*, Vol. 369, pp. 129-131.

Fang, H. P. and L. Y. Cao (1995). "Predicting and characterizing data sequences from structure-variable systems." *Physical Review E*, Vol. 51, No. 6, pp. 6254-6257.

Gao, J. and Z. Zheng (1994). "Direct dynamical test for deterministic chaos." *Europhysics Letters*, Vol. 25, No. 7, pp. 485-490.

Gilmore, C. G. (1993). "A new test for chaos." *Journal of Economic Behavior and Organization*, Vol. 22, pp. 209-237

Hoppenstead, F.C. (1993). *Analysis and Simulation of Chaotic Systems*. Springer-Verlag New York Inc.

Hubbard, J.H. and B.H. West (1995). *Differential equations: A Dynamical Systems Approach, Higher-Dimensional Systems*. Springer-Verlag, New York, Inc.

Kadtke, J. (1995). "Classification of highly noisy signals using global dynamic models." *Physics Letters A*, Vol. 203, No. 4, pp. 196-202.

Kang, S. K, Chung J., Lee S. and Yum K. (1995). "Seasonal variability of the M<sub>2</sub> tide in the seas adjacent to Korea." *Continental Shelf Research*, Vol. 15, No. 9, pp. 1087-1113.

Kesaraju, R. V. and S. T. Noah (1994). "Characterization and Detection of Parameter Variations of Nonlinear Mechanical Systems." *Nonlinear Dynamics*, Vol. 6, No. 4, pp. 433-457.

Kugiumtzis, D., B. Lillekjendlie and N. Christophersen (1994). "Chaotic time series Part II System identification and prediction." *Modeling, Identification and Control*, Vol. 15, No. 4, pp. 225-243.

Lichtenberg, A.J. and M.A. Lieberman (1983). *Regular and Stochastic Motion*. Springer-Verlag, New York, Inc.

Navone, H. D. and H. A. Ceccatto (1995). "Forecasting chaos from small data sets: a comparison of different nonlinear algorithms." *Journal of Physics A-Mathematical and General*, Vol. 28, pp. 3381-3388.

Solét, R. V. and J. Bascompte (1995). "Measuring Chaos from Spatial Information." *Journal of Theoretical Biology*, Vol. 175, No. 2, pp. 139-147.

Tanaka, N., H. Okamoto and M. Naito (1995a). "An Optimal Metric for Predicting Chaotic Time Series." *Japanese Journal of Applied Physics, Part 1.*", Vol. 34, No. 1, pp.388-394.

Tanaka, N., H. Okamoto and M. Naito (1995b). "A Way of Distinguishing Chaos from Random Fractal Sequences Based on the Difference in Time Reversal Symmetry." *Japanese Journal of Applied Physics, Part 2-Letters*, Vol. 34, No. 7A, pp. L863-L865.

## Appendix A

### A.1. Data Sample

The first 50 points of the time series used are presented. In the original file the data were presented with records containing date and time. This information was stripped and a pseudo time added. Column 1 represents the time; the sample interval is 1 hour. Column 2 represents the tidal reading in centimetres. In order to simplify the analysis in LSSA the mean was subtracted from the data series, resulting in a zero mean time series. This explains the number of decimal places in the data as it was not read to this accuracy. Readings were made at the centimeters level.

<u>Pseudo time</u>	<u>Reading in cm</u>
1000001	-237.97985
1000002	-126.97985
1000003	7.0201541
1000004	132.02015
1000005	213.02015
1000006	228.02015
1000007	178.02015
1000008	86.020154
1000009	-35.979846
1000010	-163.97985
1000011	-260.97985
1000012	-300.97985
1000013	-262.97985
1000014	-178.97985
1000015	-51.979846
1000016	74.020154
1000017	179.02015
1000018	217.02015
1000019	194.02015
1000020	118.02015
1000021	12.020154
1000022	-123.97985
1000023	-242.97985
1000024	-312.97985
1000025	-309.97985
1000026	-230.97985
1000027	-114.97985



1000028	24.020154
1000029	162.02015
1000030	226.02015
1000031	260.02015
1000032	210.02015
1000033	105.02015
1000034	-21.979846
1000035	-157.97985
1000036	-259.97985
1000037	-295.97985
1000038	-259.97985
1000039	-163.97985
1000040	-35.979846
1000041	103.02015
1000042	211.02015
1000043	260.02015
1000044	234.02015
1000045	146.02015
1000046	37.020154
1000047	-105.97985
1000048	-239.97985
1000049	-291.97985
1000050	-279.97985

## Appendix B

### B.1. LSSA Command File

The command file used for the final LSSA run is given below.

```
LSSA Output:\mathcad\work\sj_30th.dat      Input data file name
e:\fortran\lssa\ident\id26.OUT           Output listing file name
e:\fortran\lssa\ident\id26.PLT           Output plot data file name
BATCH                                     Mode (BATCH or SQNTL)
EQ                                         Equal or UNEqual space series
N                                         Plot time series? (Y or N)
0                                         Datum biases (#,times of biases)
0                                         Linear trend switch (0=off,1=on)
78 163160.725 81580.363 10407.000 8766.231 4382.906 4268.250 661.309 354.367
327.859 12.42060 12.65834 12.00000 23.93447 25.81934 11.96723 12.19162 12.62600
12.90537 24.06589 12.22177 12.43822 12.01645 6.21030 4.14020 12.4030 26.86836
4.09239 4.11400 4.16628 4.19270 6.10334 6.15155 6.26917 6.32917 8.27952 8.38630
11.57629 11.60695 11.78613 11.98360 12.45590 12.69501 12.87176 13.08807
13.12727 13.35233 13.39313 13.63226 26.72305 11.418 11.512 11.602 11.621 11.650
11.764 11.784 11.848 11.886 11.957 12.026 12.087 12.130 12.151 12.169 12.232
12.276 12.344 12.370 12.430 12.452 12.482 12.503 12.547 12.595 13.171 12.6466
12.912 12.42515                          Forced periods (#,periods)
0                                         User function switch (0=no,1=yes)
25.00 .5000                               Cutoff for listing st.dev. and corr.
1 30 2 2000                               Band #, longest, shortest, # periods
```

### B.2. LSSA Output

The first portion of the LSSA output file is listed below. What has been removed are the listings of the residuals and the power for each of the 2000 periods used in the analysis.

```
-----
LSSA: Least Squares Spectral Analysis
      Version 3 (05 Mar 91)
-----

Saint John tidal data 1947 - 1968

INPUT COMMAND FILE                          : ident.cmd
```

```

INPUT DATA FILE           : e:\mathcad\work\sj_30th.dat

OUTPUT LISTING FILE       : e:\fortran\lssa\ident\id26.OUT

OUTPUT PLOT DATA FILE   : e:\fortran\lssa\ident\id26.PLT

MODE                       : BATCH
TIME SERIES SPACING       : EQ
PLOT TIME SERIES ?       : N
NO. OF DATUM BIASES      :      0
LINEAR TREND SWITCH (0=OFF,1=ON) :      0
NO. OF FORCED PERIODS    :      78
VALUES OF FORCED PERIODS 163160.7250000000000000
                        81580.3630000000000000
                        10407.0000000000000000
                        8766.2310000000000000
                        4382.9060000000000000
                        4268.2500000000000000
                        661.3090000000000000
                        354.3670000000000000
                        327.8590000000000000
                        12.4206000000000000
                        12.6583400000000000
                        12.0000000000000000
                        23.9344700000000000
                        25.8193400000000000
                        11.9672300000000000
                        12.1916200000000000
                        12.6260000000000000
                        12.9053700000000000
                        24.0658900000000000
                        12.2217700000000000
                        12.4382200000000000
                        12.0164500000000000
                        6.2103000000000000
                        4.1402000000000000
                        12.4030000000000000
                        26.8683600000000000
                        4.0923900000000000
                        4.1140000000000000
                        4.1662800000000000
                        4.1927000000000000
                        6.1033400000000000
                        6.1515500000000000
                        6.2691700000000000
                        6.3291700000000000
                        8.2795200000000000
                        8.3863000000000000
                        11.5762900000000000
                        11.6069500000000000
                        11.7861300000000000
                        11.9836000000000000
                        12.4559000000000000
                        12.6950100000000000
                        12.8717600000000000
                        13.0880700000000000
                        13.1272700000000000
                        13.3523300000000000

```

	13.3931300000000000
	13.6322600000000000
	26.7230500000000000
	11.4180000000000000
	11.5120000000000000
	11.6020000000000000
	11.6210000000000000
	11.6500000000000000
	11.7640000000000000
	11.7840000000000000
	11.8480000000000000
	11.8860000000000000
	11.9570000000000000
	12.0260000000000000
	12.0870000000000000
	12.1300000000000000
	12.1510000000000000
	12.1690000000000000
	12.2320000000000000
	12.2760000000000000
	12.3440000000000000
	12.3700000000000000
	12.4300000000000000
	12.4520000000000000
	12.4820000000000000
	12.5030000000000000
	12.5470000000000000
	12.5950000000000000
	13.1710000000000000
	12.6466000000000000
	12.9120000000000000
	12.4251500000000000
USER-DEFINED FUNCTION SWITCH (0=OFF,1=ON) :	0
LEVEL FOR LISTING OUTSTANDING ST.DEV. (%) :	25.0000000000000000
LEVEL FOR LISTING OUTSTANDING CORRELATIONS :	5.0000000000000000E-001
SPECTRAL BAND LABEL :	1
LONGEST PERIOD :	30.0000000000000000
SHORTEST PERIOD :	4.0000000000000000

NO. OF PERIODS

2000

SOLUTION FOR KNOWN CONSTITUENTS

NUMBER	DATUM BIAS	LINEAR TREND	FORCED PERIOD	COSINE TERM	SINE TERM	USER DEFINED	AMPLITUDE (SIGMA)	PHASE (SIGMA)
	0	0	78	78	78	0		
1- 2			163160.725	.169E+02	-.102E+02		.198E+02 ( .673E+01)	328.80 ( 7.57)
3- 4			81580.363	-.655E+01	-.663E+01		.932E+01 ( .362E+01)	225.35 ( 10.56)
5- 6			10407.000	-.398E+01	.384E+00		.400E+01 ( .182E+00)	174.49 ( 2.64)
7- 8			8766.231	-.285E+01	.283E+01		.402E+01 ( .178E+00)	135.21 ( 2.45)
9- 10			4382.906	-.198E+01	-.988E+00		.221E+01 ( .409E+00)	206.56 ( 10.00)
11- 12			4268.250	.606E+00	.523E+01		.526E+01 ( .403E+00)	83.39 ( 4.27)
13- 14			661.309	.115E+01	-.601E+00		.130E+01 ( .123E+00)	332.39 ( 5.46)
15- 16			354.367	-.599E+00	.252E+00		.650E+00 ( .123E+00)	157.19 ( 10.90)
17- 18			327.859	-.143E+00	.868E-01		.167E+00 ( .124E+00)	148.68 ( 42.41)
19- 20			12.421	.270E+03	-.119E+03		.295E+03 ( .127E+00)	336.25 ( .02)
21- 22			12.658	-.572E+02	-.268E+02		.632E+02 ( .124E+00)	205.12 ( .11)
23- 24			12.000	-.368E+02	.347E+02		.506E+02 ( .125E+00)	136.67 ( .14)
25- 26			23.934	.133E+02	.984E+01		.166E+02 ( .124E+00)	36.42 ( .43)
27- 28			25.819	-.121E+02	-.628E+01		.136E+02 ( .123E+00)	207.44 ( .52)
29- 30			11.967	.172E+02	.474E+01		.179E+02 ( .124E+00)	15.36 ( .40)
31- 32			12.192	.110E+02	-.155E+02		.190E+02 ( .124E+00)	305.45 ( .37)
33- 34			12.626	.938E+01	-.106E+02		.142E+02 ( .124E+00)	311.49 ( .50)
35- 36			12.905	.311E+01	.629E+01		.702E+01 ( .125E+00)	63.66 ( 1.02)
37- 38			24.066	.513E+01	-.937E-01		.513E+01 ( .124E+00)	358.95 ( 1.38)
39- 40			12.222	-.486E+01	-.174E+01		.516E+01 ( .124E+00)	199.72 ( 1.37)
41- 42			12.438	-.439E+01	.597E+00		.443E+01 ( .131E+00)	172.26 ( 1.69)
43- 44			12.016	.116E+01	.388E+01		.405E+01 ( .124E+00)	73.40 ( 1.76)
45- 46			6.210	-.413E+01	.994E+00		.425E+01 ( .123E+00)	166.47 ( 1.67)
47- 48			4.140	-.206E+01	-.184E+01		.276E+01 ( .123E+00)	221.77 ( 2.56)

49- 50	12.403	.222E+01	.282E+00	.224E+01	( .125E+00)	7.26	( 3.20)
51- 52	26.868	.514E+00	.258E+01	.263E+01	( .124E+00)	78.74	( 2.69)
53- 54	4.092	.112E+01	-.744E+00	.135E+01	( .123E+00)	326.46	( 5.25)
55- 56	4.114	.738E-01	-.236E+00	.247E+00	( .123E+00)	287.35	( 28.60)
57- 58	4.166	-.148E+01	.932E+00	.175E+01	( .123E+00)	147.78	( 4.05)
59- 60	4.193	-.158E+00	-.364E+00	.397E+00	( .123E+00)	246.50	( 17.82)
61- 62	6.103	.950E+00	-.101E+01	.139E+01	( .123E+00)	313.27	( 5.10)
63- 64	6.152	-.187E+00	.341E+00	.389E+00	( .123E+00)	118.69	( 18.21)
65- 66	6.269	.103E+01	.138E+01	.172E+01	( .123E+00)	53.14	( 4.11)
67- 68	6.329	.229E-01	-.349E+00	.350E+00	( .123E+00)	273.75	( 20.21)
69- 70	8.280	-.187E+00	-.330E+00	.380E+00	( .123E+00)	240.49	( 18.63)
71- 72	8.386	-.274E+00	-.109E+01	.113E+01	( .123E+00)	255.94	( 6.27)
73- 74	11.576	.300E+00	.691E+00	.753E+00	( .124E+00)	66.56	( 9.41)
75- 76	11.607	-.579E+00	-.648E-02	.579E+00	( .124E+00)	180.64	( 12.29)
77- 78	11.786	-.142E+01	.135E+01	.196E+01	( .170E+00)	136.33	( 4.97)
79- 80	11.984	-.590E+00	-.294E+00	.660E+00	( .125E+00)	206.50	( 10.84)
81- 82	12.456	.747E+00	-.136E+01	.155E+01	( .131E+00)	298.79	( 4.83)
83- 84	12.695	.433E+00	-.107E+00	.446E+00	( .124E+00)	346.10	( 15.86)
85- 86	12.872	.130E+01	-.231E+01	.265E+01	( .124E+00)	299.45	( 2.67)
87- 88	13.088	.381E+00	-.343E-01	.383E+00	( .124E+00)	354.86	( 18.49)
89- 90	13.127	-.726E+00	.165E+01	.181E+01	( .124E+00)	113.68	( 3.92)
91- 92	13.352	.292E+00	-.134E+00	.322E+00	( .124E+00)	335.42	( 22.01)
93- 94	13.393	.608E+00	.273E+00	.667E+00	( .124E+00)	24.15	( 10.62)
95- 96	13.632	-.405E+00	-.600E-01	.409E+00	( .123E+00)	188.43	( 17.28)
97- 98	26.723	-.441E+00	.304E+00	.536E+00	( .123E+00)	145.43	( 13.21)
99-100	11.418	-.105E+00	-.329E+00	.345E+00	( .124E+00)	252.20	( 20.51)
101-102	11.512	-.126E+00	-.622E-01	.141E+00	( .124E+00)	206.24	( 50.28)
103-104	11.602	-.604E+00	.169E-01	.604E+00	( .124E+00)	178.39	( 11.78)
105-106	11.621	-.128E+00	-.235E+00	.268E+00	( .124E+00)	241.39	( 26.46)
107-108	11.650	.270E+00	.133E+00	.301E+00	( .124E+00)	26.27	( 23.59)
109-110	11.764	.909E-02	.256E+00	.256E+00	( .124E+00)	87.97	( 27.66)
111-112	11.784	-.853E-01	-.418E-03	.853E-01	( .170E+00)	180.28	(114.22)
113-114	11.848	-.416E+00	.123E+00	.434E+00	( .124E+00)	163.52	( 16.31)
115-116	11.886	-.716E-02	.746E+00	.746E+00	( .124E+00)	90.55	( 9.49)
117-118	11.957	.291E+00	-.334E+00	.444E+00	( .124E+00)	311.06	( 16.02)
119-120	12.026	-.116E-01	-.134E+00	.134E+00	( .124E+00)	265.05	( 52.89)
121-122	12.087	-.396E+00	.555E+00	.682E+00	( .124E+00)	125.49	( 10.39)
123-124	12.130	-.283E+00	.116E+00	.306E+00	( .124E+00)	157.72	( 23.17)

125-126	12.151	-.255E+00	.664E+00	.712E+00 (	.124E+00)	111.00	(	10.00)
127-128	12.169	-.579E-01	.208E-02	.580E-01 (	.124E+00)	177.95	(	122.85)
129-130	12.232	.114E+00	-.332E+00	.351E+00 (	.124E+00)	288.93	(	20.21)
131-132	12.276	.351E+00	.670E+00	.756E+00 (	.124E+00)	62.36	(	9.37)
133-134	12.344	-.366E-01	.423E+00	.425E+00 (	.124E+00)	94.94	(	16.67)
135-136	12.370	-.857E-01	-.868E+00	.873E+00 (	.124E+00)	264.36	(	8.13)
137-138	12.430	.215E+00	-.571E+00	.610E+00 (	.128E+00)	290.59	(	12.05)
139-140	12.452	-.758E+00	-.535E+00	.928E+00 (	.132E+00)	215.22	(	8.13)
141-142	12.482	-.637E+00	.243E-01	.637E+00 (	.124E+00)	177.81	(	11.13)
143-144	12.503	-.487E+00	-.371E+00	.612E+00 (	.124E+00)	217.32	(	11.58)
145-146	12.547	-.930E+00	.217E+00	.955E+00 (	.124E+00)	166.86	(	7.42)
147-148	12.595	.424E-01	-.276E+00	.279E+00 (	.124E+00)	278.75	(	25.41)
149-150	13.171	.523E+00	-.746E+00	.912E+00 (	.124E+00)	305.05	(	7.77)
151-152	12.647	.547E+00	-.319E+00	.633E+00 (	.124E+00)	329.75	(	11.23)
153-154	12.912	.274E+01	.140E+01	.308E+01 (	.125E+00)	27.03	(	2.33)
155-156	12.425	-.234E+01	.287E+01	.370E+01 (	.127E+00)	129.22	(	1.97)

OUTSTANDING STANDARD DEVIATIONS OF KNOWN CONSTITUENTS  
(LARGER THAN 25.0 % OF ESTIMATED MAGNITUDE)

NUMBER STANDARD DEVIATION

1	.707E+01
4	.369E+01
6	.184E+00
10	.391E+00
11	.391E+00
16	.124E+00
17	.124E+00
18	.124E+00
38	.124E+00
50	.125E+00
55	.123E+00
56	.123E+00
59	.123E+00
60	.123E+00
63	.123E+00
64	.123E+00
67	.123E+00
68	.123E+00
69	.123E+00
70	.123E+00
71	.123E+00
73	.124E+00
76	.124E+00
80	.125E+00
83	.124E+00
84	.124E+00
87	.124E+00
88	.124E+00
91	.124E+00
92	.124E+00
94	.124E+00
95	.123E+00
96	.124E+00
97	.123E+00
98	.124E+00
99	.124E+00
100	.124E+00
101	.124E+00
102	.124E+00
104	.124E+00
105	.124E+00
106	.124E+00
107	.124E+00
108	.124E+00
109	.124E+00
110	.124E+00
111	.170E+00
112	.170E+00
113	.124E+00
114	.124E+00
115	.124E+00
117	.124E+00
118	.124E+00



119	.124E+00
120	.124E+00
121	.124E+00
123	.124E+00
124	.124E+00
125	.124E+00
127	.124E+00
128	.124E+00
129	.124E+00
130	.124E+00
131	.124E+00
133	.124E+00
134	.124E+00
135	.124E+00
137	.128E+00
142	.124E+00
143	.124E+00
144	.124E+00
146	.124E+00
147	.124E+00
148	.124E+00
152	.124E+00

OUTSTANDING CORRELATIONS BETWEEN KNOWN CONSTITUENTS  
(LARGER IN ABSOLUTE VALUE THAN .50)

NUMBER	CORRELATION
1- 2	-.89624592
1- 3	-.89429985
1- 4	-.99775900
1- 6	-.56790736
2- 3	.99726391
2- 4	.87066392
2- 6	.54568585
3- 4	.86955151
3- 6	.53613124
4- 6	.55490796
5- 8	-.70335286
6- 7	.65789060
9- 12	-.93746551
10- 11	.92854799
77-111	.62753286
78-112	.62744163

## Appendix C - Source Listings after Wolf et al. (1985).

### C.1. Source listing for BASGEN

```
$LARGE
$NOFLOATCALLS
$NODEBUG
c
c THE ABOVE STATEMENT IS ONLY REQUIRED FOR MICROSOFT FORTRAN
c COMPILER FOR IBM PC. IF PC WITH MATH CHIP IS USED PERFORMANCE
c IS IMPROVED IF RECOMPILED WITH $NOFLOATCALLS OPTION.
c
  program basgen
c
  parameter (maxdat=32000,maxbox=6000,maxdim=8)
c
  integer*2 nxtbox(maxbox,maxdim),where(maxbox,maxdim)
  integer*2 datptr(maxbox),nxtdat(maxdat),target(maxdim)
  integer*4 tau,datcnt,boxcnt,runner,chaser,used
  dimension data(maxdat)
          logical tru
c
c      storage requirements: 2*maxdat + maxbox*(2*maxdim+1)
c
  write(*,111)
111  format(1x,'ASCII data file=1 : ',\ )
  read(*,*) iform
  write(*,222) maxdat
222  format(1x,'number of data points (<=,i7,') : ',\ )
  read(*,*) datcnt
c
  if(iform.eq.1) then
    open(unit=1,file='data.',status='old')
      inquire(file='t.1',exist=tru)
      if(tru) then
        open(unit=2,file='t.1')
        close(unit=2,status='delete')
      endif
    open(unit=2,file='t.1',form='unformatted')
    do 10 i=0,(datcnt/8)-1
      read(1,*) (data(8*i+j),j=1,8)
      write(2) (data(8*i+j),j=1,8)
10    continue
    close(unit=1)
    close(unit=2)
  else
    open(unit=1,file='t.1',status='old',form='unformatted')
    do 20 i=0,(datcnt/8)-1
      read(1) (data(8*i+j),j=1,8)
20    continue
    close(unit=1)
```

```

endif
c
datmin=data(1)
datmax=data(1)
do 30 i=1,datcnt
    datmin=amin1(datmin,data(i))
    datmax=amax1(datmax,data(i))
30    continue
c ENLARGE GRID SO NO POINTS ON OUTER BOUNDARY
    datmin=datmin-.01*(datmax-datmin)
    datmax=datmax+.01*(datmax-datmin)
c
40    write(*,333)
333    format(1x,'time delay (samples) : ',\ )
    read(*,*) tau
    write(*,444) maxdim
444    format(1x,'embedding dimension (<=',i4,') : ',\ )
    read(*,*) ndim
    write(*,555) maxbox
555    format(1x,'grid resolution (maxbox =',i7,') : ',\ )
    read(*,*) ires
c
    boxlen=(datmax-datmin)/ires
c
c INITIALIZE THE GRID
c
    boxcnt=1
c
    do 60 i=1,maxbox
        datptr(i)=0
    do 50 j=1,ndim
        nxtbox(i,j)=0
        where(i,j)=0
50    continue
60    continue
c
    do 70 i=1,maxdat
        nxtdat(i)=0
70    continue
c
c MAIN LOOP
c
    do 140 i=1,datcnt-(ndim-1)*tau
c
c         DETERMINE TARGET COORDINATES
c
        do 80 j=1,ndim
            target(j)=(data(i+(j-1)*tau)-datmin)/boxlen
80            continue
c
c         GO TO TARGET BOX, DIMENSION BY DIMENSION
c         IF BOX DOESN'T EXIST, CREATE IT
c
            runner=1
            chaser=0
            do 130 j=1,ndim
90                if(where(runner,j)-target(j)) 100,130,110
100                chaser=runner

```

```

        runner=nxtbox(runner,j)
        if(runner.ne.0) goto 90
110         boxcnt=boxcnt+1
        if(boxcnt.eq.maxbox) then
c           TOO MANY BOXES - QUIT
            write(*,*) 'grid overflow at i = ',i
            goto 40
        endif
        do 120 k=1,ndim
            where(boxcnt,k)=where(chaser,k)
120         continue
            where(boxcnt,j)=target(j)
            nxtbox(chaser,j)=boxcnt
            nxtbox(boxcnt,j)=runner
            runner=boxcnt
130         continue
c
c           RUNNER IS TARGET BOX - ADD DATA POINT TO THIS BOX
c
            nxdat(i)=datptr(runner)
            datptr(runner)=i
140         continue
c
            used=0
            do 150 i=1,boxcnt
                if(datptr(i).ne.0) used=used+1
150             continue
c
            write(*,*) '# boxes allocated : ',maxbox
            write(*,*) '# boxes created   : ',boxcnt
            write(*,*) '# boxes non-empty : ',used
            write(*,*)
            write(*,666)
666         format(1x,'ok=1 : ',\ )
            read(*,*) iok
            if(iok.ne.1) goto 40
c
c WRITE OUT DATA BASE
c (EMPTY BOXES WRITTEN OUT - WASTES SOME STORAGE SPACE)
c
            inquire(file='database.',exist=tru)
            if(tru) then
                open(unit=1,file='database.')
                close(unit=1,status='delete')
            endif
            open(unit=1,file='database.',form='unformatted')
            write(*,*) 'writing the database...'
c
            write(1) ndim,ires,tau,boxcnt,datcnt,datmax,datmin,boxlen
c
            do 160 i=1,boxcnt
                write(1) datptr(i)
                write(1) (nxtbox(i,j),j=1,ndim)
                write(1) ( where(i,j),j=1,ndim)
160             continue
c
            do 170 i=1,datcnt
                write(1) nxdat(i)

```

```

170     continue
      close(unit=1)
c
      end

```

## C.2. Source listing for FET

```

$LARGE
$NOFLOATCALLS
$NODEBUG
c
  program fet
c
  parameter (maxdat=32000,maxdim=8,maxbox=6000)
c
  common ndim,ires,tau,boxcnt,datcnt,datmax,datmin,boxlen,nxtbox,
     1  where,datptr,nxtdat,data,delay,oldpnt,newpnt,bstpnt,
     2  runner,datuse,dismin,dismax,bstdis,thmax,thbest,evolve
c
  dimension data(maxdat)
  integer*2  nxtbox(maxbox,maxdim),where(maxbox,maxdim)
  integer*2  datptr(maxbox),nxtdat(maxdat),delay(maxdim)
  integer*4  tau,boxcnt,datcnt,datuse,evolve
  integer*4  oldpnt,bstpnt
  integer*2  xs,xso,ys,yso,xf,xfo,yf,yfo
           logical tru
c
c READ IN THE DATA BASE
c
  open(unit=1,file='database.',status='old',form='unformatted')
  write(*,*)
  write(*,*) 'reading the database...'
c
  read(1) ndim,ires,tau,boxcnt,datcnt,datmax,datmin,boxlen
c
  do 10 i=1,boxcnt
      read(1) datptr(i)
      read(1) (nxtbox(i,j),j=1,ndim)
      read(1) ( where(i,j),j=1,ndim)
10    continue
c
  do 20 i=1,datcnt
      read(1) nxtdat(i)
20    continue
c
  close(unit=1)
c
  write(*,*)
  write(*,*) 'ndim   : ',ndim
  write(*,*) 'ires   : ',ires
  write(*,*) 'tau    : ',tau
  write(*,*) 'boxcnt : ',boxcnt

```

```

write(*,*) 'datcnt : ',datcnt
write(*,*) 'datmax : ',datmax
write(*,*) 'datmin : ',datmin
write(*,*) 'boxlen : ',boxlen
write(*,*)
c
c READ IN THE TIME SERIES
c
open(unit=1,file='t.1',status='old',form='unformatted')
write(*,*) 'reading the time series...'
c
do 30 i=1,datcnt/8
    read(1) (data(8*(i-1)+j),j=1,8)
30    continue
c
close(unit=1)
c
c READ IN PARAMETERS
c
write(*,*)
write(*,111)
111    format(1x,'time-step (seconds or iterations) : ',\ )
read(*,*) dt
write(*,222)
222    format(1x,'evolution time (number of samples) : ',\ )
read(*,*) evolve
write(*,333)
333    format(1x,'minimum separation at replacement : ',\ )
read(*,*) dismin
write(*,444)
444    format(1x,'maximum separation for replacement : ',\ )
read(*,*) dismax
write(*,555)
555    format(1x,'maximum orientation error : ',\ )
read(*,*) thmax
write(*,*)
c
c INITIALIZE GRAPHICS ROUTINES, INSERT SCREEN LIMITS
c
call qsmode(6)
scalex=639./(datmax-datmin)
scaley=199./(datmax-datmin)

inquire(file='fet.out',exist=tru)
if(tru) then
    open(unit=1,file='fet.out')
    close(unit=1,status='delete')
endif
open(unit=1,file='fet.out',status='new')
c
do 40 i=1,ndim
    delay(i)=(i-1)*tau
40    continue
c
c some data points at the end are lost...
datuse=datcnt-(ndim-1)*tau-evolve
c
its=0

```

```

sum=0.0
savmax=dismax
c
oldpnt=1
newpnt=1
c
c SEARCH FOR NEAREST NEIGHBOR - IGNORE ORIENTATION
c
50     call search(0)
      if(bstpnt.eq.0) then
          dismax=dismax*2.0
          goto 50
      endif
c
dismax=savmax
newpnt=bstpnt
disold=bstdis
iang=-1
c
c EVOLVE POINTS, FIND FINAL SEPARATION, UPDATE EXPONENT
c
60     oldpnt=oldpnt+evolve
      newpnt=newpnt+evolve
c
c GRAPHICS INTERFACE
c *****
call qsmode(6)
do 70 i=0, evolve
    indo=oldpnt-evolve+i
    indn=newpnt-evolve+i
    xso=xs
    yso=ys
    xfo=xf
    yfo=yf
c     SCALE DATA TO FIT SCREEN
    xs=int((data(indo) -datmin)*scalex)
    ys=int((data(indo+tau)-datmin)*scaley)
    xf=int((data(indn) -datmin)*scalex)
    yf=int((data(indn+tau)-datmin)*scaley)
c     CLEAR THE SCREEN, DRAW CONNECTING LINES
    call qline(xs,ys,xf,yf,1)
    if(i.gt.0) then
        call qline(xso,yso,xs,ys,1)
        call qline(xfo,yfo,xf,yf,1)
    endif
70     continue
c *****
c
c CALCULATION FINISHED
    if(oldpnt.ge.datuse) goto 110
c
c FELL OFF TIME SERIES - IN DESPERATION - FIND NEAREST NEIGHBOR
    if(newpnt.ge.datuse) then
        oldpnt=oldpnt-evolve
        goto 50
    endif
c
disnew=0.0

```

```

do 80 i=1,ndim
    p1=data(oldpnt+delay(i))
    p2=data(newpnt+delay(i))
    disnew=disnew+(p2-p1)**2.
80    continue
    disnew=sqrt(disnew)
    if (disnew.lt.0.1*dismin) disnew=0.1*dismin
c
    its=its+1
    sum=sum+alog(disnew/disold)
    zlyap=sum/(its*evolve*dt*alog(2.0))
c
c POSITION THE TEXT CURSOR WHILE IN GRAPHICS MODE
write(*,666)
666    format(\
    call qcmov(0,24)
c
    if(iang.eq.-1) then
        write(*,777) evolve*its,disold,disnew,zlyap
        write(1,777) evolve*its,disold,disnew,zlyap
    else
        write(*,888) evolve*its,disold,disnew,zlyap,iang
        write(1,888) evolve*its,disold,disnew,zlyap,iang
    endif
777    format(1x,i8,6x,f12.4,3x,f12.4,8x,f10.4)
888    format(1x,i8,6x,f12.4,3x,f12.4,8x,f10.4,8x,i5)
c
c LOOK FOR REPLACEMENT ONLY IF FINAL DISTANCE > DISMAX
c
    if(disnew.le.dismax) goto 90
    call search(1)
    if(bstpnt.ne.0) goto 100
c
c NO ACCEPTABLE REPLACEMENT - TAKE NEAREST NEIGHBOR
c
    goto 50
c
c NO NEED FOR REPLACEMENT - KEEP EVOLVING
c
90    disold=disnew
    iang=-1
    goto 60
c
c REPLACEMENT SUCCESSFUL - START NEW EVOLUTION
c
100    newpnt=bstpnt
    disold=bstdis
    iang=int(thbest)
    goto 60
c
110    continue
    end
c
c
c
subroutine search(iflag)
c
parameter(maxdat=32000,maxdim=8,maxbox=6000)

```



```

c
common ndim, ires, tau, boxcnt, datcnt, datmax, datmin, boxlen, nxtbox,
1  where, datptr, ntxtdat, data, delay, oldpnt, newpnt, bstpnt,
2  runner, datuse, dismin, dismax, bstdis, thmax, thbest, evolve
c
dimension data(maxdat), oldcrd(maxdim), zewcrd(maxdim),
1  bstcrd(maxdim)
integer*2  nxtbox(maxbox, maxdim), where(maxbox, maxdim)
integer*2  datptr(maxbox), ntxtdat(maxdat), delay(maxdim)
integer*4  igcrds(maxdim), target(maxdim)
integer*4  tau, boxcnt, datcnt, datuse, evolve
integer*4  oldpnt, bstpnt, runner
c
c IF BSTPNT <> 0 ON RETURN - A REPLACEMENT HAS BEEN FOUND.
c ...BSTPNT POINTS TO IT
c ...THBEST IS THE CHANGE IN ORIENTATION
c ...BSTDIS IS THE NEW SEPARATION FROM THE FIDUCIAL POINT
c ...BSTCRD HAS ITS COORDINATES (NOT PASSED BACK TO "MAIN")
c
c SET UP GRID COORDINATES
c
do 10 i=1, ndim
    oldcrd(i)=data(oldpnt+delay(i))
    zewcrd(i)=data(newpnt+delay(i))
    igcrds(i)=(oldcrd(i)-datmin)/boxlen
10  continue
c
c FIND DISTANCE FROM OLDPNT TO NEWPNT
c (NOT NECESSARILY 'DISNEW' OF MAIN PROGRAM)
c
oldist=0.0
do 20 i=1, ndim
    abc=oldcrd(i)-zewcrd(i)
    oldist=oldist+abc**2.
20  continue
oldist=sqrt(oldist)
c
c SKIP BOXES CLOSER THAN DISMIN, INITIALIZE 'BEST' VARIABLES
c
irange=int(dismin)/boxlen
if(irange.eq.0) irange=1
c
thbest=thmax
bstdis=dismax
bstpnt=0
c
30  do 140 icnt=0, ((2*irange+1)**ndim)-1
    icounter=icnt
c
do 40 i=1, ndim
    ipower=(2*irange+1)**(ndim-i)
    ioff=icounter/ipower
    icounter=icounter-ioff*ipower
    target(i)=igcrds(i)-irange+ioff
    if(target(i).lt.0)      goto 140
    if(target(i).gt.ires-1) goto 140
40  continue
c

```

```

c      CHECK ALL BOXES ON OUTER PERIMETER OF SEARCH AREA
c      (EXCEPT FIRST TIME THROUGH)
c
      if(irange.eq.1) goto 60
      iskip=1
      do 50 i=1,ndim
          if(iabs(target(i)-igcrds(i)).eq.irange) iskip=0
50         continue
      if(iskip.eq.1) goto 140
c
c      SEARCH FOR TARGET BOX
c
60         runner=1
      do 80 i=1,ndim
70         if(where(runner,i).eq.target(i)) goto 80
          runner=nxtbox(runner,i)
          if(runner.ne.0) goto 70
          goto 140
80         continue
c
      if(runner.eq.0) goto 140
      runner=datptr(runner)
      if(runner.eq.0) goto 140
c
c      FOR POINTS IN THIS BOX CHECK...
c      DISTANCE, ANGLE, NON-ADJACENCY
c
90         if(iabs(runner-oldpnt).lt.evolve) goto 130
      if(iabs(runner-datuse).lt.(2*evolve)) goto 130
c
      do 100 i=1,ndim
          bstcrd(i)=data(runner+delay(i))
100        continue
c
      tdist=0.0
      dot=0.0
      do 110 i=1,ndim
          abc1=oldcrd(i)-bstcrd(i)
          abc2=oldcrd(i)-zewcrd(i)
          tdist=tdist+abc1*abc1
          dot=dot+abc1*abc2
110        continue
      tdist=sqrt(tdist)
c
      if(tdist.lt.dismin) goto 130
      if(tdist.ge.bstdis) goto 130
      if(tdist.eq.0) goto 130
      if(iflag.eq.0) goto 120
      ctheta=amin1(abs(dot/(tdist*olddist)),1.0)
      theta=57.3*acos(ctheta)
      if(theta.ge.thbest) goto 130
      thbest=theta
120        bstdis=tdist
          bstpnt=runner
c
c      GO TO NEXT POINT IN BOX
c
130        runner=nxtdat(runner)

```

```
        if(runner.ne.0) goto 90
c
140     continue
c
c RETURN IF POINT FOUND, ELSE CHECK NEXT LAYER
c
c NOTE DEPENDENCE OF # OF BOXES SEARCHED ON DISMAX
c DISMAX < 1.5*BOXLEN  -> 3**NDIM BOXES (1 LAYER)
c DISMAX < 2.5*BOXLEN  -> 5**NDIM BOXES (2 LAYERS)   ETC...
    irange=irange+1
    if(irange.le.int(0.5+(dismax/boxlen))) goto 30
    return
end
```

## Appendix D

### D.1. Autocorrelation computation

Computation of the logistic equation, the two point correlation measure as described in Casti (1992, p.57) and the autocorrelation measure as described by Bendat and Piersol, (1986, p.385).

Compute the logistic map

$N := 1000$        $i := 0..N$        $x1_0 := 0.1$        $n := 4$       Set initial values

$\log\_dat_0 := x1_0$

$\log\_dat_{i+1} := n \cdot \log\_dat_i \cdot (1 - \log\_dat_i)$

Set the maximum lag (r) and limit n

$n := 0..N - 40$        $r := 0..39$

Compute the two point correlation and normalise to 1 for zero lag.

$Sm_n := \log\_dat_n$

$Smr_{r,n} := \log\_dat_{n+r}$

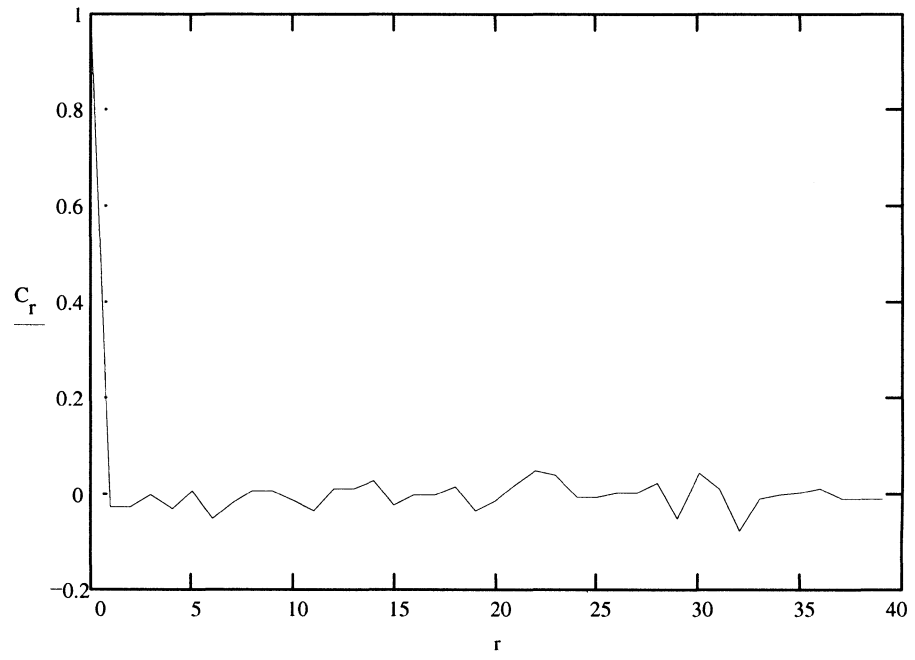
$SmSmr := \frac{Smr \cdot Sm}{N - 39}$

$SmMean := \frac{\sum(Sm)}{N - 39}$        $SmMean = 0.499$

$V_r := \sum_n Smr_{r,n}$        $SmrMean := \frac{V}{N - 39}$

$SMSMR := SmMean \cdot SmrMean$

$C := SmSmr - SMSMR$        $C := \frac{C}{C_0}$



## **Vita**

Edward Earnest Bartlett

Date of Birth : 21 November 1959      Zomba, Malawi

Fjorveien 85c  
Høvik, N-1322  
Norway

University of Natal, Durban      1977 - 1980    BSc (Survey)